ICFO – The Institute of Photonic Sciences
Castelldefels (Barcelona), Spain

PhD thesis

Local temperature and correlations in quantum many-body systems

Senaida Hernández Santana

March 11, 2019

Thesis supervisor: Dr. Antonio Acín
Thesis cosupervisor: Dr. Christian Gogolin

Acknowledgements

Abstract

Quantum Mechanics was established as the theory of the microscopic world, which allowed to understand processes in atoms and molecules. Its emergence led to a new scientific paradigm that quickly spread to different research fields. Two relevant examples are Quantum Thermodynamics and Quantum Many-Body Theory, where the former aims to characterize thermodynamic processes in quantum systems and the latter intends to understand the properties of quantum many-body systems. In this thesis, we tackle some of the questions in the overlap between these disciplines, focusing on the concepts of temperature and correlations. Specifically, it contains results on the following topics: locality of temperature, correlations in long-range interacting systems and thermometry at low temperature. The problem of locality of temperature is considered for a system at thermal equilibrium and consists in studying whether it is possible to assign a temperature to any of the subsystems of the global system such that both local and global temperatures are equal. We tackle this problem in two different settings, for generic one-dimensional spin chains and for a bosonic system with a phase transition at non-zero temperature. In the first case, we consider generic one-dimensional translation-invariant spin systems with short-range interactions and prove that it is always possible to assign a local temperature equal to the global one for any temperature, including at criticality. For the second case, we consider a three-dimensional discretized version of the Bose-Einstein model at the grand canonical ensemble for some temperature and particle density, and characterize its non-zero-temperature phase transition. Then, we show that temperature is locally well-defined at any temperature and at any particle density, including at the phase transition. Additionally, we observe a qualitative relation between correlations and locality of temperature in the system. Moving to correlations, we consider fermionic two-site long-range interacting systems at thermal equilibrium. We show that correlations between anti-commutative operators at non-zero temperature are upper bounded by a function that decays polynomially with the distance and with an exponent that is equal to the interaction exponent, which characterizes the interactions in the Hamiltonian. Moreover, we show that our bound is asymptotically tight and that the results extend to density-density correlations as well as other types of correlations for quadratic and fermionic Hamiltonians with long-range interactions. Regarding the results on thermometry, we consider a bosonic model and prove that strong coupling between

the probe and the system can boost the thermal sensitivity for low temperature. Furthermore, we provide a feasible measurement scheme capable of producing optimal estimates at the considered regime.

List of publications

Publications forming part of the thesis

- *Locality of temperature in spin chains*, Senaida Hernández-Santana, Arnau Riera, Karen V. Hovhannisyan, Martí Perarnau-Llobet, Luca Tagliacozzo, and Antonio Acín, New Journal of Physics **17**, 085007 (2015).

- *Correlation decay in fermionic lattice systems with power-law interactions at non-zero temperature*, Senaida Hernández-Santana, Christian Gogolin, Juan Ignacio Cirac, and Antonio Acín, Physical Review Letters **119**, 110601 (2017).

- *Low-temperature thermometry enhanced by strong coupling*, Luis A. Correa, Martí Perarnau-Llobet, Karen V. Hovhannisyan, Senaida Hernández-Santana, Mohammad Mehboudi, and Anna Sanpera, Phys. Rev. A **96**, 062103 (2017).

Non-published results forming part of the thesis

- *Locality of temperature and correlations in the presence of non-zero temperature phase transitions*, Senaida Hernández-Santana, Andras Molnar, Christian Gogolin, Juan Ignacio Cirac, and Antonio Acín. In preparation.

Contents

x

1. Introduction

At the beginning of the last century, Quantum Mechanics was established as the theory of the microscopic world, which allowed to understand processes in atoms and molecules. However, it caused a big controversy at the time due to its counterintuitive and probabilistic nature, which was completely opposed to the determinism of Classical Physics. The most remarkable examples of this controversy are the debates between Albert Einstein and Niels Bohr [Boh49], where Bohr defended the need of Quantum Theory to explain the microscopic world. In fact, there are many phenomena that cannot be explained by Classical Physics alone, for example, the wave-particle duality or the photoelectric effect. In 1927 at the Fifth Solvay Conference, it was clear that Quantum Physics was already widely accepted. A revolution had started, both fundamental and technological.

Most of the intriguing properties in Quantum Mechanics are based on the phenomena of Quantum Entanglement and Quantum Superposition. These two phenomena have opened the door to new possibilities in a variety of fields, but they have also led to numerous open questions. In fact, there has been a rising of new fields devoted to understanding quantum mechanics in the most diverse contexts, from quantum engineering to quantum chemistry, including new theories in biology or applications of quantum-based technologies on medicine.

In this new era, the field of Quantum Thermodynamics became immediately part of the discussion, aiming to solve questions regarding the effects of quantum phenomena in thermodynamic processes. One of the most prominent examples in this direction is the work by Von Neumann in 1929 [VN29], where he proved that states evolved towards maximum entropy and conceptualized many of the ideas in equilibration of quantum systems. Another great example is one of the first proposals of quantum heat engines, made by Scovil and Schulz-DuBois in 1959 [SSD59]. In the last decades, the field has experienced a renewed interest due to three factors. First, there has been spectacular experimental progress that allows for direct observation of thermodynamic phenomena in a variety of quantum systems, such as ultra-cold atoms in optical lattices, ion traps, superconductor qubits, etc [BDN12, PSSV11, KRJP13, SBM$^+$11]. Second, there have been numerous advances in numerical methods and computation power, enabling us to study quantum systems under different conditions, such as few-body
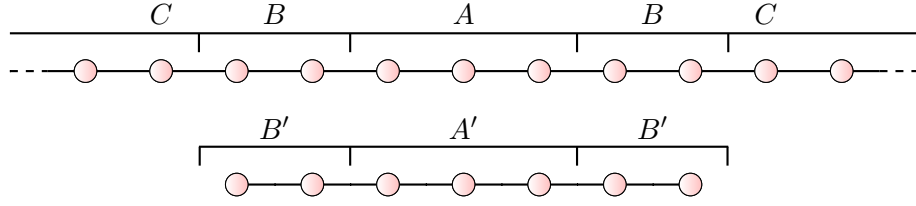
Figure 1.1.: Scheme of the 1D setting for the problem of locality of temperature.

or many-body systems, or systems at equilibrium and at non-equilibrium. And at last, there has been an outburst of theoretical works that have led to a deeper understanding in the field, such as, the proposal of thermal machines consisting of few qubits [LPS10] or the derivation of statistical mechanics principles directly from quantum mechanics [PSW06].

Quantum Thermodynamics has led to many intriguing questions, some of them in overlap with fields such as Condensed Matter Physics or Estimation Theory. In this thesis, we aim to tackle some of these questions in the context of many-body systems. We will focus on fundamental concepts, such as temperature or correlations, and consider a variety of scenarios, including different types of particles and interactions.

1.1. Contributions

In the following, we review the different works that conform this thesis, giving the motivations and explaining the main results.

1.1.1. Locality of temperature for one-dimensional spin systems

1.1.1.1. State of the art and motivation

One of the most fundamental questions in Quantum Thermodynamics is whether the Thermodynamic Laws are still valid in quantum systems or whether they need to be modified. As a consequence, fundamental concepts like temperature are now questioned since they are defined in terms of the Thermodynamic Laws. In particular, the concept of temperature, originally defined by the standard Zeroth Law, is understood as a statistical parameter and, thus, becomes unclear when dealing with few-body systems or quantum systems. In fact, there is not yet an agreement on the fundamental

meaning of temperature in Quantum Physics: while theoreticians associate temperature to a mathematical parameter that characterizes the thermal state, experimentalists relate it to particles kinetic energy. Understanding the Zeroth Law becomes then necessary to find a common understanding of temperature in quantum systems. The Zeroth Law is stated in the following way: if two bodies are each in thermal equilibrium with a third body, they are in thermal equilibrium with each other [Rei98, Bal07]. This implicitly means that: (i) There is a thermal equilibrium state that is well defined by a parameter called temperature, and isolated systems tend to this state; (ii) Each subsystem of the system is at the thermal equilibrium state; (iii) All the subsystems have the same temperature, i.e., temperature is intensive. Since the first point is verified by the known thermal state, we need to understand the last two points to understand the Zeroth Law. In recent years, many works have tried to solve this question, also known as the problem of locality of temperature.

The general setting of this problem consists of a quantum system described by a Hamiltonian H and at a thermal state with temperature T. A typically studied model is a periodic quantum lattice system where the Hamiltonian is a sum of local terms interacting according to some underlying graph. For weak interactions, the thermal state of the system can be well approximated by a product of thermal states acting on different subsystems, which allows one to assign locally the same global temperature T to each of these subsystems. However, in the presence of strong interactions the partial state of a subsystem will not generally have the same form as the thermal state. Hence, it is not obvious how to assign a temperature to it. In 2012, a first step to circumvent the problem was made by Ferraro et al. in [FGSA12], where they considered coupled harmonic oscillators on a lattice at thermal equilibrium at temperature T. They studied how to assign a temperature to a subsystem A by dividing the whole system into three regions: the subsystem A, a boundary region around it B and the rest C (see Figure 1.1). Given this, they considered a different system at thermal equilibrium at temperature T which consists of two regions A' and B' which are equivalent to the subsystem A and its boundary B, respectively. Then, they showed that it is sufficient to compute the state of the subsystem A' to obtain a very close approximation to the actual state of the subsystem A, which we also refer as effective thermal state. In this way, the correlations and the boundary effects around A are taken into account and it is possible to assign the same temperature to the subsystem A provided that the boundary region B is independent of the total system size. In the next years, this approach has been taken as the default starting point for locality of temperature in the upcoming works.

For instance, in 2014 Kliesch et al. [KGK$^+$14] proved the first generic result for fermionic and spin local Hamiltonians for any spatial dimension following the same approach. They showed that for high enough temperature both partial states of the

subsystem A and its equivalent A' were approximately equal with an error that decayed exponentially with the size of the boundary B. Furthermore, they proved that correlations were directly related to the distinguishability between both states, playing a fundamental role in the locality of temperature. Nevertheless, it is far from clear what occurs at low temperatures.

Motivated by these works, we consider one dimensional translation-invariant spin systems and study whether the temperature can be considered local in such systems, with emphasis on how temperature affects the locality of temperature.

1.1.1.2. Main result

We show that, for one dimensional translation-invariant spin systems with short-range interactions, it is always possible to assign a local temperature for any temperature. More specifically, we prove that the trace distance between the actual state of the system A and the effective thermal state is upper-bounded by a function that decays with the boundary size. The function decays differently depending on the presence of criticality: exponentially away from criticality and as a power law at criticality. Therefore, it is always possible to guarantee that the partial state of any subsystem can be described as an effective thermal state with the same global temperature T for a large enough boundary size. Regarding our methods, we make use of the theory of tensor networks for the off-criticality case, and results from conformal field theory for the criticality case. Finally, we exemplify our analytical findings by analysing a model of a quantum Ising chain. This system is complex enough to have a quantum phase transition point, but simple enough to allow for an exact diagonalization by standard tools of statistical mechanics, thereby serving as a perfect test-bed for our analytical upper bounds.

1.1.2. Locality of temperature and correlations in the presence of non-zero temperature phase transitions

1.1.2.1. State of the art and motivation

We also consider here the problem of locality of temperature. As we have seen above, temperature can be locally well defined under different circumstances. More specifically, it has been proven local in some specific bosonic systems: 1D and 2D interacting harmonic oscillators [FGSA12]; and in fermionic systems under different constraints: (i) for generic one-dimensional systems and at arbitrary temperature, result present in this thesis, [HSRH$^+$15], (ii) for fermionic and spin systems with ar-

bitrary dimension and at high temperature [KGK$^+$14], and (iii) for the Ising model [GSFA09, HSRH$^+$15]. Morover, it has been observed that locality is also valid at quantum phase transitions in one-dimensional fermionic systems provided that the boundary region is large enough [GSFA09, HSRH$^+$15].

However, phase transitions in 1D systems with short-range interactions are exclusively driven by quantum fluctuations, that is, they only occur at zero temperature in these systems. This is far from true when it comes to higher dimensional systems, where phase transitions can also occur at non-zero temperature and are driven by both thermal and quantum fluctuations. Non-zero-temperature phase transitions are an important feature in many-body systems which holds interesting phenomenology. In fact, there have been studies suggesting a relation between these phase transitions and correlations or even entanglement negativity [LG18], a purely quantum measure. It is natural then to wonder whether and how the concept of local temperature is affected by the presence of non-zero-temperature phase transitions. Motivated by this question, we characterize a three-dimensional bosonic system with a non-zero-temperature phase transition, which corresponds to a discrete version of the Bose-Einstein model [PS16], and study the problem of locality of temperature and its relation to the correlations in the system.

1.1.2.2. Main result

We study a three-dimensional discrete version of the Bose-Einstein model at the grand canonical ensemble for temperature T and particle density n. We show that the system undergoes a non-zero-temperature phase transition in a similar fashion to the Bose-Einstein model, i.e., the system condensates to the ground state below a critical temperature T_c. Regarding the locality, we consider a three-dimensional system ABC with length L and study whether the temperature is local in a subsystem A consisting of a $2 \times 2 \times 2$ cube. In the same way as in the previous section (see Figure 1.1), we compare the partial state of the subsystem A with the partial state of an equivalent subsystem A' only surrounded by a boundary region. Concretely, we prove that temperature is locally well defined at any temperature and at any particle density. We make use of the fidelity as our distinguishability measure between partial states and observe different behaviours depending on the temperature. Below the critical temperature T_c, the fidelity goes to 1 as a power-law with the boundary size; and above T_c, it goes to 1 exponentially. In addition, we analyse the correlations of the system and observe that they decay polynomially to n_0^2 below the critical temperature T_c, where n_0 is the zero-momentum particle density, and exponentially above T_c. While we observe long-distance correlations below the critical temperature, the qualitative

behaviour of the correlations is consistent with the results on the study of locality.

1.1.3. Correlations in long-range interacting systems

1.1.3.1. State of the art and motivation

In the last years, long-range interacting systems (with power-law decaying interactions) have started to gain attention. This recent interest is fundamentally due to two reasons. First, these systems offer many fascinating properties that set them apart from systems with merely finite-range or exponentially decaying (short range) interactions. For instance, they allow for faster processes in physics, as it has been observed in the spreading of correlations [RGL+14, MGFFG16], in equilibration dynamics [Kas11, BK13, Kas17] or in state transfer [EGM+17]. Also, they show new violations of the area law [KLT12] and topological effects, and they support Majorana edge modes [VLE+14, PNP17]. Second, recently there has been an outbreak of experimental techniques to simulate these systems [PC04, DPC05, HCMH+10, GTHC+15], for instance via polar molecules [MBZ06], ultra-cold ions[IEK+11, SPS12, BSK+12, JLH+14, RGL+14], or Rydberg atoms [LBR+16].

Many typical interactions in nature are actually long-range, such as dipole-dipole interactions, the van der Waals force and the Coulomb interaction. However, condensed matter physics has typically focused on the properties of short-range interacting systems. One example is given by the spatial correlations, which have been thoughtfully characterized in these systems. More concretely, it has been shown that they decay exponentially with the distance in a variety of systems at thermal equilibrium. For instance, it has been proven for short-range fermionic systems at non-zero temperature for anti-commutative operators [Has04b] and at zero temperature provided there is a non-vanishing spectral gap [HK06], and for short-range spin and fermionic systems above certain threshold temperature [KGK+14]. A similar level of understanding of the correlations in long-range interacting systems is lacking so far, but it is of fundamental interest given their recent experimental feasibility and their intriguing properties. Our goal is to understand how correlations behave in long-range interacting systems at thermal equilibrium.

1.1.3.2. Main result

We prove an upper bound for a type of spatial correlations in long-range interacting systems. Specifically, we consider fermionic two-site long-range interacting systems

and show that correlations between anti-commutative operators at non-zero temperature are upper bounded by a decaying function with the distance. This function decays polynomially with a exponent that is equal to the interaction exponent, which characterizes the interactions in the Hamiltonian. Our result implies that correlations cannot decay slower than a power-law with the interaction exponent. The proof is based on a previous work on correlations by Hastings [Has04b] and on recent advances on the dynamical spreading of correlations in long-range interacting systems [FFGCG15]. Furthermore, we prove that our bound is asymptotically tight by means of a high temperature expansion and by numerical simulations of a fermionic model with long-range interactions, whose ground state phase diagram has been extensively studied [VLEP16, VLE$^+$14].

1.1.4. Low-temperature thermometry enhanced by strong coupling

1.1.4.1. State of the art and motivation

Nanoscale thermometry [CP15] aims to measure the temperature of a quantum system at thermal equilibrium. Recently, this field has experienced great advances due to its potential applications to micro-electronics [WW86, ATMC05, LV05], biochemistry, or to disease diagnosis [KN09, KMY$^+$13, SCLD14, SG14]. In particular, thermometer miniaturization may be taken to the extreme of engineering individual quantum thermometers [FVV$^+$11, MB13, SHS$^+$14, HIK14, NJD$^+$13, KMY$^+$13, JCM$^+$16, HBPLB17]. This approach has the advantage of providing a nanometric spatial resolution and leaving the sample mostly unperturbed provided that the heat capacity of the probe is low enough, in contrast to the direct manipulation of the sample, such as time-of-flight measurements of ultra-cold trapped atoms. The typical setting consists of a sample at equilibrium at some temperature T and a measuring device or probe that is thermally coupled and acts as the thermometer. After equilibration, one can estimate the temperature T by monitoring some temperature-dependent features of the thermometer via a suitable measurement and data analysis scheme. Nonetheless, if the sample is too cold, the probe may not equilibrate [NA02]; and if the probe is too small, boundary effects become relevant and need to be taken into account to properly describe thermalisation [GE16, FGSA12, KGK$^+$14, HSRH$^+$15]. A way to tackle this problem is to decrease the interaction between the sample and the probe, but this decreases the thermal sensitivity of the probe considerably [Deb12], providing futile results. This is an inherent problem of low-temperature thermometry [DRFG16]. In this chapter, we show how to make use of strong interactions to fight such a fundamental limitation.

1.1.4.2. Main result

We show that strong coupling between the probe and the system can boost the thermal sensitivity in the low temperature regime. To that end, we make use of the Caldeira-Leggett Hamiltonian [Wei08], where the system at equilibrium is represented by a bosonic reservoir [CL83, RHW85], and the probe is described by a single harmonic oscillator. In particular, we analytically obtain the exact steady state of the probe and show that the maximum sensitivity attainable at low temperature is significantly enhanced by increasing the coupling strength. Furthermore, we provide a concrete and feasible measurement scheme capable of producing nearly optimal temperature estimates in the low temperature regime.

1.2. Outline of the thesis

This thesis is organized as follows:

- Chapter 2 introduces the fundamental concepts that appear in the thesis.

- Chapter 3 is dedicated to the investigation of the problem of locality of temperature in one-dimensional spin chains. This chapter refers to the original results published in [HSRH$^+$15].

- In Chapter 4, we study locality of temperature for a three-dimensional model of free bosons that has a phase transition at non-zero temperature. The publication presenting these results is in preparation.

- In Chapter 5 we show how correlations behave in long-range interacting systems regardless of the dimension. These results refer to the published work [HSGCA17].

- In Chapter 6, we propose a way to tackle low-temperature thermometry by considering strong interactions. This chapter is based on the results published in [CPLH$^+$17].

2. Preliminaries

In this chapter, we introduce the basic concepts and tools that appear in the thesis. It consists of three main sections: the first explains the necessary fundamental concepts of quantum mechanics, the second is devoted to quantum many-body physics and the last contains the basic notions of quantum thermometry. Many of the concepts explained here can be found in the book by Nielsen and Chuang [NC00], and in the review by Gogolin and Eisert [GE16].

2.1. Fundamental concepts

In this section, we explain some basic concepts of quantum mechanics, going from operators and trace distance to correlations and entanglement.

2.1.1. Hilbert space and operators

Let us consider a complex separable Hilbert space $\mathcal{H}$ with dimension d and inner product $\langle\varphi|\psi\rangle$ for $|\varphi\rangle, |\psi\rangle \in \mathcal{H}$. Given this, it is possible to define the following subspaces:

- The space of bounded operators, $\mathcal{B}(\mathcal{H})$: $A \in \mathcal{B}(\mathcal{H}) \leftrightarrow A$ has finite eigenvalues.

- The space of trace class operators, $\mathcal{T}(\mathcal{H}) \subset \mathcal{B}(\mathcal{H})$: $A \in \mathcal{T}(\mathcal{H}) \leftrightarrow \mathrm{tr}(A)$ is finite.

- The space of quantum states, $\mathcal{S}(\mathcal{H}) \subset \mathcal{T}(\mathcal{H})$: $\rho \in \mathcal{S}(\mathcal{H}) \leftrightarrow \mathrm{tr}(\rho) = 1$ and ρ is non-negative, that is, $\mathrm{tr}(\rho\, A) \geq 0, \forall A \geq 0$.

- The space of observables, $\mathcal{O}(\mathcal{H}) \subset \mathcal{B}(\mathcal{H})$: $A \in \mathcal{O}(\mathcal{H}) \leftrightarrow A$ is self-adjoint, i.e. $A = A^\dagger$.

Moreover, an operator $U \in \mathcal{B}(\mathcal{H})$ is unitary if $U^\dagger U = U U^\dagger = \mathbb{1}$ and an operator $\Pi \in \mathcal{B}(\mathcal{H})$ is a projector if $\Pi\,\Pi = \Pi$. For finite dimensional systems, $\rho \in \mathcal{S}(\mathcal{H})$ is non-negative, it has unit trace and it is also self-adjoint and, therefore, $\mathcal{S}(\mathcal{H}) \subset \mathcal{O}(\mathcal{H})$.

The extreme points of this set are called pure states and are rank-one[1] projectors, and the rest refers to mixed states. In a formal way, a quantum state $\rho \in \mathcal{S}(\mathcal{H})$ is said to be pure if it can be expressed as $\rho = |\psi\rangle\langle\psi|$ for a single vector $\psi \in \mathcal{H}$. A mixed state cannot be represented in this way and it can be given by a combination of pure states, that is, $\rho = \sum_i^d p_i |\psi_i\rangle\langle\psi_i|$ where $\{\psi_i\}$ are the vectors that constitute the Hilbert space basis, $p_i \geq 0 \, \forall i$ and $\sum_i p_i = 1$. The state is also called completely mixed if $p_i = d^{-1} \, \forall i$.

2.1.1.1. Expectation value of an observable

Given an observable $A \in \mathcal{O}(\mathcal{H})$ and a quantum state $\rho \in \mathcal{S}(\mathcal{H})$, the **expectation value** of A for the state ρ is defined as

$$\langle A \rangle_\rho := \mathrm{tr}(A\,\rho). \tag{2.1}$$

More generally, this definition applies to any bounded operator. However, we will only work with observables since they correspond to valid physical operators.

2.1.1.2. Norm of an observable

For any finite $p \geq 1$, the **Schatten p-norm** [Bha97] of an observable $A \in \mathcal{O}(\mathcal{H})$ is defined as

$$\|A\|_p := \left[\sum_{j=1}^d (s_j(A))^p \right]^{1/p}, \tag{2.2}$$

where $\{s_j(A)\}_{j=1}^d$ is the ordered set of real and non-negative singular values of A. We refer to the Schatten ∞-norm as the operator norm and to the Schatten 1-norm as the trace norm. As previously, we highlight that this is also valid for any bounded operator.

2.1.1.3. Purity

For any quantum state $\rho \in \mathcal{S}(\mathcal{H})$, the **purity** corresponds to a measure of how much the state is mixed and it is given by

$$\mathcal{P}(\rho) = \mathrm{tr}\,\rho^2. \tag{2.3}$$

The purity satisfies $\frac{1}{d} \leq \mathcal{P} \leq 1$ where $\mathcal{P} = 1$ implies that the state ρ is a pure state and $\mathcal{P} = d^{-1}$ means that it is completely mixed.

---

[1]The rank of an operator is the dimension of its image.

2.1.2. Hamiltonian: Properties and evolution

The Hamiltonian $H \in \mathcal{O}(\mathcal{H})$ of a finite dimensional quantum system is characterized by a **spectral decomposition**

$$H = \sum_{k=1}^{d'} E_k \, \Pi_k, \tag{2.4}$$

where $\Pi_k \in \mathcal{O}(\mathcal{H})$ and E_k represent the orthogonal spectral projectors and the energy eigenvalues of H, respectively, and $d' \leq d := \dim(\mathcal{H})$ is the number of different eigenvalues. If H is non-degenerate, $d' = d$ and the projectors $\Pi_k = |E_k\rangle\langle E_k|$ where $\{|E_k\rangle\}_{k=1}^{d}$ are the orthonormal energy eigenstates of H. A fundamental parameter of the Hamiltonian is the **spectral gap**, which is defined as the energy difference between its lowest energy value E_0 and its next lowest energy value E_1 such that the spectral gap $\Delta := E_1 - E_0$. The spectral gap allows one to study whether the system has a **quantum phase transition** (QPT), an abrupt change in the properties of the system. More concretely, given a parameter-dependent Hamiltonian characterized by $H := H_0 + h \, H_1$ with parameter h and spectral gap $\Delta = \Delta(h)$, a QPT is said to occur if Δ goes to 0 for some critical value h_{crit}. These transitions only happen at zero temperature and, thus, are only driven by quantum fluctuations. Nonetheless, phase transitions at non-zero-temperature also exist, which are driven by both thermal (classical) and quantum fluctuations.

2.1.2.1. Evolution

Given a quantum system at state ρ and described by a time independent Hamiltonian H, the evolution of its state $\rho(t)$ is described by the **Liouville–von Neumann equation Neumann equation**, which in the **Schrödinger picture** is

$$\frac{\partial}{\partial t}\rho(t) = -\mathrm{i}\,\hbar^{-1}[H, \rho(t)], \tag{2.5}$$

where $\hbar$ is the reduced Planck constant. Its solution is given by $\rho(t) := U^\dagger(t)\,\rho\,U(t)$ with $t \in \mathbb{R}$ and the time evolution operator $U(t) := \mathrm{e}^{-\mathrm{i}\,H\,t} \in \mathcal{B}(\mathcal{H})$. Equivalently, the evolution equation can be expressed in terms of operators via the **Heisenberg picture**, which for an observable $A \in \mathcal{O}(\mathcal{H})$ reads as

$$\frac{\partial}{\partial t}A(t) = \mathrm{i}\,\hbar^{-1}[H, A(t)]. \tag{2.6}$$

The solution is now given by $A(t) := U(t)\,A(0)\,U^\dagger(t)$ with the same time evolution operator $U(t)$. The equivalence between both pictures can be clearly justified when

computing the temporal evolution of the observable A, as

$$\langle A \rangle_t = \mathrm{tr}\left(A\, U^\dagger(t)\, \rho\, U(t) \right) = \mathrm{tr}\left(U(t)\, A\, U^\dagger(t)\, \rho \right), \qquad (2.7)$$

which implies that $\langle A \rangle_t = \langle A \rangle_{\rho(t)} = \langle A(t) \rangle_\rho$ and, thus, both pictures are equivalent.

2.1.3. State distinguishability

One of the most frequent measures of distinguishability between any two states $\rho_1, \rho_2 \in \mathcal{S}(\mathcal{H})$ is the **trace distance** [NC00], defined as

$$\mathcal{D}\left(\rho_1, \rho_2 \right) := \frac{1}{2} \left\| \rho_1 - \rho_2 \right\|_1, \qquad (2.8)$$

which is symmetric and satisfies that $\mathcal{D}(\rho_1, \rho_2) \in [0, 1]$, where $\mathcal{D}(\rho_1, \rho_2) = 0$ means that $\rho_1 \equiv \rho_2$. Other important relation of the trace distance is of the form

$$\mathcal{D}\left(\rho_1, \rho_2 \right) = \max_{A \in \mathcal{O}(\mathcal{H}):\, 0 \leq A \leq \mathbb{1}} \mathrm{tr}(A\, \rho_1) - \mathrm{tr}(A\, \rho_2), \qquad (2.9)$$

where the trace distance is given by the maximum difference between expectation values of an operator A satisfying $0 \leq A \leq \mathbb{1}$ for the states ρ_1 and ρ_2. Another typically used measure of distinguishability is the **fidelity** [NC00], which is defined for any two quantum states $\rho_1, \rho_2 \in \mathcal{S}(\mathcal{H})$ as

$$\mathrm{F}\left(\rho, \sigma \right) := \left[\mathrm{tr}\left(\sqrt{\rho^{1/2}\, \sigma\, \rho^{1/2}} \right) \right]^2, \qquad (2.10)$$

which is also symmetric and verifies that $\mathrm{F}(\rho_1, \rho_2) \in [0, 1]$, where $\mathrm{F}(\rho_1, \rho_2) = 1$ means that $\rho_1 \equiv \rho_2$. Moreover, the fidelity is related to the trace distance via the relation [FV99] given by

$$1 - \mathrm{F}\left(\rho_1, \rho_2 \right)^{1/2} \leq \mathcal{D}\left(\rho_1, \rho_2 \right) \leq \left(1 - \mathrm{F}\left(\rho_1, \rho_2 \right) \right)^{1/2}. \qquad (2.11)$$

2.1.4. Correlations

Correlations in quantum mechanics are often measured via the **covariance**, which for a system at a quantum state ρ and two operators A, B is defined as

$$\mathrm{cov}_\rho(A, B) := \mathrm{tr}(\rho\, A\, B) - \mathrm{tr}(\rho\, A)\, \mathrm{tr}(\rho\, B). \qquad (2.12)$$

We will only be interested in the correlations between any two observables A, B acting on disjoint subsystems X and Y defined as $X := \mathrm{supp}(A)$ and $Y := \mathrm{supp}(B)$. In this typical scenario, the state $\rho \in \mathcal{S}(\mathcal{H})$ is uncorrelated with respect to the bipartition XY if and only if $\mathrm{cov}_\rho(A, B) = 0$.

2.1.5. Entanglement

Consider a bipartite system with Hilbert space $\mathcal{H}$ consisting of two disjoint subsystems X and Y. In this setting, a quantum state $\rho \in \mathcal{S}(\mathcal{H})$ is said to be a **product state** with respect to this bipartition if $\rho = \rho^X \otimes \rho^Y$. In this case, the state ρ is said to be uncorrelated with respect to this bipartition. Moreover, it is possible to define a quantum state as **separable state** with respect to the bipartition XY if it can be expressed as

$$\rho = \sum_j p_j \, \rho_j^X \otimes \rho_j^Y \tag{2.13}$$

with $(p_j)_j$ a probability vector, i.e., $\sum_j p_j = 1$ and $p_j \geq 0$ for all j, and $\rho_j^X \in \mathcal{S}(\mathcal{H}_X)$ and $\rho_j^Y \in \mathcal{S}(\mathcal{H}_Y)$ for all j. This state is correlated in general, but a classical mechanism is responsible for the correlations present. If a quantum state is not separable, it is called **entangled**.

2.2. Quantum many-body physics

In this section, we focus on the necessary definitions to understand the variety of many-body systems that are considered in this manuscript. We also explain other relevant concepts in these systems, such as locality of temperature and Lieb-Robinson bounds.

2.2.1. Locally interacting quantum systems

Through out this thesis, we will always consider **locally interacting quantum systems**, which are defined by an interaction hypergraph $\mathcal{G} := (\mathcal{V}, \mathcal{E})$, where $\mathcal{V}$ is the vertex set and $\mathcal{E}$ is the edge set. The **vertex set** $\mathcal{V}$ refers to the indices labelling the sites in the system and a subset of this set $X \subset \mathcal{V}$ is defined as a subsystem. The **edge set** $\mathcal{E}$ refers to all the subsystems X which have associated a Hamiltonian term H_X with support[2] $\mathrm{supp}(H_X) = X$ that couples all the sites in X. The Hilbert space $\mathcal{H}$ of the system is equal to the tensor product of the individual Hilbert spaces $\mathcal{H}_x$ for the sites $x \in \mathcal{V}$, that is, $\mathcal{H} = \bigotimes_{x \in \mathcal{V}} \mathcal{H}_x$.

Regarding the Hamiltonian, any locally interacting quantum system is characterized by a **local Hamiltonian**, defined as a sum of local[3] Hamiltonians on the subsystems

---

[2]The support of an operator is the smallest subsystem where the operator acts non-trivially.

[3]A local observable has a support that is independent of the system or small compared to it.

$X \in \mathcal{E}$ and expressed as

$$H = \sum_{X \in \mathcal{E}} H_X. \tag{2.14}$$

Another important concept is the **graph distance** $\mathrm{dist}(X, Y)$, which is defined for any two subsystems $X, Y \subset \mathcal{V}$ as the size[4] of the smallest subsystem of $\mathcal{E}$ that connects X and Y, which is zero if only if the subsystems overlap. The graph distance can also be defined for operators such that for any two operators A, B it is equal to the graph distance between their supports, that is, $\mathrm{dist}(A, B) := \mathrm{dist}(\mathrm{supp}(A), \mathrm{supp}(B))$.

2.2.2. Fermionic and bosonic systems

In the following, we describe locally interacting fermionic and bosonic systems. The Hilbert space of these systems can be represented as a tensor product of each individual Hilbert space of the fermionic or bosonic sites. In particular, for fermions each individual Hilbert space $\mathcal{H}^f_{\{x\}} = \mathbb{C}^2$ with orthonormal basis $((|n\rangle_f)^1_{n=0}$, and for bosons $\mathcal{H}^b_{\{x\}} = \ell^2$, the Hilbert space of square-summable sequences[5], with orthonormal basis $(|n\rangle_b)^\infty_{n=0}$. Nonetheless, the full Hilbert space is more conveniently represented by the Fock layer, which is characterized by a number of sites M and a total particle number N. The **Fock layer** represents the span of the orthonormal **Fock states** $|n_1, \dots, n_M\rangle$ satisfying that $\sum_{x \in [0, M]} n_x = N$, where the particle number $n_x \in \{0, 1\}$ for fermions or $n_x \in [0, N]$ for bosons. The Hilbert space corresponds then to the **Fock space**, defined as the direct sum of the Fock layers for each possible total particle number N. The Fock space for fermions is finite dimensional, as $N \leq M$ due to the Pauli exclusion principle[6]. For bosons, however, the Fock space is infinite, since N is independent of M in this case.

In this scenario, any operator is defined in terms of the so-called **fermionic and bosonic operators** (single-site operators). There are two types of these operators, the **annihilation operators** f_x (fermionic) and b_x (bosonic), which annihilate a particle on site x, and the **creation operators** $f^\dagger_x$ and $b^\dagger_x$, which create a particle instead. More formally, they act on the Fock states $|\overrightarrow{n}\rangle := |n_1, \dots, n_M\rangle$ in the following way

$$f_x|\overrightarrow{n}\rangle_f = (-1)^{\theta_x} n_x |\overrightarrow{n_x - 1}\rangle_f, \qquad f^\dagger_x|\overrightarrow{n}\rangle_f = (-1)^{\theta_x}(1 - n_x)|\overrightarrow{n_x + 1}\rangle_f, \tag{2.15}$$

$$b_x|\overrightarrow{n}\rangle_b = \sqrt{n_x}|\overrightarrow{n_x - 1}\rangle_b, \quad \text{and} \quad b^\dagger_x|\overrightarrow{n}\rangle_b = \sqrt{n_x + 1}|\overrightarrow{n_x + 1}\rangle_b. \tag{2.16}$$

---

[4]The size of a subsystem is equal to the number of sites included in it.

[5]By definition, the elements of the space of square-summable sequences have finite norm.

[6]The Pauli exclusion principle implies that two or more identical fermions cannot occupy the same position simultaneously

where $\theta_x := \sum_{y=1}^{x-1} n_y$, $|\overrightarrow{n_x - 1}\rangle := |n_1, \ldots, n_{x-1}, n_x - 1, n_{x+1}, \ldots, n_M\rangle$, and $|\overrightarrow{n_x + 1}\rangle := |n_1, \ldots, n_{x-1}, n_x + 1, n_{x+1}, \ldots, n_M\rangle$. Moreover, they satisfy the commutation relations

$$\{f_x, f_y\} = \{f_x^\dagger, f_y^\dagger\} = 0, \qquad\qquad \{f_x, f_y^\dagger\} = \delta_{x,y}, \qquad (2.17)$$

$$[b_x, b_y] = [b_x^\dagger, b_y^\dagger] = 0, \qquad\qquad [b_x, b_y^\dagger] = \delta_{x,y}, \qquad (2.18)$$

where for any two operators $A, B \in \mathcal{B}(\mathcal{H})$, $[A, B] := A\,B - B\,A$ is the **commutator** and $\{A, B\} := A\,B + B\,A$ the **anti-commutator**.

Another important restriction for fermionic systems is that all the physical observables, Hamiltonians and density matrices of these systems are even[7] polynomials in the fermionic operators, a condition imposed by the fermion number parity superselection rule [BCW09].

2.2.3. Short-range and long-range interactions

Let us consider a system with a Hilbert space $\mathcal{H}$ and a local Hamiltonian H (2.14), characterized by an interaction hypergraph $\mathcal{G} := (\mathcal{V}, \mathcal{E})$, with $\mathcal{V}$ the vertex set and $\mathcal{E}$ the edge set. In this setting, the interactions of the system are classified depending on how for any subsystem $X \subset \mathcal{V}$ the local interacting terms h_X behave with respect to the diameter[8] of X. In particular, they are divided into short-range ang long-range interacting systems:

- The **short-range interactions** can be divided into two types:

    - Finite-range interactions, which are only non-zero for subsystems whose diameter is upper-bounded by a given constant.

    - Exponentially decaying interactions that decay with the diameter of the subsystem.

    In these cases, the local interacting terms h_X satisfy that [HK06]

    $$\sum_{X \ni x,y} \|h_X\| \leq \lambda_0 \exp[-\mu \operatorname{dist}(x,y)] \quad \text{with} \quad \lambda_0, \mu > 0. \qquad (2.19)$$

- The **long-range interactions** are stronger than short-range interactions and, thus, violate the inequality (2.19). In particular, we will study interactions decaying as a power-law with the diameter of the subsystem. In a formal way,

---

[7] An even/odd polynomial of fermionic operators refers to a linear combination of odd/even monomials of these operators.

[8] The diameter of a subsystem is the longest graph distance between any two sites in it.

these interactions are defined by local interacting terms h_X that verify [HK06]

$$\sum_{X \ni x,y} \|h_X\| \leq \frac{\lambda_0}{[1 + \text{dist}(x,y)]^\eta} \quad \text{with} \quad \lambda_0, \eta > 0. \tag{2.20}$$

2.2.4. Canonical, micro-canonical and grand-canonical quantum states

In the following, we define different types of quantum states for a system with a Hamiltonian H, each being a quantum analogous to the known statistical canonical, micro-canonical and grand-canonical ensembles:

- The **canonical quantum state** or **(quantum) thermal state** (also known as Gibbs state) of a system described by a Hamiltonian H at inverse temperature β is defined as

$$\Omega_\beta[H] := \frac{e^{-\beta H}}{Z_\beta[H]} \in \mathcal{S}(\mathcal{H}), \tag{2.21}$$

where $Z_\beta[H]$ is the canonical partition function given by $Z_\beta[H] := \text{tr}(e^{-\beta H})$, $\beta = 1/k_B T$ and k_B is the Boltzmann constant.

- The **micro-canonical quantum state** of the system for an energy interval $[E, E + \Delta]$ is defined as

$$\Omega_{\{E,\Delta\}}[H] := \frac{\sum_{k \in \zeta(E,\Delta)} |E_k\rangle\langle E_k|}{Z_{E,\Delta}[H]}, \tag{2.22}$$

where $\zeta(E, \Delta) := \{k : E_k \in [E, E + \Delta]\}$ and $Z_{E,\Delta}[H]$ is the micro-canonical partition function defined as $Z_{E,\Delta}[H] := \text{tr}(\sum_{k \in \zeta(E,\Delta)} |E_k\rangle\langle E_k|)$.

- The **grand-canonical quantum state** of the system with a total particle number N, and at inverse temperature β and chemical potential μ, is given by

$$\Omega_{\{\beta,\mu\}}[H] := \frac{e^{-\beta H + \mu N}}{Z_{\beta,\mu}}, \tag{2.23}$$

where $Z_{\beta,\mu}[H]$ is the grand-canonical partition function defined as $Z_{\beta,\mu}[H] := \text{tr}(e^{-\beta H + \mu N})$.

An important property of the thermal state is that it is the unique quantum state that maximises the von Neumann entropy

$$S(\rho) := -\text{tr}(\rho \log_2 \rho) \tag{2.24}$$

for a given expectation value of the Hamiltonian [Thi02]. The micro-canonical and grand-canonical states also maximise the entropy given a certain set of conditions for each case. In particular, the micro-canonical state maximises the entropy in a space spanned by the eigenvalues $|E_k\rangle$ with energy $E_k \in [E, E + \Delta]$ for some E and Δ. On the other hand, the grand-canonical state maximises it for given expectation values of the Hamiltonian H and the particle number N. Another relevant property is that canonical and micro-canonical states do not evolve in time, since they are defined in terms of the energy projectors $\Pi_k := |E_k\rangle\langle E_k|$.

2.2.5. Locality of temperature

The problem of locality of temperature aims to study whether it is possible to locally assign a temperature to a subsystem embedded in a system at thermal equilibrium at temperature T such that the local temperature is equal to the global temperature T. The general setting of this problem is given by a lattice system with a local Hamiltonian H (2.14) and at a thermal state at some temperature T (2.21). If the interactions are weak enough, the global thermal state can be well-approximated by a product state of thermal states, each acting on non-overlapping subsystems of the whole. It is said then that the temperature is locally well defined as each subsystem is at a thermal state. However, this is not usually the case since the interactions are generally strong and, thus, it is unclear how one can assign a temperature to a subsystem. A concrete way to circumvent the problem was first proposed by Ferraro et al. [FGSA12], where they consider a locally interacting system (2.14) with a subsystem A, a shell region around it B and its environment $C = (A \cup B)^c$ (see Figure 2.1). In this setting, the problem can be tackled by studying the distinguishability between the partial state of the subsystem A and the partial state of an equivalent subsystem where the Hamiltonian is now truncated, that is, $H_0 = H_C \otimes H_{AB}$ (see Fig. 3.1). Given this, the temperature is said to be local if the distinguishability between the states is negligible for a width L_B of the boundary region B that is independent of the total system size L_{ABC}.
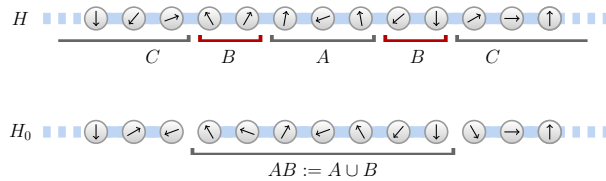
Figure 2.1.: Scheme of the subsystem of interest A, the boundary region B, and their environment C for a spin chain.

2.2.6. Lieb-Robinson bounds

The **Lieb-Robinson bound** is an expression that characterizes the propagation of information in quantum lattice systems described by a local Hamiltonian (2.14) with short-range interactions (2.19). In particular, for any two operators A, B with support X, Y, respectively, the bound [LR72] is as follows

$$\|[A_X(t), B_Y]\| \leq C|X||Y|\|A_X\|\|B_Y\|e^{v|t| - \mu \operatorname{dist}(X,Y)}, \qquad (2.25)$$

where the positive constants C, μ, v depend on the system. This bound implies that given a perturbation A on the lattice system, the effects on a measurement B at a distance $r := \operatorname{dist}(X, Y)$ are exponentially small for short times $t \leq t_{min} = r/v$, where t_{min} refers to the minimum time needed for detection and v corresponds to the maximum speed of propagation (see Figure 2.2). Therefore, the propagation of information in short-range systems is bounded by a linear function in time with a maximum speed v depending on the system.

For long-range interacting systems with polynomial decay (2.20), the most general bound [HK06] states that for any two operators A, B with supports X, Y, respectively, the following holds,

$$\|[A_X(t), B_Y]\| \leq C|X||Y|\|A_X\|\|B_Y\|\frac{e^{v|t|}}{\operatorname{dist}(X,Y)^\alpha}, \qquad (2.26)$$

where the positive constants C, α, v depend on the system. Following the previous detection-measurement setting, the minimum time $t_{min} \propto \log r$ (see Figure 2.2 for a 1D example).
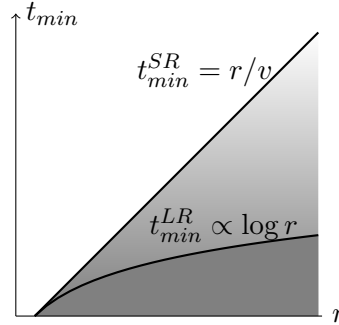
Figure 2.2.: Lower bounds on detection time t_{min} vs the distance r between the operators A, B. The curves defined by t_{min}^{SR} and t_{min}^{LR} refer to the short-range and long-range cases, respectively.

In comparison to short-range interactions, the spreading of information may be faster in long-range systems since it is not possible to define a maximum speed and the propagation is upper-bounded by a function that is exponentially increasing with time. However, this does not necessarily imply that propagation is faster in general for long-range interactions, as we have only access to upper bounds.

2.3. Quantum estimation theory

In this section, we focus on the basic elements of quantum estimation theory and explain its application to quantum thermometry.

2.3.1. Fundaments

Estimation theory is a field within statistics which aims to estimate the value of an unknown parameter from a set of experimental measurements of an estimator. There are two estimation approaches depending on the parameter: (i) the **frequentist approach** when the parameter is deterministic with a fixed value; and (ii) the **bayesian approach** when the parameter is a random variable itself with a range of possible values. In the following, we will focus on the frequentist approach for a single-parameter estimation, as we will only consider this case throughout the thesis.

Assuming a quantum system with a positive state ρ_θ with unit trace and parametrized by a single parameter $\theta \in \mathbb{R}$, quantum estimation theory aims to obtain a correct estimation of θ by making a large and independent number of quantum measurements on the state ρ_θ. Quantum measurements are described by a **positive operator valued measurement** (POVM), whose elements are positive operators $\{E_m\}$ which satisfy $\sum_m E_m = \mathbb{1}$. For a quantum state ρ, the measurement is described by probabilities $p_m(\theta) = \mathrm{tr}(\rho_\theta E_m)$, which refers to the probability of obtaining a measurement m. After repeating this measurement scenario a large number of times, we obtain an outcome dataset $\mathbf{x}$ that we eventually use with an estimator function to map the dataset to some estimate $\overline{\theta}$ of the parameter θ. Due to the randomness of the measurement outcomes, the estimation has an uncertainty which is characterized by the **quantum Cramér–Rao bound** [Cra99], that is,

$$\Delta\overline{\theta} \geq 1/\sqrt{\nu\mathcal{F}_\theta}, \tag{2.27}$$

which applies to unbiased estimators[9] and where $\Delta\overline{\theta}$ is the variance of the estimate

---

[9]Unbiased estimators always give on average the true parameter over all possible dataset $\mathbf{x}$: $\langle\overline{\theta}(\mathbf{x})\rangle_{\mathbf{x}} = \theta$.

$\bar{\theta}$, ν is the number of measurements and $\mathcal{F}_\theta$ is the quantum Fisher information (QFI) of the parameter θ. This expression (2.27) implies that the precision of the estimation increases with the number of measurements and the quantum Fisher information. The **quantum Fisher information** is a quantity that bounds how much information can be obtained about the unknown parameter θ [BC94] and it is given by

$$\mathcal{F}_\theta := -2 \lim_{\delta \to 0} \frac{\partial^2 F(\rho_\theta, \rho_{\theta+\delta})}{\partial \delta^2}, \tag{2.28}$$

where the fidelity $F(\rho_\theta, \rho_{\theta+\delta})$ is given by the expression (2.10) and is related to the **Bures distance** via the expression $D_B(\rho, \sigma) = \sqrt{2\left(1 - \sqrt{\mathrm{F}(\rho, \sigma)}\right)}$. The QFI can also be expressed in terms of the so-called symmetric logarithmic derivate (SLD) [MSC18] such that

$$\mathcal{F}_\theta = \mathrm{tr}(\rho_\theta \Lambda_\theta^2), \tag{2.29}$$

where the SLD is given by the self-adjoint operator Λ_θ, defined by

$$\Lambda_\theta \rho_\theta + \rho_\theta \Lambda_\theta = 2\partial_{\theta'} \rho_{\theta'}|_{\theta'=\theta}. \tag{2.30}$$

Moreover, the QFI characterizes the efficiency of the estimation protocol and allows two types of estimation error depending on its scaling with the number of measurements, the **Standard Quantum Limit** (SQL) and the **Heisenberg limit**. The SQL refers to the case where the QFI is independent of the number of measurements ν and the variance $\Delta\bar{\theta}$ scales with $1/\sqrt{\nu}$. On the other hand, the Heisenberg limit occurs when the QFI increases linearly with ν and the variance $\Delta\bar{\theta}$ scales with $1/\nu$.

2.3.2. Quantum thermometry

Quantum thermometry aims to measure the temperature of a system at thermal equilibrium at a given temperature T (2.21). The standard setting consists of two systems, a system at thermal equilibrium at temperature T and another system which acts as a measurement device, the probe system. The system and the probe are weakly interacting such that the probe can thermalise to the same temperature T. Notice here that the heat capacity[10] of the probe must be much smaller than the system's heat capacity, since this condition avoids perturbations on the system due to the probe and allows a proper thermalisation of the probe at temperature T. Once the probe thermalises, the temperature can be estimated by monitoring some temperature-dependent features of its steady state via a suitable measurement and data analysis scheme. As previously

---

[10]The heat capacity is a quantity that represents the ratio of change between heat (δQ) and temperature (dT): $\mathcal{C} = \delta Q/\mathrm{d}T$.

described, the uncertainty of the estimate is bounded by the quantum Cramér-Rao bound (2.27), decreasing with the number of measurements and the quantum Fisher information (QFI). The QFI is thus referred as the optimal thermal sensitivity, since the precision increases with it.

In order to give some intuition, let us consider an example of a probe described by a Hamiltonian $H := \sum_n \varepsilon_n |\varepsilon_n\rangle\langle\varepsilon_n|$. Assuming the probe has thermalised to the thermal state Ω_T (2.21), we can compute the SLD (2.30) via the expression for a thermal state [MSC18], that is,

$$\Lambda_T = \frac{\beta^2}{2}(H - \langle H \rangle). \tag{2.31}$$

Thus, we can obtain the QFI via the equation (2.29), such that

$$\mathcal{F}_\theta = \beta^4 \Delta H^2_{\rho_T} = \beta^2 \mathcal{C}_T, \tag{2.32}$$

where ΔH_{ρ_T} is the variance of the Hamiltonian at the state ρ_T and $\mathcal{C}_T$ refers to the heat capacity of the probe. Therefore, we observe that the thermal sensitivity of a probe at equilibrium is completely limited by its heat capacity. This phenomenon is typical in quantum thermometry.

2. Preliminaries

3. Locality of temperature for one-dimensional spin systems

In traditional thermodynamics, temperature is a local quantity, that is, a subsystem of a large thermal system is in a thermal state at the same temperature as the large system. For strongly interacting systems, however, the locality of temperature breaks down. We study the possibility of associating an effective thermal state to subsystems of chains of interacting spin particles with arbitrary finite dimension. We study the effect of correlations and criticality in the definition of this effective thermal state and discuss the possible implications for the classical simulation of thermal quantum systems.

3.1. Introduction

The question whether the standard notions of thermodynamics are still applicable in the quantum regime has experienced a renewed interest in recent years. This refreshed motivation can be explained as the consequence of two factors. On the one hand, the progress on experimental techniques allows for a direct observation of thermodynamic phenomena in many different quantum systems, such as ultra-cold atoms in optical lattices, ion traps, superconductor qubits, etc [BDN12, PSSV11, KRJP13, SBM$^+$11]. On the other hand, the inflow of ideas from quantum information theory provided significant insight into the thermodynamics of quantum systems [MNV09, PSW06, HO13, dRrR$^+$11]. Specifically, qualitative improvements have been made in understanding how the methods of statistical mechanics can be justified from quantum mechanics as its underlying theory [PSW06, GLTZ06, GMM04, PSSV11, SF12, BC15].

One of the fundamental postulates of thermodynamics is the so called Zeroth Law: two bodies, each in thermodynamic equilibrium with a third system, are in equilibrium with each other [Rei98, Bal07]. This law stands behind the notion of temperature [Rei98, Bal07]. In fact, the above formulation of the Zeroth law consists of three parts: (i) there exists a thermal equilibrium state which is characterized by a single parameter called temperature, and isolated systems tend to this state [PSSV11, PSW06, GLTZ06,

GMM04]; (ii) the temperature is local, namely, each part of the whole is in a thermal state [Rei98, Bal07]; and (iii) the temperature is an intensive quantity: if the whole is in equilibrium, all the parts have the same temperature [Rei98, Bal07, FGSA12, GSFA09, KGK$^+$14, PTZB14]. The last two points are usually derived from statistical mechanics under the assumption of weakly interacting systems. Nevertheless, when the interactions present in the system are non negligible, the points (ii) and (iii) need to be revised. Following the direction given by Refs. [FGSA12, GSFA09], in this work we concentrate on the clarification and generalization of the aforementioned aspects of the Zeroth Law of the thermodynamics for spin chains with strong, short-range interactions.

The general setting of the problem is as follows. The system with Hamiltonian H is in thermal equilibrium, given by a canonical state at inverse temperature β (2.21),

$$\Omega_\beta[H] = \frac{\mathrm{e}^{-\beta H}}{\mathrm{tr}\left(\mathrm{e}^{-\beta H}\right)}, \tag{3.1}$$

and we seek to understand the thermal properties of a finite part of the system.

Obviously, in the presence of strong interactions, the reduced density matrix of a subsystem of the global system will not generally have the same form as (3.1). In systems where the Hamiltonian is a sum of local terms interacting according to some underlying graph, it is unclear how one can locally assign temperature to a subsystem. More precisely, the reduced density matrix of the subsystem A (see Figure 3.1) of a global thermal state is described by

$$\rho_A = \mathrm{tr}_{\bar{A}}(\Omega_\beta[H]), \tag{3.2}$$

which will not be thermal unless the particles in A do not interact with its environment $\bar{A}$. Hence, given only a subsystem state ρ_A and its Hamiltonian H_A, it is not possible to assign a temperature to it, since this would totally depend on the features of the environment and the interactions that couple the subsystem to it.

In the context of quantum information, a first step to circumvent the problem of assigning temperature to a subsystem was made in Ref. [FGSA12] where for harmonic lattices it was shown that it is sufficient to extend the subsystem A with a boundary region B that when traced out disregards the correlations and the boundary effects (see Figure 3.1). If the size of such a boundary region is independent of the total system size, temperature can still be said to be local.

More explicitly, given a lattice Hamiltonian H with a subsystem A, a shell region around it B and its environment $C = (A \cup B)^c$, see Figure 3.1, we aim to understand how the expectation values of operators that act non-trivially only on A for the global
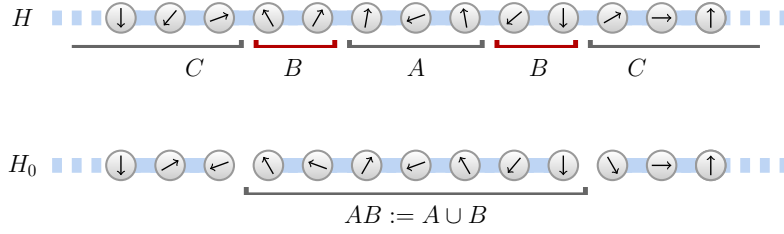
Figure 3.1.: Scheme of the subsystem of interest A, the boundary region B, and their environment C for a spin chain. Expectation values on A for the thermal state of the full Hamiltonian H (above) are expected to be approximated by expectation values for thermal state of the truncated Hamiltonian H_{AB} (below) if the boundary region B is sufficiently large.

thermal state $\Omega_\beta[H]$ differ from those taken for the thermal state of the truncated Hamiltonian H_{AB} (with $AB = A \cup B$) as the width ℓ_B of the boundary region B increases:

$$\left| \mathrm{tr}\left(O\,\rho_A\right) - \mathrm{tr}\left(O\,\rho'_A\right) \right| \leq ||O||_\infty f(\ell_B), \tag{3.3}$$

where $\rho'_A = \mathrm{tr}_B \Omega_\beta[H_{AB}]$ is the state of A for the chain truncated to AB, and $f(\ell_B)$ is expected to be a monotonically decreasing function in ℓ_B. The width of the boundary region ℓ_B is defined as the graph-distance between the sets of vertices (regions) A and C.

Surely, the differences (3.3) fully characterize the distance of ρ_A from ρ'_A. Indeed, the trace distance (2.8), $\mathcal{D}(\rho_A, \rho'_A) = \frac{1}{2}||\rho_A - \rho'_A||_1$, has the following representation (2.9):

$$\mathcal{D}(\rho_A, \rho'_A) = \max_{0<O<I} \mathrm{tr}\left(O(\rho_A - \rho'_A)\right) \leq f(\ell_B), \tag{3.4}$$

where I is the identity operator in the Hilbert space of A.

In Ref. [KGK$^+$14], it is proven that the correlations responsible for the distinguishability between the truncated and non-truncated thermal states are quantified by a generalized covariance. For any two operators O and O', full-rank quantum state ρ, and parameter $\tau \in [0, 1]$, the generalized covariance is defined as

$$\mathrm{cov}_\rho^\tau(O, O') := \mathrm{tr}\left(\rho^\tau O \rho^{1-\tau} O'\right) - \mathrm{tr}(\rho O)\mathrm{tr}(\rho O'), \tag{3.5}$$

and the difference between expectation values of some observable O for the truncated and non-truncated thermal states reads as

$$\mathrm{tr}\left(O\,\Omega_\beta[H_{AB}]\right) - \mathrm{tr}\left(O\,\Omega_\beta[H]\right) = 2\int_0^1 \mathrm{d}s \int_0^{\beta/2} \mathrm{d}t\, \mathrm{cov}_{\Omega_s}^{t/\beta}(H_I, O), \tag{3.6}$$

25

where H_I is the corresponding Hamiltonian term that couples B and C, $H_{AB} = H - H_I$ is the truncated Hamiltonian (see Figure 3.1) and $\Omega_s = \Omega_\beta[H_s]$ is the thermal state of the interpolating Hamiltonian $H_s := H - (1-s) H_I$. Hence, the generalized covariance is the quantity that measures the response in a local operator of perturbing a thermal state and ultimately at what length scales temperature can be defined.

Temperature is known to be a local quantity in a high temperature regime. More specifically, in Ref. [KGK$^+$14], it is shown that for any local Hamiltonian there is a threshold temperature (that only depends on the connectivity of the underlying graph) above which the generalized covariance decays exponentially. Nevertheless, it is far from clear what occurs below the threshold, and, especially, at low temperatures ($\beta \gg 1$). Note that, in that case, the right hand side of the truncation formula (3.6) could be significantly different from zero since the integration runs up until $\beta/2$, while the covariance is expected to decay only algebraically for critical systems.

In this chapter we show that, for one-dimensional translationally-invariant systems with short-range interactions, temperature is local for any β. Away from criticality, we rigorously bound the truncation formula (3.6) by mapping the generalized covariance to the contraction of a tensor network and exploiting some standard results in condensed matter. At criticality, we use some results from conformal field theory [DFMS97, Car06]. Finally, the results in [MAMW15], where the equivalence of microcanonical and canonical ensembles is proven for translation-invariant lattices with short-range interactions, render our results valid also when, instead of being canonical, (3.1), the global state $\Omega_\beta[H]$ is, e.g., microcanonical.

3.2. Tensor network representation of the generalized covariance

We start by representing the generalized covariance (3.5) as a tensor network contraction for a spin system with short-range interactions.

3.2.1. Mapping the partition function of a D-dimensional quantum model to the contraction of a tensor network of $D + 1$ dimensions

Let us consider a system of spins described by a short-range Hamiltonian. The structure of the Hamiltonian is given by a graph $G(V, E)$. The spins correspond to the set of vertices V and the two-body interactions to the edges E. Such a Hamiltonian (2.14)

Figure 3.2.: Diagrammatic representation of a) the operator $\mathrm{e}^{-\beta H}$ with H the Hamiltonian of a spin chain, b) its decomposition $\left(\exp(-\beta/mH)\right)^m$, c) the tensor network that approximates $\mathrm{e}^{-\beta H}$ after performing the Trotter-Suzuki decomposition for a one-dimensional short-ranged Hamiltonian and (d) the same tensor network after a convenient arrangement of the tensors. We use the Penrose notation: tensors are represented as geometric shapes, open legs represent their indices and legs connecting different tensors encode their contraction over the corresponding indices.

can be written as

$$H = \sum_{u \in E} h_u \tag{3.7}$$

where h_u are the Hamiltonian terms acting non-trivially on the adjacent vertices of u. For simplicity, the energy units are taken such that $\|h_u\|_\infty \le 1$ with $\|\cdot\|_\infty$ the operator norm.

In Ref. [Has06, MSVC14], it is shown that, for any error $\delta > 0$, the matrix $\mathrm{e}^{-\beta H}$ of a local Hamiltonian can be approximated in one norm by its Trotter-Suzuki expansion,

$$\tilde{\rho}_{TN} = \left(\left(\prod_{u \in E} \mathrm{e}^{-\frac{\beta}{2m}h_u} \right) \left(\prod_{v \in E} \mathrm{e}^{-\frac{\beta}{2m}h_v} \right)^\dagger \right)^m, \tag{3.8}$$

such that

$$\left\| \mathrm{e}^{-\beta H} - \tilde{\rho}_{TN} \right\|_1 \le \delta \left\| \mathrm{e}^{-\beta H} \right\|_1, \tag{3.9}$$

where $m > 360\beta^2|E|^2/\delta$ and the products over u and v in Equation (3.8) are realized in the same order.

To illustrate the previous approximation, let us consider in detail the one-dimensional case: a spin chain with the nearest neighbour interactions. By decomposing in the

standard way the Hamiltonian in its odd and even terms, the tensor network $\tilde{\rho}_{TN}$ becomes in this case

$$\tilde{\rho}_{TN} = \left(e^{-\frac{\beta}{2m} H_{\text{odd}}} e^{-\frac{\beta}{m} H_{\text{even}}} e^{-\frac{\beta}{2m} H_{\text{odd}}} \right)^m , \tag{3.10}$$

where $H_{\text{odd/even}} = \sum_{u \in \text{odd/even}} h_u$ and $H = H_{\text{odd}} + H_{\text{even}}$.

Let us think about each $\exp(\beta/m h_u)$ as a tensor. In this way, $\tilde{\rho}_{TN}$ can be seen as the contraction of several of such tensors, that is, a tensor network (see c) in Figure 3.2). Starting from a one-dimensional quantum system, $\tilde{\rho}_{TN}$ can be interpreted as a tensor network spanning two dimensions, with the extra dimension of length m. We will refer to this extra dimension as the β direction, while the original dimension will be called spatial direction.

In Figure 3.2 a), the diagrammatic representation of $\tilde{\rho}_{TN}$ is presented. Its tensors can be decomposed and arranged in order to form a square lattice of elementary tensors as shown in Figure 3.2 b).

3.2.2. Generalized covariance as the contraction of tensor networks

The expectation value of a local operator is given by

$$\langle O \rangle = \text{tr}(O\,\Omega_\beta[H]) = \frac{\text{tr}(O\,e^{-\beta H})}{\text{tr}(e^{-\beta H})} . \tag{3.11}$$

By using Equation (3.9), the fact that $\left\| e^{-\beta H} \right\|_1 = \text{tr}(e^{-\beta H})$ and some elementary algebra, the expectation value of a local operator A can be approximated by the ratio between the contraction of two tensor networks

$$\left| \langle O \rangle - \frac{\text{tr}(O\tilde{\rho}_{TN})}{\text{tr}(\tilde{\rho}_{TN})} \right| \leq 2 \left\| O \right\|_\infty \delta . \tag{3.12}$$

This is represented diagrammatically in a) in Figure 3.3.

The generalized covariance can be rewritten as

$$\text{cov}^\tau_{\Omega_s}(O, O') = \frac{\text{tr}\left(\tilde{O} e^{-\tau \beta H} \tilde{O}' e^{-(1-\tau)\beta H} \right)}{\text{tr}\left(e^{-\beta H} \right)} , \tag{3.13}$$
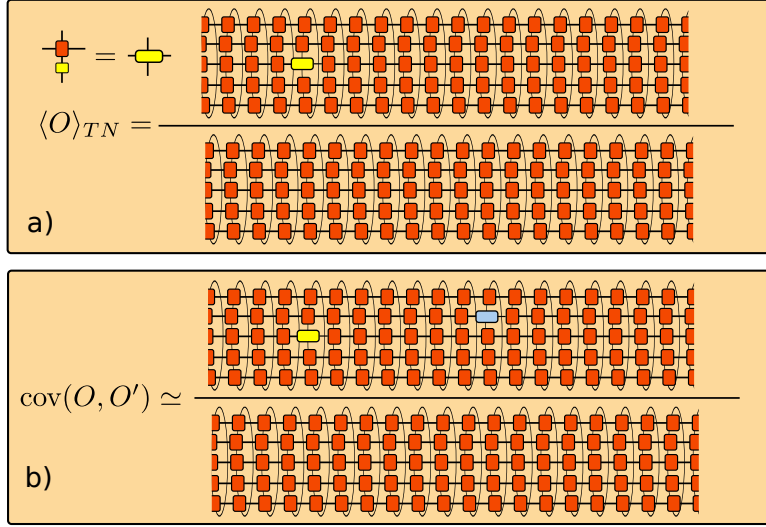
Figure 3.3.: Diagrammatic representation of a) the expectation value of a one site operator and b) the generalized covariance (a two-point correlation function) between two one site operators. In both cases, the final result is computed as the ratio between the contraction of two tensor networks.

where $\tilde{O} = O - \text{tr}(O\,\Omega_\beta[H])$ for any operator O. Hence, in a similar way as it has been made for the expectation values, the generalized covariance can be also approximated as the ratio between two tensor network contractions as shown in b) in Figure 3.3

$$\left| \text{cov}^\tau_{\Omega_s}(O, O') - \frac{\text{tr}(\tilde{O}\tilde{\rho}^\tau_{TN}\tilde{O}'\rho^{(1-\tau)}_{TN})}{\text{tr}(\tilde{\rho}_{TN})} \right| \leq 2 \left\| O \right\|_\infty \left\| O' \right\|_\infty \delta. \qquad (3.14)$$

From this perspective, the generalized covariance can be seen as a two point correlation function on a 2-dimensional lattice in which τm is the separation in the β direction and the distance between the non-trivial supports of O and O' is the separation in the spatial direction (see Figure 3.3).

This construction can be generalized to approximate expectation values of local operators and n-point correlation functions of a D dimensional quantum model by the the ratio of the contraction of two $D + 1$ dimensional tensor networks.

3.2.3. Transfer matrices

It is also very useful to define two extra objects: the transfer matrices along the spatial T and β directions T_β. The first is obtained by contracting a column of the elementary tensors of the network, while the second is obtained by contracting several rows of elementary tensors.

The number of rows that need to be contracted in order to obtain the transfer matrix in the β direction is chosen such that the gap of T_β is independent of both β and m. This can be achieved by contracting m/β rows, leading to a transfer matrix with two largest eigenvalues λ_1 and λ_2

$$\frac{\lambda_2}{\lambda_1} = \mathrm{e}^{-\Delta} \tag{3.15}$$

where Δ is the gap of the Hamiltonian. Both matrices are represented in Figure 3.4.

3.3. Locality of temperature at non-zero temperature

Let us consider now the case in which β is of order one. The physical distinguishability in A between the full and the truncated Hamiltonians can be bounded by

$$\mathrm{tr}\left(O\,\Omega[H_{AB}]\right) - \mathrm{tr}\left(O\,\Omega_\beta[H]\right) \leq \beta \max_{s\in[0,1]} \max_{\tau\in[0,1]} \mathrm{cov}_{\Omega_s}^\tau(H_I, O). \tag{3.16}$$

In order to bound the generalized covariance, let us rewrite it as a 3-point correlation function

$$\mathrm{cov}_{\Omega_s}^\tau(H_I, O) = \frac{\langle 1_L | X T^\ell Y T^\ell X | 1_R \rangle}{\langle 1_L | T_s T^{2\ell+1} T_s | 1_R \rangle} - \frac{\langle 1_L | T_s T^\ell Y T^\ell T_s | 1_R \rangle}{\langle 1_L | T_s T^{2\ell+1} T_s | 1_R \rangle} \frac{\langle 1_L | X T^{2\ell+1} X | 1_R \rangle}{\langle 1_L | T_s T^{2\ell+1} T_s | 1_R \rangle} \tag{3.17}$$

where T is the transfer matrix in the spatial direction, see Figure 3.4 (left), and $|1_{L/R}\rangle$ is the left/right dominant eigenvector of T i. e. the eigenvector associated to its largest eigenvalue. The matrix T_s is the transfer matrix corresponding to the boundaries BC where the elementary tensors of the network are different from the rest for $s \neq 1$. The matrix Y corresponds to the slice of the region A where the operator O is supported, and the matrix X is the transfer matrix T_s with the insertion of the operators H_I located at a distance $\tau\beta$ from O in the transverse direction.

To bound the generalized covariance (3.17) it is useful to rewrite it in terms of local expectation values, and 2-point and 3-point correlation functions of the uniform

Figure 3.4.: Diagrammatic representation of the transfer matrix in the spatial direction (left) and the β direction (right).

system with transfer matrix T

$$
\begin{aligned}
\text{cov}_{\Omega_s}^{\tau}(H_I, O) &= \frac{\langle X \rangle_T^2 + \text{cov}_2(2\ell + 1; T, X, X)}{\left(\langle T_s \rangle_T^2 + \text{cov}_2(2\ell + 1; T, T_s, T_s) \right)^2} \text{cov}_3(\ell; T_s, Y) \\
&+ \frac{\text{cov}_3(\ell; X, Y)}{\langle T_s \rangle_T^2 + \text{cov}_2(2\ell + 1; T, T_s, T_s)}
\end{aligned}
\tag{3.18}
$$

where

$$
\langle X \rangle_T := \frac{\langle 1_L | X | 1_R \rangle}{\langle 1_L | T | 1_R \rangle},
\tag{3.19}
$$

$$
\text{cov}_2(\ell; T, X, Y) := \frac{\langle 1_L | X T^{\ell} Y | 1_R \rangle}{\langle 1_L | T^{2\ell_B + 3} | 1_R \rangle} - \langle X \rangle_T \langle Y \rangle_T,
\tag{3.20}
$$

$$
\text{cov}_3(\ell; T, X, Y) := \frac{\langle 1_L | X T^{\ell} Y T^{\ell} X | 1_R \rangle}{\langle 1_L | T^{2\ell_B + 3} | 1_R \rangle} - \frac{\langle 1_L | X T^{2\ell+1} X | 1_R \rangle}{\langle 1_L | T^{2\ell+3} | 1_R \rangle} \langle Y \rangle_T.
\tag{3.21}
$$

In short-range one-dimensional systems, the absence of phase transitions at non-zero temperature certifies that the transfer matrix T is gapped, with a gap related to the spatial correlation length as

$$
\xi := - \left(\ln |\lambda_2| \right)^{-1} > 0,
\tag{3.22}
$$

where λ_2 is the second largest eigenvalue of the transfer matrix T.

The 3-point correlation function can be proven to be upper-bounded by

$$
\begin{aligned}
|\text{cov}_3(\ell; X, Y, T)| &\leq 2 \|Y\|_{\infty} \sigma_L(X^{\dagger}) \sigma_R(X) / \|T\|_{\infty}^3 e^{-2\ell/\xi} \\
&+ \langle X \rangle_T \left(\sigma_L(X^{\dagger}) \sigma_R(Y) + \sigma_L(Y^{\dagger}) \sigma_R(X) \right) e^{-\ell/\xi}
\end{aligned}
\tag{3.23}
$$

where $\| \cdot \|_{\infty}$ is the operator norm, and $\sigma_{L/R}(O) = \left\| \left(O - \langle 1_L | O | 1_R \rangle \right) | 1_{L/R} \rangle \right\|$ can be interpreted as the fluctuations of the operator O for the state $|1_{L/R}\rangle$. The complete

proof of the previous statement can be found in the Appendix A.1, in particular, in Lemma 5.

Equation (3.6) can then be upper-bounded by

$$\operatorname{tr}\left(O\,\Omega_\beta[H_{AB}]\right) - \operatorname{tr}\left(O\,\Omega_\beta[H]\right) \leq 3\beta^2 \mathrm{e}\|O\|_\infty e^{-\ell_B/\xi} \tag{3.24}$$

where we have used that $\|Y\|_\infty \leq \beta\mathrm{e}\,\|O\|_\infty$, $\sigma_{L/R}(X) \leq 1$, $\sigma_{L/R}(Y) \leq \|O\|_\infty$ and $\langle 1_L|X|1_R\rangle \leq \beta\mathrm{e}$. This means that the difference between expectation values of the operator O for the truncated and the full Hamiltonians is upper-bounded by a function that decays exponentially with the boundary length l_B, that is, the trucanted Hamiltonian H_{AB} offers a good approximation for the expectation value if the length l_B is large enough. Note that the above argument only works for a finite β.

3.4. Zero temperature

We consider the case at zero-temperature and distinguish between two situations: when the Hamiltonian of the system is gapped (gapped system), and when it is gapless and the system undergoes a quantum phase transition, i.e, it is at the criticality point.

3.4.1. Gapped systems

Given a Hamiltonian with gap Δ, here we study the regime in which $\beta^{-1} \ll \Delta$. This implies that the lattice in its β direction is much larger than the correlation length

$$\xi_\beta = \left(\ln\left(\frac{\lambda_1}{\lambda_2}\right)\right)^{-1} = \Delta^{-1}. \tag{3.25}$$

In the limit of temperature tending to zero, the 2D network that represents the partition function becomes infinite in the β direction (see Figure 3.5).

In order to see that the temperature is also local in this case, let us decompose the integral over t of the generalized covariance into two pieces

$$\begin{aligned}
\operatorname{tr}\left(O\,\Omega_\beta[H_{AB}]\right) \quad - \quad \operatorname{tr}\left(O\,\Omega_\beta[H]\right) &= 2\int_0^{\beta/2} \mathrm{d}t\, \operatorname{cov}_{\Omega_s}^{t/\beta}(H_I, O) \\
&= 2\int_0^L \mathrm{d}t\, \operatorname{cov}_{\Omega_s}^{t/\beta}(H_I, O) + 2\int_L^{\beta/2} \mathrm{d}t\, \operatorname{cov}_{\Omega_s}^{t/\beta}(H_I, O) \quad (3.26)
\end{aligned}$$
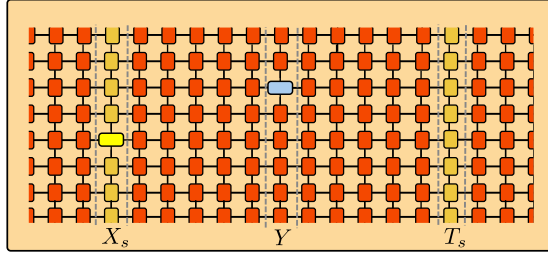
Figure 3.5.: Diagrammatic representation of a 3-point correlation function for a system at zero temperature. The network is infinite in both directions.

where L is a cut-off that will be chosen afterwards to minimize a bound on the right hand side, and β will be made to tend to infinity.

Concerning the integral over $0 \leq t \leq L$, we will exploit the fact that the system is gapped, and hence its ground state is known to have a finite correlation length ξ in the spatial direction and to be represented by a Matrix Product State of bond dimension D, with $D \propto \text{poly}(\xi)$ [VC06, PGVWC07, PVVT12]. As argued in the previous section, a finite correlation length guarantees a gap in the transfer matrix in the corresponding direction. By performing an analogous calculation to the one described in the previous section, one obtains

$$\int_0^L \mathrm{d}t\, \text{cov}_{\Omega_s}^{t/\beta}(H_I, O) \leq \frac{3}{2}\mathrm{e}L^2 D^2 \|O\|_\infty e^{-\ell_B/\xi} \,. \tag{3.27}$$

The second integral over $t > L$ can be bounded by taking the transfer matrix in the β direction which is also gapped for gapped Hamiltonians. More specifically, the generalized covariance can be written as

$$\text{cov}_{\Omega_s}^{t/\beta}(H_I, O) = \frac{\langle GS|OT_\beta^t H_I|GS\rangle}{\langle GS|T_\beta^t|GS\rangle} - \frac{\langle GS|OT_\beta^t|GS\rangle}{\langle GS|T_\beta^t|GS\rangle}\frac{\langle GS|T_\beta^t H_I|GS\rangle}{\langle GS|T_\beta^t|GS\rangle} \,. \tag{3.28}$$

where we have identified T_β as the transfer matrix for which the ground state of the Hamiltonian $|GS\rangle$ is its dominant eigenvector. In Lemma 4 in the Appendix A.1, such covariance is proven to decay exponentially in ℓ_B, leading to

$$\left|\text{cov}_{\Omega_s}^{t/\beta}(H_I, O)\right| \leq \|O\|_\infty \|H_I\|_\infty \mathrm{e}^{-t/\xi_\beta} \leq \|O\|_\infty \mathrm{e}^{-t/\xi_\beta} \,. \tag{3.29}$$

The integration is then bounded by

$$\lim_{\beta \to \infty} \int_L^{\beta/2} \mathrm{d}t\, \text{cov}_{\Omega_s}^{t/\beta}(H_I, O) \leq \xi_\beta \|O\|_\infty e^{-L/\xi_\beta} \,. \tag{3.30}$$

Let us mention that although the statement of Lemma 4, that a gapped transfer matrix implies an exponential decay of the correlations, is common knowledge in condensed matter, we didn't find an explicit proof of it elsewhere. For that reason, this result is presented in the form of a Lemma in the Appendix.

Putting the previous bounds together, and after an optimization over L and a maximization over s, we get

$$\mathrm{tr}\left(O\,\Omega_\beta[H_{AB}]\right) - \mathrm{tr}\left(O\,\Omega_\beta[H]\right) \le \frac{3}{2}\mathrm{e}D^2\|O\|_\infty L_o\left(L_o + 2\xi_\beta\right)\mathrm{e}^{-\ell_B/\xi}, \quad (3.31)$$

where L_o is the optimal value of L and corresponds to the solution of the equation $3/2\mathrm{e}D^2 L_o\mathrm{e}^{-\ell_B/\xi} = \mathrm{e}^{-L_o/\xi_\beta}$. For large ℓ_B, the previous bound becomes

$$\mathrm{tr}\left(O\,\Omega_\beta[H_{AB}]\right) - \mathrm{tr}\left(O\,\Omega_\beta[H]\right) \le \frac{3\mathrm{e}}{2}D^2\|O\|_\infty\left(\frac{\xi_\beta}{\xi}\ell_B\right)^2\mathrm{e}^{-\ell_B/\xi}, \quad (3.32)$$

showing that temperature can be locally assigned to subsystems for arbitrarily large β and gapped Hamiltonians.

3.4.2. Criticality

A system at zero temperature is said to be critical when the gap between the energy ground state (space) and the first excited state closes to zero in the thermodynamic limit. The critical exponents z and ν control how the gap Δ tends to zero

$$\Delta \propto n^{-z\,\nu}, \quad (3.33)$$

where ν is the critical exponent that controls the divergence of the correlation length

$$\xi \propto n^\nu. \quad (3.34)$$

The previous divergences are a signature of the scale invariance that the system experiences at criticality. If the critical exponent $z = 1$, there is a further symmetry enhancement and the system becomes conformal invariant. The group of conformal transformations includes, in addition to scale transformations, translations and rotations.

In 1+1 dimensions, conformal symmetry completely dictates how correlation functions behave and how local expectation values of local observables of infinite systems differ from those taken for finite ones. Hence, conformal field theory establishes that

$$\mathrm{tr}\left(O\,\Omega_\beta[H_{AB}]\right) - \mathrm{tr}\left(O\,\Omega_\beta[H]\right) \simeq \frac{1}{\ell_B^y} \quad (3.35)$$

up to higher order terms, where y is the scaling dimension of the operator H_I [Car84, Car86]. If H_I is a standard Hamiltonian term, in the sense that the system is homogeneous, its leading scaling dimension is $y = 2$.

Once more, we see that by increasing the boundary region temperature can be arbitrarily well assigned as the difference between expectation values decays polynomially with the boundary length l_B.

3.5. A case study: The Ising chain

Now we illustrate our results for the quantum Ising chain, which is described by the Hamiltonian

$$H_N = \frac{1}{2} \sum_{i=1}^{N-1} \sigma_i^x \otimes \sigma_{i+1}^x - \frac{h}{2} \sum_{i=1}^{N} \sigma_i^z, \tag{3.36}$$

where σ_i^x and σ_i^z correspond to the Pauli matrices, h characterizes the strength of the magnetic field and N is the number of spins. Notice that the interactions in the above Hamiltonian are of finite range, a crucial assumption in our derivations, see (3.7). This model has a quantum phase transition at $h = 1$, so it well exemplifies the different regimes discussed above: criticality (only at zero temperature) and away from it (for zero and non-zero temperatures).

3.5.1. Generalized covariance

First of all, as in the previous sections, we split the chain in three regions, which are shown Figure 3.6. For such a splitting, and in the context of equation (3.6), we compute the generalized covariance $\text{cov}_{\Omega_s}^{t/\beta}(O, O')$ taking for O a local operator in A, $O = \sigma_{N/2}^z$, and for O' the boundary Hamiltonian between B and C, $O' = H_I$, given by

$$H_I = \frac{1}{2} \left(\sigma_{N/2-3}^x \otimes \sigma_{N/2-2}^x + \sigma_{N/2+2}^x \otimes \sigma_{N/2+3}^x \right) .. \tag{3.37}$$
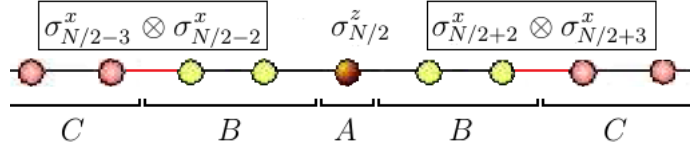
Figure 3.6.: Scheme of the subsystem A, the boundary region B and their environment C. The local operator $\sigma^z_{N/2}$ acts on the subsystem A and the interaction term H_I corresponds to the red lines (connection between the subsystems AB and C).

In order to compute $\mathrm{cov}^{t/\beta}_{\Omega_s}(\sigma^z_{N/2}, H_I)$, we first diagonalize the Hamiltonian (3.36) using standard techniques from statistical mechanics, such as the Jordan-Wigner and the Bogoliubov transformation (see Appendix A.2). Once the Hamiltonian is diagonalized, we can straightforwardly construct the corresponding thermal state for every large but finite N, and compute $\mathrm{cov}^{t/\beta}_{\Omega_s}(\sigma^z_{N/2}, H_I)$ using expression (3.5).

Figure 3.7 shows $\mathrm{cov}^{t/\beta}_{\Omega_s}(\sigma^z_{N/2}, H_I)$ as a function of t/β for several temperatures ($\beta = 5, 20, 1000$), and for $h = 0.9, 1$ (i.e., near and at criticality). We take $N = 40$, which already describes well the thermodynamic limit (recall that we are only interested on the local state, and that the correlations decay exponentially). The area below the curves correspond to the first integral in (3.6), which measures how well the local state in A can be approximated by a thermal state in AB.

The results in Figure 3.7 are in agreement with properties (i) and (ii) from Lemma 6 in Appendix A.1. The first property implies that the covariance is symmetric with respect to $t = \beta/2$, and it follows by taking $l = t$ and $n = \beta$ in (A.18). Second, property (ii) implies that it is bounded by a convex function of t with a maximum at $t = 0$ and $t = \beta$ and with a minimum at $t = \beta/2$. Therefore, the covariance satisfies the bound (A.19).

On the other hand, the covariance is not monotonic in s (see Figure 3.8). This is somehow counterintuitive, as it shows that the outcomes of two non-overlapping observables (located in A and in the intersection between B and C) do not always become more correlated as s, which quantifies the strength of the interaction between B and C, increases.
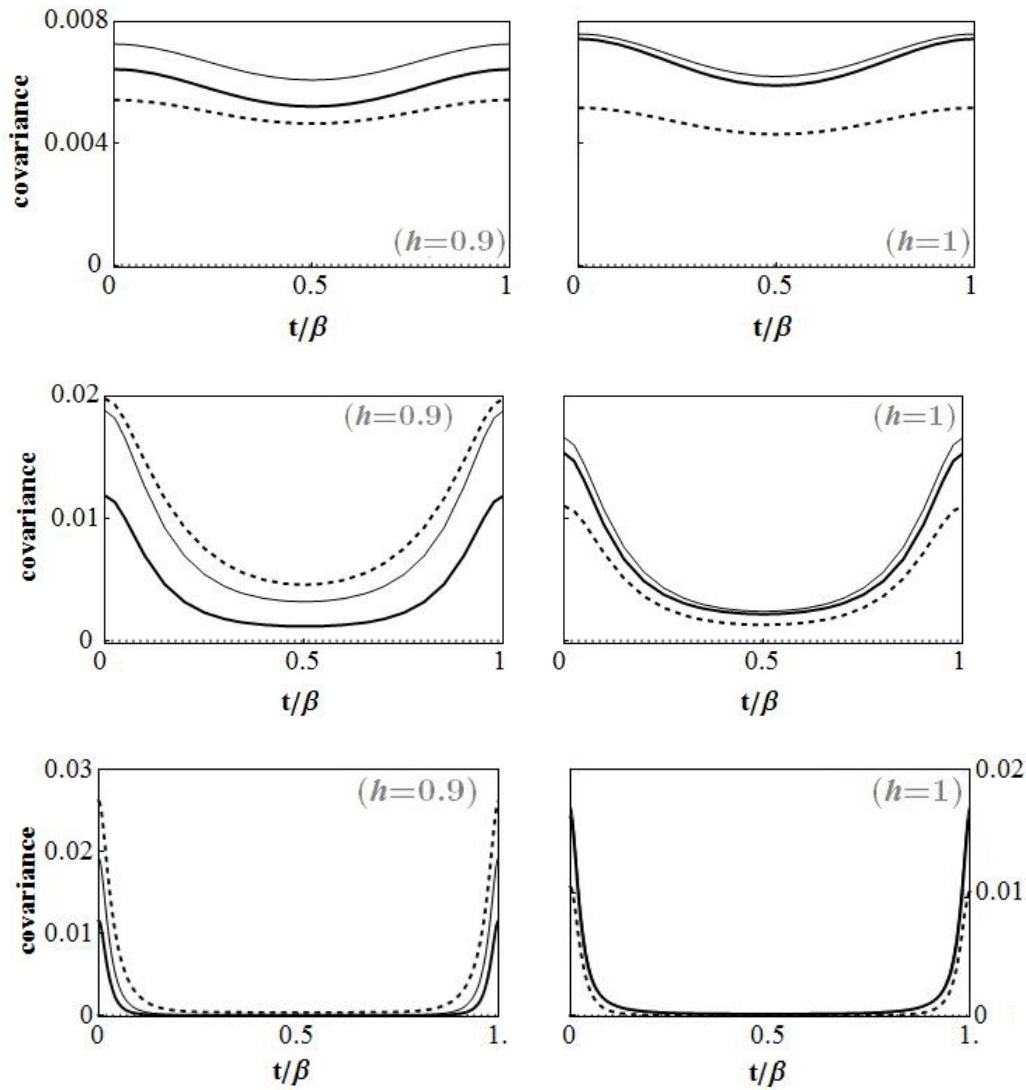
Figure 3.7.: Generalized covariance as a function of t for different values of s: $s = 0, 1/3, 2/3, 1$ for the dotted, dashed, black and thick lines. The figures correspond to inverse temperature $\beta = 5$ (top), $\beta = 20$ (at the middle) and $\beta = 100$ (bottom) and field strength $h = 0.9$ (left) and $h = 1$ (right).
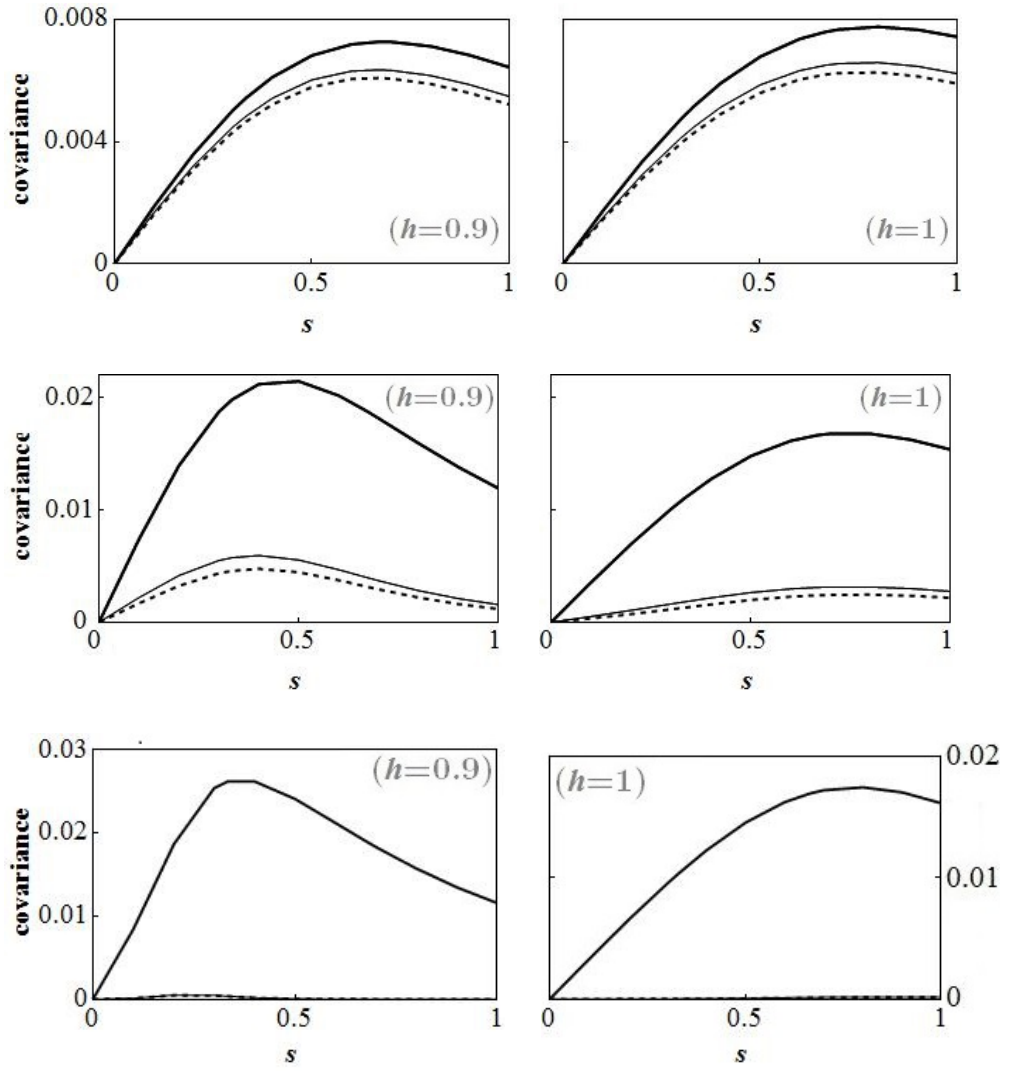
Figure 3.8.: Generalized covariance as a function of s for different values of t: $t/\beta = 0, 1/3, 1/2$ for the thick, black and dashed lines. The figures correspond to inverse temperature $\beta = 5$ (top), $\beta = 20$ (at the middle) and $\beta = 100$ (bottom) and field strength $h = 0.9$ (left) and $h = 1$ (right). Notice that, due to the symmetry in t, the values $t/\beta = 2/3, 1$ are also considered.

3.5.2. Locality of temperature in the quantum Ising chain

In our analytical findings, the generalized covariance naturally appeared as a tool to solve the locality of temperature problem, see (3.6). This motivated the previous section, where we studied its properties in the context of the quantum Ising chain. Nevertheless, in order to obtain (3.6), one still needs to integrate $\mathrm{cov}^{t/\beta}_{\Omega_s}(O, H_I)$ over s and τ. While this approach is useful when dealing with arbitrary generic systems, here we are dealing with a specific model that is furthermore solvable, so we can take a more direct approach. Concretely, we first compute

$$\rho_A = \mathrm{Tr}_{\bar{A}}(\Omega_\beta[H]), \qquad \text{with} \quad H \equiv H_\infty \qquad (3.38)$$

and

$$\rho'_A = \mathrm{Tr}_{\bar{A}}(\Omega_\beta[H_{AB}]), \qquad \text{with} \quad H_{AB} \equiv H_N, \qquad (3.39)$$

for different sizes N of the region AB. Secondly, we measure the distinguishability between such states via the quantum fidelity, which is advantageous for computational reasons. We remind here that the fidelity (2.10) for two states ρ_A and ρ'_A is defined as

$$\mathrm{F}(\rho_A, \rho'_A) = \mathrm{tr}\left(\sqrt{\sqrt{\rho_A}\rho'_A\sqrt{\rho_A}}\right). \qquad (3.40)$$

and it satisfies $0 \le F \le 1$ where $\mathrm{F}(\rho_A, \rho'_A) = 1$ if and only if $\rho_A = \rho'_A$. In order to relate this approach to our previous considerations, we note the relation (2.11) between the trace distance, $\mathcal{D}(\rho_A, \rho'_A)$, and $\mathrm{F}(\rho_A, \rho'_A)$, given by

$$1 - \mathrm{F}(\rho_A, \rho'_A) \le \mathcal{D}(\rho_A, \rho'_A) \le \sqrt{1 - \mathrm{F}(\rho_A, \rho'_A)^2}. \qquad (3.41)$$

Therefore, the fidelity provides us with upper and lower bounds to (3.4). In particular, when $\mathcal{D}(\rho_A, \rho'_A) \to 0$ then $\mathrm{F}(\rho_A, \rho'_A) \to 1$, and in that case we say that the temperature is locally well defined.

From now on, we take for A a two spin subsystem, an infinite chain as the total system, and we compute $\mathrm{F}(\rho_A, \rho'_A)$ as a function of the size of AB, with $N = 2 + 2l_B$, and the different parameters of the Hamiltonian.

In order to compute ρ_A and ρ'_A, it is convenient to apply the Jordan-Wigner transformation to (3.36), which maps spin operators $\sigma^{x,y,z}_i$ to fermionic operators $a_i, a^\dagger_i$ (see Appendix A.2 for details). The Hamiltonian (3.36) takes then the form,

$$H_N = \sum_{i,j=1}^{N} A_{ij}a_i a^\dagger_j + \frac{1}{2}\sum_{i,j=1}^{N} B_{ij}(a^\dagger_i a^\dagger_j - a_i a_j), \qquad (3.42)$$

which is quadratic in terms of the fermionic operators. It follows that thermal states, as well as their local states, are gaussian operators. Therefore it is possible to describe them by their covariant matrix, whose size is only $\mathcal{O}(N^2)$. This allows us to compute ρ'_A in (3.39) for finite but large l_B; while in the limit $N \to \infty$, i.e. to compute ρ_A in (3.38), we rely on the analytical results from [BM71]. The explicit calculations are done in Appendix A.2.

3.5.2.1. Non-zero temperature

Figure 3.9 shows $\text{F}(\rho_A, \rho'_A)$ as a function of β and h, for $N = 4$ (left) and $N = 20$ (right). Recall that N, with $N = 2 + 2l_B$, defines the size of the boundary region which is used to approximate ρ_A by ρ'_A. Even if the boundary is small, $N = 4$, the fidelity is close to 1 for all values of β and h, and thus the temperature is locally well-defined. As expected, $\text{F}(\rho_A, \rho'_A)$ increases with N (see Figure 3.10).

We also observe in Figure 3.9 that the fidelity becomes minimal near $h = 1$, which is the phase transition point. As N increases, this minimum is shifted to $h = 1$. At this point the spatial correlations also increase, which suggests a relation between both quantities.

In order to further explore this connection, we compute the scaling of $\text{F}(\rho_A, \rho'_A)$ with N, and compare it to the decay of the correlations. The behaviour of $\text{F}(\rho_A, \rho'_A)$ is plotted in Figure 3.10, which clearly shows that the fidelity follows an exponential law with N, given by

$$\text{F}(\rho_A, \rho'_A) \sim 1 - e^{-\frac{N}{2\xi_S}}, \tag{3.43}$$

where ξ_S is a parameter that characterizes the slope of the function. On the other hand, the correlations between a local observable in A, σ_i^z, and one in the intersection of B and C, σ_{i+d}^z,

$$\text{corr}(\sigma_i^z, \sigma_{i+d}^z) = \langle \sigma_i^z \sigma_{i+d}^z \rangle - \langle \sigma_i^z \rangle \langle \sigma_{i+d}^z \rangle,$$

can be obtained through the two-spin correlation function $\langle \sigma_i^z \sigma_{i+d}^z \rangle$ in [BM71]. Their asymptotic behaviour is also exponential with d,

$$\text{corr}(\sigma_i^z, \sigma_{i+d}^z) \sim e^{-\frac{d}{\xi}},$$

where ξ is the correlation length. Now, identifying d, the distance between particles, with $N/2$, which is roughly the size of B, we obtain from the numerical results in Figure 3.11 the following simple relation,

$$\xi = 2\xi_S.$$

Roughly speaking, the quality of the approximation ρ'_A is directly related to the strength of the correlations in the system. This relation is in good agreement with previous considerations in [LCB14], where the correlation length is related to the error of the cluster approximation.

In summary, temperature can be assigned to the local system for all h, finite β by taking a small boundary region (with $N \geq 4$, and thus $l_B \geq 2$). We have shown that this is directly connected to the exponential decay of the correlations with the distance, which makes the local state of a thermal state only be sensible to its closest boundary.
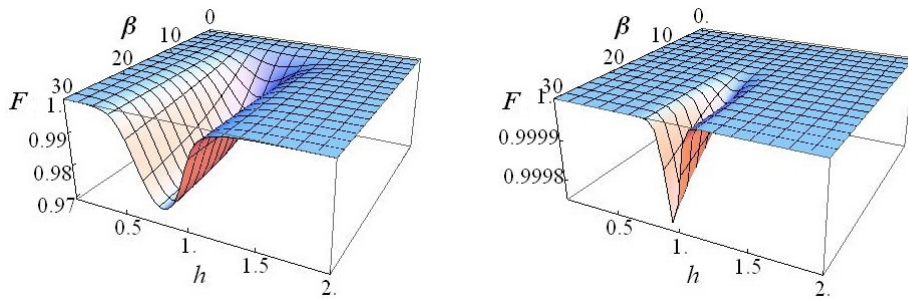
Figure 3.9.: Fidelity $F(\rho_A, \rho'_A)$ as a function of β and the strength of the magnetic field h for $N = 4$ (left) and $N = 20$ (right). The temperature is locally well-defined provided that $F(\rho_A, \rho'_A) \approx 1$.
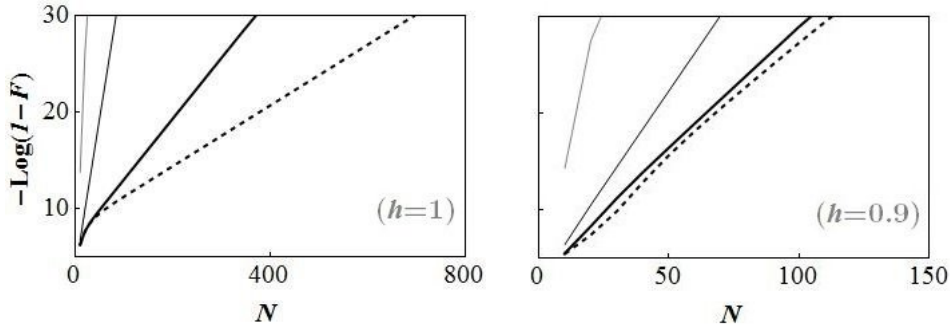
Figure 3.10.: Function of fidelity, $-Log(1 - F(\rho_A, \rho'_A))$, as a function of N for $h = 1$ (left) and $h = 0.9$ (right). The inverse temperature is $\beta = 5, 20, 100, 200$ for the grey, black, thick and dashed lines.
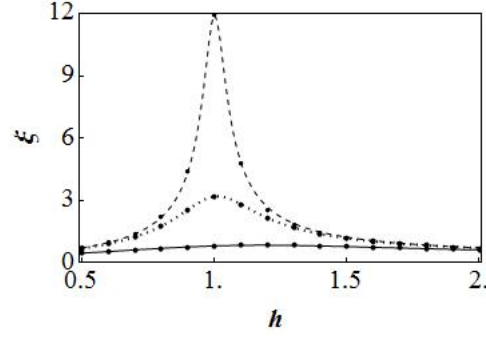
Figure 3.11.: Correlation length, ξ, as a function of h. The black spots correspond to the numerical values for $2\xi_S$. The inverse temperature is $\beta = 5, 20, 75$ for the black, dotted and dashed lines.

3.5.2.2. Zero temperature

The same conclusions apply at zero temperature, as the fidelity is also close to 1 for all h and $N \geq 4$. It also has a minimum near the critical point.

Nonetheless, the scaling of the fidelity (or more precisely $1 - F$) with N can differ from the previous case. While the scaling is generally exponential at zero temperature, it becomes a power law at the phase transition point (see Figure 3.12),

$$F(\rho_A, \rho'_A) \sim 1 - N^{-C_s}.. \tag{3.44}$$

This type of decay is also obtained for the correlations as a function of the distance, which again shows a direct connection between the quality of the approximation (quantified by $F(\rho_A, \rho'_A)$) and the strength of the correlations.
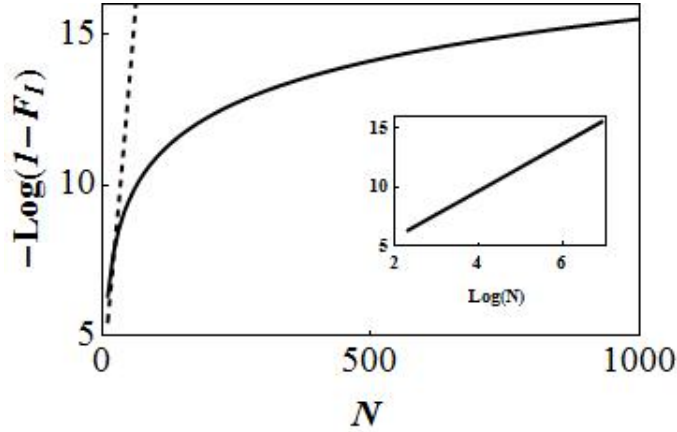
Figure 3.12.: Function of fidelity, $-Log(1 - \mathrm{F}(\rho_A, \rho'_A))$, as a function of N for $\beta \to \infty$. The field strength is $h = 0.9, 1.$ for the dashed and black lines.

3.6. Conclusions

We studied the problem of locality of temperature for quantum spin chains with strong but finite-range interactions. Upon noting that in the presence of strong interactions the marginal states of a global thermal state do not take the canonical form themselves, we go on defining an effective thermal state for a subsystem. The effective thermal state refers to the reduced density matrix of the subsystem considered as a part of a slightly bigger, enveloping thermal system (see Figure 3.1). Borrowing concepts from quantum information theory and employing methods from quantum statistical mechanics, we relate the accuracy with which the effective thermal state describes the actual state of the subsystem to the correlations present in the whole system (see Eqs. (3.4, 3.5, 3.6) and the discussion around them). Furthermore, we utilize techniques from tensor networks [Has06, MSVC14] for any temperature, except at the phase transition point. At this critical point, we make use of already existing formulas from conformal field theory.

Finally, we exemplify our analytical findings by analysing the quantum Ising chain. In particular, we find that, e.g., away from criticality, the envelope which is bigger than the system only by one layer of spins, is enough to approximate the actual state with good precision (see, e.g., Figure 3.9).

3. Locality of temperature for one-dimensional spin systems

4. Locality of temperature and correlations in the presence of non-zero-temperature phase transitions

Temperature is typically understood as an intensive quantity in standard thermodynamics. Nonetheless, it is far from known whether this still holds in quantum systems at thermal equilibrium, that is, whether each subsystem is at an effective thermal state at the same global temperature. In this chapter, we are interested to understand how the problem of the locality of temperature is affected by a phase transition at non-zero temperature. For that aim, we consider a three-dimensional discrete version of the Bose-Einstein model at the grand canonical ensemble with temperature T and particle density n, and characterize its phase transition at non-zero temperature T_c. We find that temperature is locally well defined in the system regardless of the temperature T. We characterize the correlations in the system and discuss its relation to the locality of temperature.

4.1. Introduction

Since the beginning of quantum mechanics, there have been strong attempts to understand thermodynamic processes in quantum systems [GMM04]. It is not clear how thermodynamic quantities should be defined in microscopic systems or whether their properties differ from those in classical systems, as they are originally defined as statistical magnitudes. For example, in standard thermodynamics the temperature has an intensiveness property, but it is not known whether this holds in quantum systems. This property implies that any subsystem within a system at thermal equilibrium at temperature T is also at thermal equilibrium at the same temperature T, i.e., the temperature is locally well defined. In quantum systems, however, systems at thermal equilibrium correspond to systems at a thermal state and, thus, temperature can only be defined in such case. Thus, the problem can be reformulated in terms of two ques-

45

tions: (i) is it is possible to define temperature for a subsystem of a system at thermal equilibrium at temperature T?; and (ii) if temperature can be defined, does it correspond to the global temperature T?

In the following, we formalize the general setting of the problem. First, we assume a system described by a Hamiltonian H and at a canonical state at temperature T (2.21). We then attempt to understand the thermal properties of a finite part (subsystem) of the system. More concretely, we take into account the partial state of the subsystem and analyse whether it is possible to assign a temperature that is equivalent to the global one, T. This partial state is not thermal in general, except for subsystems that weakly interact with the rest of the system. Therefore, it is not straightforward how to assign a temperature to it in general, since this depends on the environment and the interactions that couple the subsystem to it. A way to solve this problem was proposed by Ferraro et al. [FGSA12]. They show for coupled harmonic oscillators on a lattice that it is possible to assign a temperature to the subsystem via an effective thermal state at temperature T which constitutes a very good approximation to the partial state of the subsystem. The effective thermal state refers to the partial state of another subsystem (reference) surrounded by a a sufficiently large boundary region such both reference subsystem and boundary constitute a composed system at thermal equilibrium at the same temperature T. If the size of such a boundary region is independent of the total system size, temperature can still be said to be local.

During the last decades, there have been several works based on the same approach of Ferraro et al. [FGSA12] where it is shown that temperature is locally well defined for different systems and conditions. More specifically, it has been shown in bosonic systems: 1D and 2D interacting harmonic oscillators [FGSA12]; and in fermionic systems under different constraints: (i) for generic one-dimensional systems and at arbitrary temperature [HSRH+15], (ii) for fermionic and spin systems with arbitrary dimension and at high temperature [KGK+14], and (iii) for the Ising model [HSRH+15]. It has been also observed that locality is valid at quantum phase transitions in one-dimensional fermionic systems provided that the boundary region is large enough [GSFA09], which are the only type of phase transitions for 1D systems and only happen at zero temperature. However, this is far from true when it comes to higher dimensional systems, where phase transitions can also occur at non-zero temperature and are driven by both thermal and quantum fluctuations. In fact, non-zero-temperature phase transitions are an important feature in many-body systems which holds interesting phenomenology, which has been observed the study of correlations or entanglement negativity [LG18]. In this chapter, we aim to investigate how non-zero-temperature phase transitions affect the locality of temperature.

We consider a three-dimensional bosonic system that correspond to a discrete version

of the Bose-Einstein model and assume the system is at a grand canonical ensemble at temperature T and at chemical potential μ with a fixed particle n. We show then that the system undergoes a phase transition at non-zero temperature in a similar fashion to the Bose-Einstein condensate, i.e., all the particles of the system are at the ground state below the critical temperature. We observe that temperature is local at any temperature and at any density n. We also analyse the correlations of the system for the same settings and observe that correlations decay polynomially to n_0^2 below the critical temperature T_c, where n_0 is the zero-momentum particle density, and exponentially above T_c. While we observe long-distance correlations below the critical temperature, the behaviour of the correlations is in agreement with the observations in the locality section.

4.2. Model

We consider a free bosonic system in a three-dimensional lattice of size L^3 with periodic boundary conditions (PBC) and described by the Hamiltonian

$$H := -t \sum_{<\mathbf{n},\mathbf{m}>} b_{\mathbf{m}}^{\dagger} b_{\mathbf{n}} + 6t \sum_{\mathbf{n}} b_{\mathbf{n}}^{\dagger} b_{\mathbf{n}}, \tag{4.1}$$

where t is the hopping strength, b and $b^{\dagger}$ are annihilation and creation bosonic operators, and $\mathbf{n} = (n_x, n_y, n_z)$ with $n_i = j - L/2$ and $j \in [0, L-1]$ for each $i \in \{x, y, z\}$. This system corresponds to a discretized version of the well-known Bose-Einstein model [PS16], which is known to have a phase transition at non-zero temperature for a fixed particle density, below which all the particles are at 0-momentum and the system condensates. In fact, we show that the system (4.1) is analogous to it at the continuous limit (see Appendix B.1) and that it is able to reproduce the condensate when its physical dimension $D > 2$ (see Appendix B.2). We expect then to observe an analogous phase transition and condensate for a large enough system size, $L >> 1$, and a fixed particle density n. Taking this into account, we assume the system to be at the grand canonical state (4.2) with a fixed particle density $n := N/V$, given by

$$\Omega_{\{\beta,\mu\}} := e^{-\beta H + \mu N} / \operatorname{tr}(e^{-\beta H + \mu N}) \tag{4.2}$$

where μ is the chemical potential, the inverse temperature $\beta := 1/(k_B T)$ with fixed Boltzmann constant $k_B = 1$, and the total particle number $N := \sum_{\mathbf{n}} \langle b_{\mathbf{n}}^{\dagger} b_{\mathbf{n}} \rangle_{\beta}$.
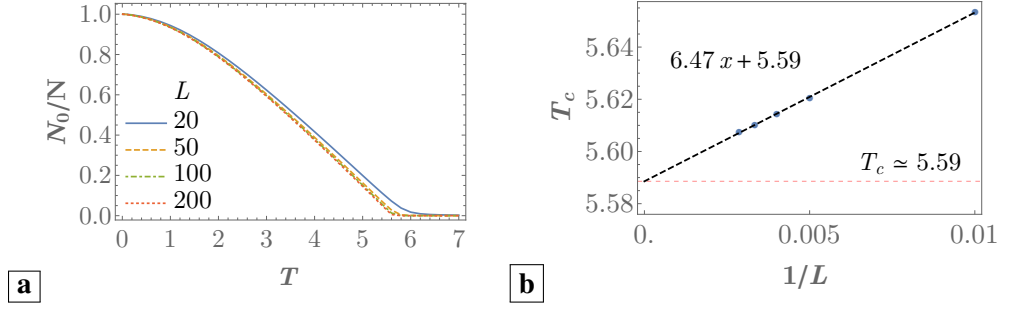
Figure 4.1.: a. Zero-momentum density, N_0/N, vs temperature, T, for density $n = 1$. The system size, L, is set to $20, 50, 100$ and 200 for the solid, dashed, dotted and dotdashed lines. b. Critical temperature, T_c vs inverse distance, $1/L$, for density $n = 1$. Data involves system sizes $L = 100, 200, 250, 300, 350$. The red dashed line highlights the critical temperature at the thermodynamic limit T_c.

4.2.1. Phase transition and phase diagram

In this section, we verify the equivalence of the system (4.1) to the Bose-Einstein model and characterize its phase transition and phase diagram.

For this aim, we assume a particle density $n = 1$ and obtain the values of the chemical potential μ for each inverse temperature β that guarantee a grand canonical state $\Omega_{\{\beta,\mu\}}$ with $n = 1$ at any temperature. We analyse then the population ratio between ground-state particles and total number of particles, N_0/N, as a function of the temperature, T, for different system sizes, L (see Figure 4.1.a). We observe that there is a phase transition at a critical temperature, T_c, and a condensate for any temperature $T \leq T_c$. As the phase transition only makes sense at the thermodynamic limit, we obtain that the critical temperature $T_c \approx 5.59$ by computing an estimation for each system size, L, and making a finite size analysis (see Figure 4.1.b). The estimation of the temperature was computed by fitting the non-negligible data for $N_0/N \in [0.01, 0.05]$ and extracting the temperature at which the fitting function goes to zero.

We also study how the critical temperature, T_c, depends on the particle density, n, and show that T_c increases monotonically with the density (see Figure 4.2.a). This can be qualitatively explained in terms of the energy: since we increase the particle density, n, in a periodic system, we are increasing the site population homogeneously and, thus, each site requires higher energy to guarantee the same state for each particle.

Regarding the phase diagram of the system, we study how the chemical potential, μ, depends on the temperature, T, for different values of the particle density n (see
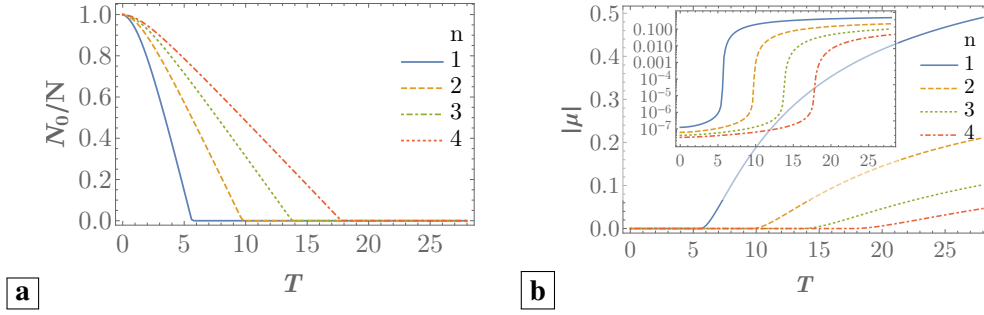
Figure 4.2.: Analysis for values of particle density $n = 1, 2, 3, 4$ and system size $L = 200$. a. Zero-momentum density, N_0/N, vs temperature, T. b. Chemical potential, μ, vs temperature, T.

Figure 4.2.b). We observe that the chemical potential μ increases with the temperature T for $T > T_c$ and that $\mu \approx 0$ for $T \leq T_c$, a clear sign of the phase transition. Thus, the condensate is linked to zero chemical potential, $\mu \approx 0$, and adding or removing particles to the ground state requires no energy, which is consistent with the analogy of this model to the standard Bose-Einstein condensate [PS16].

4.3. Locality of temperature

In this section, we analyse whether the temperature can be locally well defined in the considered system and how this depends on the presence of a phase transition at non-zero temperature.

4.3.1. The problem

We consider a cubic global system **ABC** with L_0^3 sites described by the discrete version of the Bose-Einstein model (4.1) with periodic boundary conditions, where $L_0 := L_{\mathbf{ABC}}$ and $L_{\mathbf{ABC}}$ is defined as the number of sites in the extremal edge of the system **ABC** (see Figure 4.3). We also assume that the system is at thermal equilibrium at temperature T and with a fixed particle density n, that is, the system is at the grand canonical state 4.2. Given this, we want to know whether the temperature is locally well defined in the system. From a practical point of view, we aim to understand if it is possible to assign the same global temperature T to any typical subsystem **C**. In practice, we select a $2 \times 2 \times 2$ cube as subsystem **C** with $L_{\mathbf{C}} = 2$ and compare its partial state to the partial state of a reference system. This reference system has $L_{\mathbf{BC}}^3$
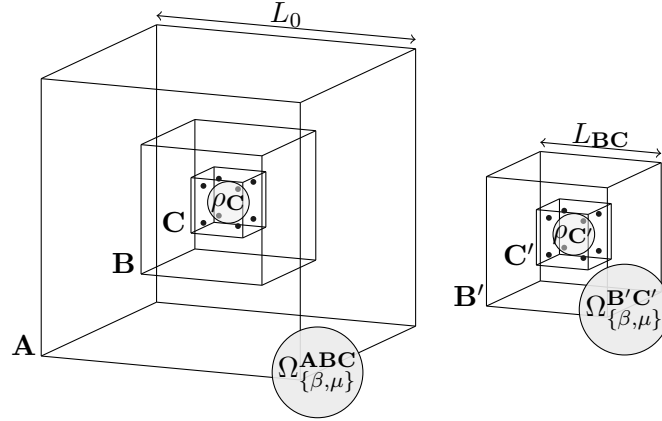
Figure 4.3.: Left: Setting of the subsystem of interest C, the boundary region B and their environment C. Right: Setting of the reference system with the subsystem C' and the boundary B', which are equivalent to C and B respectively.

sites and consists of a core $\mathbf{C'}$ with the same characteristics than $\mathbf{C}$ and a boundary region $\mathbf{B'}$ around it. By comparing these two partial states $\rho_{\mathbf{C}}$ and $\rho_{\mathbf{C'}}$, we are able to tackle the question and its distinctive behaviour depending on the temperature T, the phase transition and the size of $\mathbf{B'}$, $L_{\mathbf{B}} = L_{\mathbf{BC}} - 2$.

4.3.2. Methods

In order to compare both states, ρ_C and $\rho_{C'}$, we obtain the distinguishability between such states via the quantum fidelity (2.10). The fidelity can be computed from the covariance matrices of the states provided that the states are Gaussian [PS99]. Since the partial state of a Gaussian state is also Gaussian and the Grand Canonical state of a quadratic Hamiltonian is Gaussian, $\rho_{\mathbf{C}}$ and $\rho_{\mathbf{C'}}$ are both Gaussian.

The covariance matrix of the system described by the Hamiltonian (4.1), with size L^3, and at the state $\Omega_{\{\beta,\mu\}}$ (4.2) can be exactly solved by Fourier transform (B.19). In fact, its elements are given by the expressions

$$\langle b_{\mathbf{n}}^{\dagger} b_{\mathbf{m}} \rangle_{\{\beta,\mu\}} = \frac{1}{\sqrt{L^3}} \sum_{\mathbf{k}} \frac{e^{-I(\mathbf{n}-\mathbf{m})\mathbf{k}}}{e^{\beta\varepsilon(\mathbf{n})+\mu} - 1}, \tag{4.3}$$

$$\langle b_{\mathbf{n}} b_{\mathbf{m}}^{\dagger} \rangle_{\{\beta,\mu\}} = 1 + \langle b_{\mathbf{n}}^{\dagger} b_{\mathbf{m}} \rangle_{\{\beta,\mu\}}, \text{ and} \tag{4.4}$$

$$\langle b_{\mathbf{n}} b_{\mathbf{m}} \rangle_{\{\beta,\mu\}} = \langle b_{\mathbf{n}}^{\dagger} b_{\mathbf{m}}^{\dagger} \rangle_{\{\beta,\mu\}} = 0; \tag{4.5}$$
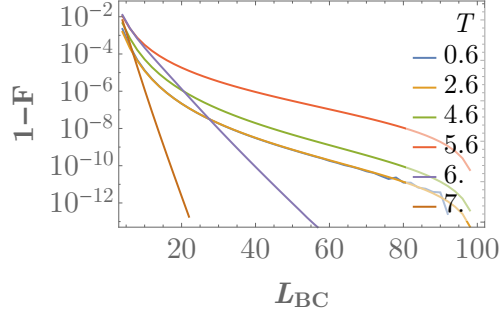
Figure 4.4.: Fidelity, F($\rho_{\mathbf{C}}, \rho_{\mathbf{C}'}$), vs reference system length, $L_{\mathbf{BC}}$, for different temperatures $T = 0.6, 2.6, 4.6, 5.6, 6, 7$.

where $\mathbf{k}$ is the momentum vector (B.19) and $\varepsilon(\mathbf{n})$ is the eigenvalue of the Hamiltonian B.2. Given this, we extract the covariance matrix of any subsystem by taking the matrix elements corresponding to the sites within that subsystem. At last, we obtain the fidelity between $\rho_{\mathbf{C}}$ and $\rho_{\mathbf{C}'}$ by means of their covariance matrices and the formula of Paraoanu et al. [PS99].

4.3.3. Results

We study the problem of locality of temperature for a subsystem $\mathbf{C}$ of dimensions $2 \times 2 \times 2$ embedded in a system with length $L_0 = 100$ and particle density $n = 1$, and a reference system $\mathbf{B}'\mathbf{C}'$ with length $L_{\mathbf{BC}} \in [4, 100]$, that is, $L_{\mathbf{B}} \in [2, 98]$. We also consider different temperatures around the critical temperature $T_c \approx 5.6$ to investigate how a non-zero-temperature phase transition affects the locality of temperature.

First, we observe that the fidelity between the states $\rho_{\mathbf{C}}$ and $\rho_{\mathbf{C}'}$ increases when the length $L_{\mathbf{BC}}$ increases, i.e., when the boundary region B increases (see Figure 4.4). It also behaves differently depending on whether we are below or at the critical temperature, $T \leq T_c$, or above, $T > T_c$.

Below and at the phase transition, the fidelity, F($\rho_{\mathbf{C}}, \rho_{\mathbf{C}'}$), increases polynomially to F $= 1$ with the length $L_{\mathbf{BC}}$ (see Figure 4.5.a), described by

$$1 - \mathrm{F}\left(\rho_{\mathbf{C}}, \rho_{\mathbf{C}'}\right) \propto \frac{1}{L_{\mathbf{BC}}^{\nu_F}}, \tag{4.6}$$

with exponent ν_F. Moreover, we analyse how the exponent, ν_F, behaves as a function of the temperature, T, for different system sizes L_0 and make a finite size analysis (see Figure 4.5.b). At the continuous limit, we estimate that the exponent $\nu_F \approx 6$ for
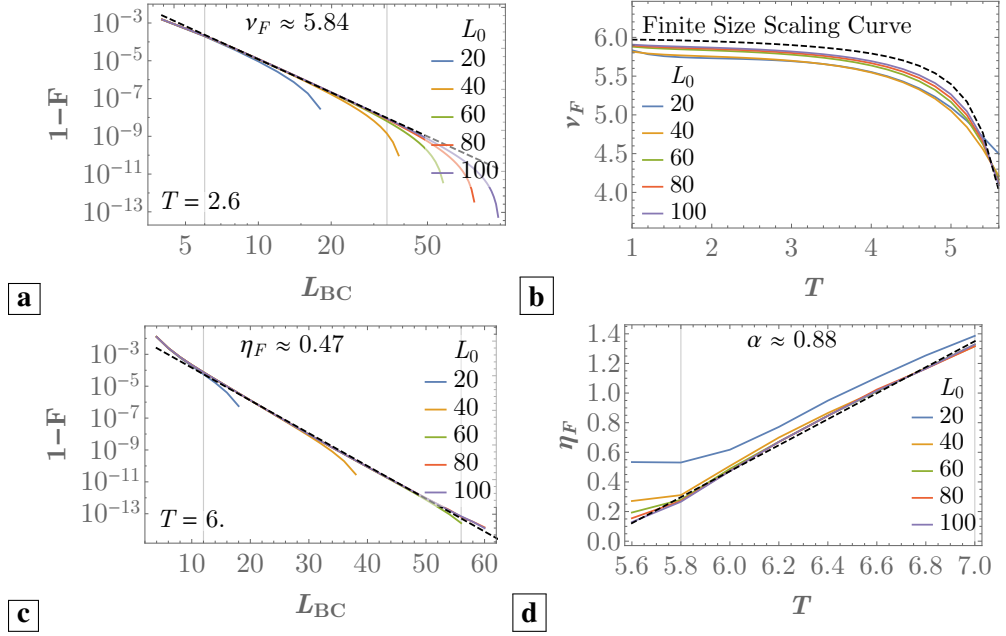
Figure 4.5.: a. Fidelity error, $1 - F(\rho_{\mathbf{C}}, \rho_{\mathbf{C'}})$, vs length $L_{\mathbf{BC}}$ for lengths $L_0 = 20, 40, 60, 80, 100$ and temperature $T = 2.6$, below the critical temperature $T_c = 5.6$. b. Exponent for power-law fitting vs temperature below the phase transition ($T \leq T_c$). The dashed line corresponds to the curve resulting of finite size scaling analysis. c. Fidelity error, $1-F(\rho_{\mathbf{C}}, \rho_{\mathbf{C'}})$, vs length $L_{\mathbf{BC}}$ for system lengths $L_0 = 20, 40, 60, 80, 100$ and temperature $T = 6$, above the critical temperature T_c. d. Exponent for exponential fitting vs temperature above the phase transition ($T > T_c$). The dashed line corresponds to the fitting of data for $L_0 = 100$.

temperature $T \leq 4$, away from the phase transition, and that it suddenly decreases up to $\nu_F \approx 4$ around the phase transition, at $4 < T < 5.6$. The exponents for finite systems were computed by fitting the data of the error fidelity, $1 - F(\rho_{\mathbf{C}}, \rho_{\mathbf{C'}})$, in the range $L_{\mathbf{BC}} \in [6, 34] \times (L_0/100)$.

On the other side, we find that above the phase transition the fidelity increases exponentially to $F = 1$ with $L_{\mathbf{BC}}$ (see Figure 4.5.c), that is,

$$1 - F(\rho_{\mathbf{C}}, \rho_{\mathbf{C'}}) \propto e^{-\eta_F L_{\mathbf{BC}}}, \tag{4.7}$$

with the characteristic exponent η_F. We also make a study of the exponent η_F and observe that it increases linearly with temperature (see Figure 4.5.d). In fact, we obtain that $\eta_F = \alpha T + \beta$ with $\alpha \approx 0.9$ and $\eta_F \in [0, 1.3]$ for $T \in [5.6, 7]$. In this case, we
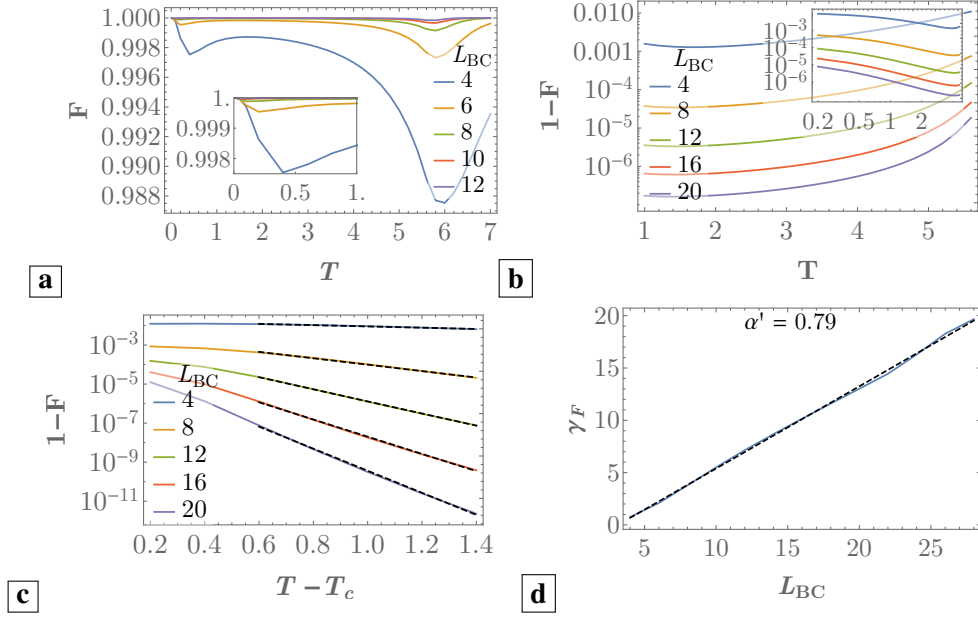
Figure 4.6.: a. Fidelity vs temperature for different lengths $L_{\mathbf{BC}} = 4, 6, 8, 10, 12$. Inset: Plot for data at temperature $T \leq 1$. b. Fidelity error, $1 - \mathrm{F}(\rho_{\mathbf{C}}, \rho_{\mathbf{C'}})$, vs temperature difference $T_c - T$ for $L_0 = 100$ and for length $L_{\mathbf{BC}} = 4, 8, 12, 16, 20$. The scaling of the plot is logarithmic, and the scaling of the inset is double logarithmic. c. Fidelity error, $1 - \mathrm{F}(\rho_{\mathbf{C}}, \rho_{\mathbf{C'}})$, vs temperature difference $T - T_c$ for $L_0 = 100$ and for length $L_{\mathbf{BC}} = 4, 8, 12, 16, 20$. The dashed line corresponds to an exponential fit. d. Exponent of exponential fit vs the length of reference system size $L_{\mathbf{BC}}$. The dashed line correspond to a linear fit.

have taken into account the data for $L_0 = 100$ as our estimation for the continuous limit since they have effectively converged from $L_0 = 60$. Exponents were computed by fitting data between the point with error fidelity $1 - \mathrm{F} = 10^{-4}$ and the closest point that satisfies $1 - \mathrm{F} = 10^{-13}$ or $L_{\mathbf{BC}} = 68 \times (L_0/100)$.

Additionally, we investigate the behaviour of the fidelity as a function of the temperature T for different lengths $L_{\mathbf{BC}}$ (see Figure 4.6.a). We observe a global minimum at the critical temperature T_c for any length $L_{\mathbf{BC}}$. Unfortunately we are not able to clearly identify the behaviour of the fidelity around the critical point at T_c. Below the critical temperature, we do not observe a clear scaling (see Figure 4.6.b), as the data could be equally fitted to an exponential or power-law function around the critical point T_c. The same occurs for temperatures that are just above the critical temperature, T_c.
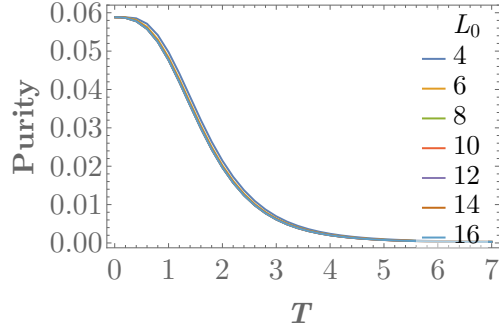
Figure 4.7.: Purity of the partial state ρ_C vs temperature T for different values of system size $L_0 = 4, 6, 8, 10, 12, 14, 16$.

However, at very large temperatures, $T >> T_c$, it is possible to see that the fidelity goes exponentially to 1 (see Figure 4.6.c), that is,

$$1 - \mathbf{F}\left(\rho_{\mathbf{C}}, \rho_{\mathbf{C}'}\right) \propto \mathrm{e}^{-\gamma_F T} \tag{4.8}$$

with exponent γ_F. We also analyse the exponent and obtain that $\gamma_F \propto \alpha' T + \beta'$ with a factor $\alpha' \approx 0.8$ (see Figure 4.6.d). At last, we notice that there is a local minimum at low temperatures, which shifts to lower temperatures when $L_{\mathbf{BC}}$ increases. This minimum is probably a consequence of numerical instabilities. There are several reasons that point in this direction: (i) some elements of the covariance matrix diverge for $T << 1$ since they contain diverging terms like $1/(e^{\varepsilon(\mathbf{k})/T} - 1)$ (see Appendix B.2), (ii) numerical errors are relatively significant because the fidelity is very high $F > 0.98$, and (iii) the fidelity is a non-trivial function between two states where the numerical instability can appear at different temperatures T, causing a minimum in the fidelity.

As a last remark, it is necessary to highlight that the fidelity is extremely high, with values $F > 0.98$ for any given parameters. We tackle why this happens by studying the purity (2.3) of ρ_C for different system sizes L (see Figure 4.7). We obtain that the purity $\mathcal{P} < 0.1$ for any system size $L \in [4, 16]$. This means that the partial state is extremely mixed for any boundary size and, thus, the state ρ_C is highly independent of the system size L, which explains why we are obtaining such a high fidelity.

4.4. Correlations

In this chapter, we analyse the behaviour of the correlations in the system depending on the temperature T.

4.4.1. Figure of merit

We make use of density-density correlations, defined as

$$\text{corr}(b_{\mathbf{i}}^{\dagger} b_{\mathbf{i}}, b_{\mathbf{j}}^{\dagger} b_{\mathbf{j}}) := \langle b_{\mathbf{i}}^{\dagger} b_{\mathbf{i}} b_{\mathbf{j}}^{\dagger} b_{\mathbf{j}} \rangle - \langle b_{\mathbf{i}}^{\dagger} b_{\mathbf{i}} \rangle \langle b_{\mathbf{j}}^{\dagger} b_{\mathbf{j}} \rangle. \tag{4.9}$$

The correlations for the state $\rho_{\{\beta,\mu\}}$ can be computed via Wick's theorem (Lemma 6 in [GKF$^+$16]) as the state is Gaussian, given by the expression

$$\langle \prod_{k=1}^{m} c_{i_k} \rangle_{\beta} = \text{Pf}(\Gamma[i_1, \ldots, i_m]), \tag{4.10}$$

where Pf is the Pfaffian and Γ has matrix elements

$$\left(\Gamma[i_1, \ldots, i_m] \right)_{a,b} := \begin{cases} \langle c_{i_a} c_{i_b} \rangle_{\beta} & \text{if } a < b, \\ -\langle c_{i_b} c_{i_a} \rangle_{\beta} & \text{if } a > b, \\ 0 & \text{otherwise.} \end{cases} \tag{4.11}$$

Applying Equation (4.10) into (4.9), the correlations are given by the covariance matrix elements such that

$$\text{corr}(b_{\mathbf{i}}^{\dagger} b_{\mathbf{i}}, b_{\mathbf{j}}^{\dagger} b_{\mathbf{j}}) = \langle b_{\mathbf{i}}^{\dagger} b_{\mathbf{j}} \rangle \langle b_{\mathbf{i}} b_{\mathbf{j}}^{\dagger} \rangle - \langle b_{\mathbf{i}}^{\dagger} b_{\mathbf{j}}^{\dagger} \rangle \langle b_{\mathbf{i}} b_{\mathbf{j}} \rangle \tag{4.12}$$

4.4.2. Results

We study the density-density correlations (4.12) between sites $\mathbf{i}_x = (i, 1, 1)$ and $\mathbf{j}_x = (j, 1, 1)$ as a function of the distance, dist $:= |i - j|$, for a system length $L_0 = 100$, a fixed particle density $n = 1$ and different temperatures T around the critical temperature $T_c \approx 5.6$.

We observe that the correlations behave differently depending on whether we are above the phase transition point or below (see Figure 4.8). At temperatures $T \leq T_c$,
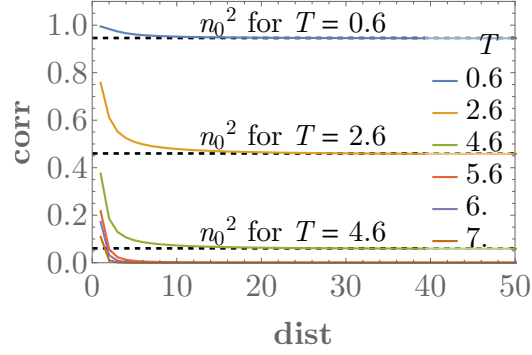
Figure 4.8.: Correlations vs distance for $L = 100$ and for temperatures $T = 0.6, 2.6, 4.6, 5.6, 6.7$.

correlations decay up to a constant value equal to the square of the ground state density, n_0^2, where $n_0 := (1/L_0^3)\langle a_0^\dagger a_0 \rangle$ and, thus,

$$n_0 = \frac{1}{L_0^3} \frac{1}{e^{-\mu} - 1}. \tag{4.13}$$

We also prove analytically this decay to n_0^2 for low temperatures $T << 1$ (see Appendix B.3). Moreover, we observe that the correlations decay as a power-law for $T \leq T_c$ (see Figure 4.9.a), that is,

$$\mathrm{corr}(a_{\mathbf{i}_x}^\dagger a_{\mathbf{i}_x}, a_{\mathbf{j}_x}^\dagger a_{\mathbf{j}_x}) - n_0^2 \propto \frac{1}{\mathrm{dist}^{\nu_C}}, \tag{4.14}$$

where the exponent ν_C increases with the temperature T. More concretely, we obtain that $\nu_C \approx 1.4$ for $T \leq 4$ and that $\nu_C \in [1.4, 2.2]$ for $T \in [4, 5.6]$ (see Figure 4.9.b). The fitting has been obtained for data with $\mathrm{dist} \in [5, 15] \times (L_0/100)$. For temperature $T > T_c$, we observe that correlations decay exponentially to 0 (see Figure 4.9.c), that is,

$$\mathrm{corr}(a_{\mathbf{i}_x}^\dagger a_{\mathbf{i}_x}, a_{\mathbf{j}_x}^\dagger a_{\mathbf{j}_x}) \propto e^{-\eta_C \, \mathrm{dist}}, \tag{4.15}$$

where the exponent η_C increases with the temperature T. In particular, it increases linearly, i.e., $\eta_C = \alpha'' T + \beta''$ with a factor $\alpha'' \approx 0.76$ and with values $\eta_C \in [0, 1.2]$ for $T \in [5.6, 7]$ (see Figure 4.9.d). The fitting has been computed for data with $\mathrm{dist} \in [20, 35] \times (L_0/100)$.

We notice that there is a correspondence between the results for the locality of temperature as a function of the reference system length $L_{\mathbf{BC}}$ (Section 4.3) and these results for the correlations. Concretely, both fidelity and correlations have a power-law behaviour for $T \leq T_c$ and an exponential behaviour for $T > T_c$. Moreover, the
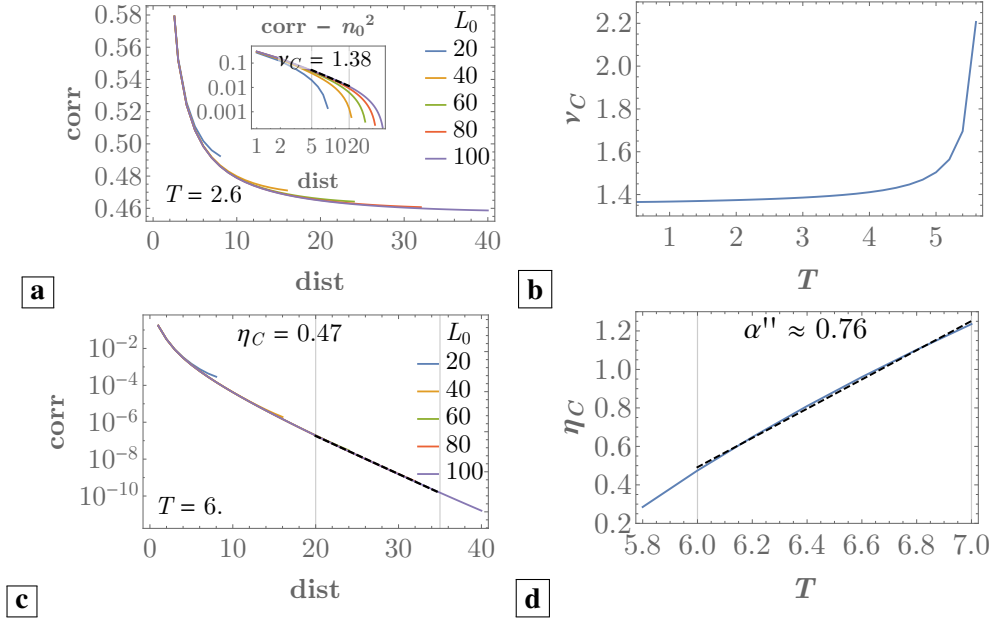
Figure 4.9.: a. Correlations for $T = 2.6 < T_c$ with a log-log scaled inset. The inset corresponds to the function $\mathrm{corr} - n_0^2$, where n_0 is the 0-momentum particle density. The dashed line corresponds to a power-law fit for $L_0 = 100$ and data between $\mathrm{dist} = 5\% \; L_0$ and $\mathrm{dist} = 15\% \; L_0$. b. Exponents for the power-law fits for $T \leq T_c$. c. Logarithmic plot of the correlations at $T = 6 > T_c$. The dashed line corresponds to a power-law fit for $L_0 = 100$ and data between $\mathrm{dist} = 20\% \; L_0$ and $\mathrm{dist} = 35\% \; L_0$. d. Exponents for the exponential fits for $T > T_c$. The dashed line corresponds to a linear fit.

power-law exponents for fidelity and correlations also behave similarly, since they are constant for $T \leq 4$ and increase with the temperature for $T \in [4, 5.6]$. This also happens for the exponential exponents, since both exponents increase linearly with the temperature. However, we also observe that the long-range correlations at temperature $T \leq T_c$ are not reflected in the fidelity, a feature that has not been observed before in the context of locality of temperature.

4.5. Conclusions

We analyse a three-dimensional discrete version of the Bose-Einstein model (4.1) at the grand canonical state (4.2) with particle density n. We show that the system under-

goes a non-zero-temperature phase transition at temperature $T_c \approx 5.6$, below which all the particles have zero-momentum and the chemical potential μ is negligible, analogously to the Bose-Einstein condensate. Regarding the locality of temperature, we find that the temperature is locally well defined in this system, as the fidelity between the partial states ρ_C and ρ'_C tends to $F = 1$ for increasing boundary length, $L_{\mathbf{B}}$. In particular, the fidelity behaves differently above and below the phase transition: for $T \leq T_c$, the fidelity behaves as a power-law; and for $T > T_c$, the fidelity behaves exponentially. We also observe that the fidelity is minimum at $T = T_c$ for any boundary size $L_{\mathbf{BC}}$ and that it increases exponentially to $F = 1$ for large temperatures $T >> T_c$. We also find that the partial state ρ_C is highly mixed for any system size. This suggests that the partial state is highly independent of the system size L and it explains the high values of the fidelity, which is $F > 0.98$ for any case. Furthermore, we study density-density correlations as a function of the distance depending on the temperature. We obtain that they behave in different ways below and above the critical temperature T_c: for $T \leq T_c$, the system has long-range correlations as they decay to n_0^2 as a power-law; and for $T > T_c$, they decay exponentially to 0. This implies that the qualitative behaviours of the fidelity and correlations are the same, that is, that they behave as a power-law function for $T \leq T_c$ and as an exponential function for $T > T_c$. However, we observe long-range correlations at $T < T_c$ that do not appear to affect the locality of temperature.

5. Correlations in long-range interacting systems

We study correlations in fermionic systems with long-range interactions in thermal equilibrium. We prove an upper-bound on the correlation decay between anti-commuting operators based on long-range Lieb-Robinson type bounds. Our result shows that correlations between such operators in fermionic long-range systems of spatial dimension D with at most two-site interactions decaying algebraically with the distance with an exponent $\alpha \geq 2D$, decay at least algebraically with an exponent arbitrarily close to α. Our bound is asymptotically tight, which we demonstrate by numerically analysing density-density correlations in a 1D quadratic (free, exactly solvable) model, the Kitaev chain with long-range interactions. Away from the quantum critical point correlations in this model are found to decay asymptotically as slowly as our bound permits.

5.1. Introduction

Systems with long-range interactions decaying algebraically (power-law like) with the distance have many fascinating properties setting them apart from systems with merely finite-range or exponentially decaying (short range) interactions. Very recently, a surge of interest in the properties of these models has lead to a wealth of new insights. For example, in such systems very quick equilibration [Kas11, BK13, Kas17] and fast spreading of correlations [RGL$^+$14, MGFFG16], as well as violations of the area law [KLT12] and very fast state transfer [EGM$^+$17] are possible. They also show topological effects and support Majorana edge modes [VLE$^+$14, PNP17]. This development is to a large extent a consequence of the fact that such systems can be realized [PC04, DPC05, HCMH$^+$10, GTHC$^+$15] in extremely well controlled experiments with polar molecules [MBZ06], ultra-cold ions [IEK$^+$11, SPS12, BSK$^+$12, JLH$^+$14, RGL$^+$14], and Rydberg atoms [LBR$^+$16]. At the same time, many of the typical interactions in physics are actually algebraically decaying, such as dipole-dipole interactions, the van der Waals force, and, last but not least, the Coulomb interaction.

In some cases, realistic systems can be approximately captured by finite-range models, for example in the limit of a tight binding approximation. The physics of such systems has been at the center of attention of theoretical condensed matter physics. In particular, it has been proven for finite-range fermionic systems that the correlations between anti-commutating operators decay exponentially at any non-zero temperature [Has04b] and the same holds at zero temperature whenever there is a non-vanishing gap above the ground state [HK06]. Similarly, arbitrary observables above a threshold temperature in finite-range spin and fermionic systems [KGK$^+$14] show exponential decay of correlations. A similar level of understanding of the correlation decay of truly long-range interacting systems is lacking so far [PNP17], but is no less desirable due to their intriguing properties [CT96, Dys69, FMN72, DB01, PC04, DPC05, HCMH$^+$10, DPZ10, Kas11, KLT12, PMWB12, BK13, Kas17, EGM$^+$17, SBC16, PNP17].

In this chapter, we consider general fermionic two-site interacting long-range systems and prove that certain type of correlations at non-zero temperature decay at least with essentially the same exponent as the interaction strength. The upper bound for the correlations holds for any physical dimension. We also demonstrate that the bound is asymptotically tight by means of a high temperature expansion and by numerical simulations of a 1D Kitaev chain of fermions with long-range p-wave pairing at finite temperature, whose ground state phase diagram has been extensively studied [VLEP16, VLE$^+$14].

5.2. Setting and notation

We study the correlations and their decay behaviour in quantum many-body systems in thermal equilibrium at finite temperature T. We focus on systems of spinless fermions in which for each site $i \in \{1 \ldots, L\}$ we have a fermionic creation $a_i^\dagger$ and an annihilation operator a_i that satisfy the anti-commutation relations $\{a_i, a_j^\dagger\} := a_i \, a_j^\dagger + a_j^\dagger \, a_i = \delta_{i,j}$ (a generalization to spin fermions is straightforward). We denote by $n_i := a_i^\dagger a_i$ the particle number operator of site i. For O and O' operators on the Fock space we define their correlation coefficient (2.12) as

$$\mathrm{corr}_\beta(O, O') := \langle O \, O' \rangle_\beta - \langle O \rangle_\beta \, \langle O' \rangle_\beta, \tag{5.1}$$

where $\langle \cdot \rangle_\beta$ is the expectation value in the thermal state (2.21)

$$\Omega_\beta := \mathrm{e}^{-\beta H} / \mathrm{tr}(\mathrm{e}^{-\beta H}) \tag{5.2}$$

at inverse temperature $\beta := 1/k_B T$. We call an operator O even (odd) if it can be written as an even (odd) polynomial of creation and annihilation operators, i.e., if it

is a sum of monomials that are all products of an even (odd) number of a_i and $a_i^\dagger$. Odd operators anti-commute when they have disjoint supports. Due to the particle number parity super-selection rule Hamiltonians of physical systems are even operators and hence $\langle O \rangle_\beta = 0$ whenever A is an odd operator. In what follows, we will mostly be interested in the correlations between operators O and O' that are either particle number operators on different sites or odd operators on disjoint regions and how $\mathrm{corr}(O, O')$ decays with the distance of their supports.

Our result is obtained for fermionic systems on a hypercubic lattices of dimension D whose Hamiltonian can, for some constant J, be written in the form

$$H = \sum_{\kappa,i,j} J_{i,j}^{(\kappa)} \, V_i^{(\kappa)} \, V_j^{(\kappa)}, \tag{5.3}$$

in terms of normalized operators $V_i^{(\kappa)}$, each acting on their respective site i, and coupling coefficients $J_{i,j}^{(\kappa)}$ satisfying $\sum_\kappa J_{i,j}^{(\kappa)} \leq J \, d_{i,j}^{-\alpha}$ with $d_{i,j}$ the L_1-distance between the sites i and j. Thus, our result holds for fermionic systems with quadratic Hamiltonians as well as non-quadratic ones with two-site interactions. Further, our main result (Theorem 3) can be extended to Hamiltonians with interactions between pairs of patches of sites as long as their diameters are bounded by a constant, as well as to systems with more than one type of fermions.

5.3. A general bound on correlation decay in fermionic long-range systems

We now derive a general bound on the decay of correlations for long-range fermionic systems at non-zero temperature. Concretely, for O, O' odd operators we obtain a bound on $\mathrm{corr}_\beta(O, O') = \langle O\, O' \rangle_\beta$. In the case of quadratic Hamiltonians, our bound also yields, via Wick's theorem, a bound on correlations between even operators, such as density-density correlations, which are directly measurable in the type of experiments mentioned above. Our result is based on two main ingredients: An integral representation of $\langle O\, O' \rangle_\beta$ that was previously used in [Has04b] and an extension to the fermionic case of a very recently derived Lieb-Robinson-type bound for systems with long-range interactions [FFGCG15].

The first ingredient for our proof is the following integral representation of the expectation value $\langle O\, O' \rangle_\beta$ (see Appendix C.1 for more details):

Lemma 1 (integral representation [Has04b])**.** *Given a fermionic system at inverse temperature $\beta > 0$ and an even Hamiltonian and any two odd operators O, O' it*

5. Correlations in long-range interacting systems

holds that

$$\langle O\,O'\rangle_\beta = \frac{\langle\{O,O'\}\rangle_\beta}{2} + \int_0^\infty \frac{\mathrm{i}}{\beta}\,\frac{\langle\{O(t)-O(-t),O'\}\rangle_\beta}{\mathrm{e}^{\pi\,t/\beta}-\mathrm{e}^{-\pi\,t/\beta}}\,\mathrm{d}t. \qquad (5.4)$$

Lieb and Robinson [LR72] first proved that the propagation of information in quantum spin systems with short-range interactions is characterized by a group velocity bounded by a finite constant (2.26), which leads to a light-cone-like causality region. These results have since been generalized and improved in various aspects [Has04a, NVZ11] (see also [KGE14] for a review). Hastings and Koma [HK06] proved an upper bound on the group velocity that grows exponentially in time in systems with power-law decaying interactions with exponent $\alpha > D$. Improving upon this, Gong et al. [GFFMG14] derived a bound for $\alpha > D$, that consists of a exponentially and a power-law like decaying contribution. Foss-Feig et al. [FFGCG15] proved a Lieb-Robinson type bound with a group-velocity bounded by a power-law for two-site long-range interacting spin systems with the same form as in Eq. (5.3) for $\alpha > 2\,D$. Further, Matsuta et al. [MKN17] proved a closely related bound for long-range interacting spin systems for all $\alpha > D$. For $\alpha < D$ energy is no longer extensive and Lieb-Robinson-like bounds can only be achieved [EVDWMK13] when time is rescaled with the system size [SVK15].

For the purpose of our proof, we extend the Lieb-Robinson bound obtained by Foss-Feig et al. [FFGCG15] to fermionic systems. Here it takes the form of a bound on the operator norm $\|\ \|$ of the anti-commutator of odd operators:

Lemma 2 (Lieb-Robinson-like bound for fermionic long-range systems). *Consider a fermionic system on a hypercubic lattice of dimension D. Let $\alpha > 2\,D$ and $\gamma := (1+D)/(\alpha-2\,D)$. Assume that the Hamiltonian can be written in the form (5.3) with J a constant. Then, for any two odd operators A and B separated by a distance l there exist constants c_0 and c_1, independent of the system size, l, and t, such that*

$$\|\{O(t),O'\}\| \le c_0\,\mathrm{e}^{v\,|t|-l/|t|^\gamma} + c_1\,\frac{|t|^{\alpha\,(1+\gamma)}}{l^\alpha}, \qquad (5.5)$$

with $v \le 8\,J\,\exp(1)\,2^D$.

The proof of Lemma 2 follows the general strategy of [FFGCG15]. We explain all necessary technical modifications in Appendix C.2.

The main result is that for fermionic systems with two-site long range interactions and at non-zero temperature, correlations decay at least algebraically to zero with an exponent essentially given by the exponent α of the decay of the long-range interactions:

Theorem 3 (Power-law decay of correlations). *Consider a fermionic system on a D dimensional hypercubic lattice with a Hamiltonian of the form given in (5.3) with J a*

constant and $\alpha > 2\,D$. For any two odd operators O, O', denoting by l the distance between their supports, then for any $0 < \epsilon < 1$

$$|\operatorname{corr}_\beta(O, O')| \in \mathcal{O}(l^{-(1-\delta)\,\alpha}) \quad (l \to \infty). \tag{5.6}$$

Before we present the proof (which actually yields a concrete bound with calculable prefactors) of this theorem, let us interpret the result. It says that the correlations between any two odd (and therefore anti-commuting) operators in long-range interacting fermionic systems in thermal equilibrium at non-zero temperature decay at least power-law like at long distances, with an exponent that is arbitrarily close to the exponent α of the long-range interactions. This holds for systems with an arbitrary spatial dimension D as long as $\alpha \geq 2\,D$.

Proof of Theorem 3. We start by using Lemma 1. As $\{O, O'\} = 0$ only the second term from Eq. (5.4) is non-zero. We split up the integral in this term $I = I_{\leq \tau(l)} + I_{>\tau(l)}$ into an integral $I_{\leq \tau(l)}$ from time zero up to some value $\tau(l)$ (whose dependence on l we will chose later) and the rest $I_{>\tau(l)}$. We bound these two integrals separately. Using that $|\langle\{O(t) - O'(-t), B\}\rangle_\beta| \leq 4\,\|O\|\,\|O'\|$, we find

$$|I_{>\varsigma(l)}| \leq \left|\int_{\varsigma(l)}^\infty \frac{1}{\beta} \frac{4\,\|O\|\,\|O'\|}{e^{\pi\,t/\beta} - e^{-\pi\,t/\beta}}\ \mathrm{d}t\right|. \tag{5.7}$$

The integral satisfies

$$\int_{\varsigma(l)}^\infty \frac{1}{\beta} \frac{\mathrm{d}t}{e^{\pi\,t/\beta} - e^{-\pi\,t/\beta}} \leq \frac{\pi^{-1}}{e^{\pi\,\varsigma(l)/\beta} - e^{-\pi\,\varsigma(l)/\beta}} \tag{5.8}$$

and therefore we have

$$|I_{>\varsigma(l)}| \leq \frac{c_2/\pi}{e^{\pi\,\varsigma(l)/\beta} - e^{-\pi\,\varsigma(l)/\beta}} \tag{5.9}$$

with $c_2 := 4\,\|O\|\,\|O'\|$.

For the second term $I_{<\tau(l)}$ we use that $|\langle\{O(t), O'\}\rangle_\beta| \leq \|\{O(t), O'\}\|$ so that

$$|I_{<\varsigma(l)}| \leq \int_0^{\varsigma(l)} \frac{1}{\beta} \frac{\|\{O(t), O'\}\| + \|\{O(-t), O'\}\|}{e^{\pi\,t/\beta} - e^{\pi\,t/\beta}}\ \mathrm{d}t. \tag{5.10}$$

Next, we apply the Lieb-Robinson-like bound from Lemma 2,

$$\begin{aligned}|I_{<\varsigma(l)}| \leq\ & \frac{2\,c_0}{\beta} \int_0^{\varsigma(l)} \frac{e^{v\,t - l/t^\gamma}}{e^{\pi\,t/\beta} - e^{\pi\,t/\beta}}\ \mathrm{d}t \\ &+ \frac{2\,c_1}{\beta} \frac{1}{l^\alpha} \int_0^{\varsigma(l)} \frac{t^{\alpha\,(1+\gamma)}}{e^{\pi\,t/\beta} - e^{\pi\,t/\beta}}\ \mathrm{d}t.\end{aligned} \tag{5.11}$$

5. Correlations in long-range interacting systems

As $(e^{\pi t/\beta} - e^{\pi t/\beta})^{-1} \le \frac{\beta}{2\pi t}$ we further have

$$|I_{<\varsigma(l)}| \le \frac{c_0}{\pi} \int_0^{\varsigma(l)} \frac{e^{v\,t - l/t^\gamma}}{t}\, dt + \frac{c_1\, \varsigma(l)^{\alpha\,(1+\gamma)}}{\pi\,\alpha\,(1+\gamma)\,l^\alpha}. \tag{5.12}$$

Now, let $g(t) := e^{v\,t}\, e^{-l/t^\gamma}/t$. Notice that $g(t)$ is a product of the monotonically increasing function e^{vt} and the function $h(t) := e^{-l/t^\gamma}/t$ which satisfies: (i) it has a local maximum at $t_h^*(l) := (\gamma\,l)^{1/\gamma}$; (ii) it is monotonically increasing in $[0, t_h^*(l)]$. Therefore, $g(t)$ is also monotonically increasing in $[0, t_h^*(l)]$ so that, provided that $\varsigma(l) < t_h^*(l)$, we can bound

$$\int_0^{\varsigma(l)} g(t)\, dt \le g(\varsigma(l))\,\varsigma(l) = e^{v\,\varsigma(l) - l/\varsigma(l)^\gamma}. \tag{5.13}$$

For all $\tau(l) < t_h^*(l)$ we hence have the upper-bound

$$|I_{<\varsigma(l)}| \le \frac{c_0}{\pi}\, e^{v\,\varsigma(l) - l/\varsigma(l)^\gamma} + \frac{c_1}{\pi}\, \frac{1}{\alpha\,(1+\gamma)}\, \frac{\varsigma(l)^{\alpha\,(1+\gamma)}}{l^\alpha}. \tag{5.14}$$

It remains to find a good choice for $\varsigma(l)$. The function ς must grow unbounded with increasing l in order for the right hand side of Eq. (5.9) to go to zero and, at the same time, it must not grow too fast, so that $\varsigma(l) < t_h^*(l)$ is satisfied and the right hand side of Eq. (5.14) goes to zero for large l. We take $\varsigma(l) = (l/v)^{\frac{1}{\gamma+1}}\, l^{-\eta}$ with $\eta \in\,]0, 1/(\gamma+1)[$. This yields that for all such η

$$\begin{aligned}
\|\langle O\,O'\rangle_\beta\| &\le \frac{c_0}{\pi}\, e^{v^{\frac{\gamma}{\gamma+1}}\, l^{\frac{1}{\gamma+1}}\,(l^{-\eta} - l^{\gamma\,\eta})} \\
&\quad + \frac{c_1/\pi}{\alpha\,(1+\gamma)\,v^\alpha}\, l^{-\eta\,(1+\gamma)\,\alpha} + \frac{c_2/\pi}{e^{\pi\,v^{\frac{-1}{\gamma+1}}\, l^{\frac{1}{\gamma+1} - \eta}/\beta} - 1}.
\end{aligned} \tag{5.15}$$

As γ and η are positive and $\eta < 1/(\gamma+1)$, both the first and the last term decay super-algebraically for large l. The dominating term is thus the middle term, which implies the result as stated, where $\delta = 1 - \eta\,(1+\gamma)$. $\qquad\square$

We remark that we were not able to prove Theorem 3 from the other Lieb-Robinson bounds for systems with long-range interactions. In particular, when using the bound from [MKN17] that is valid for all $\alpha > D$, the term corresponding to the first term in Eq. (5.12) diverges because of the behaviour of the integrand in the limit $t \to 0$. It remains open whether the restriction to $\alpha > 2\,D$ in our result is an artefact of our proof technique or whether there is a physical reason.

64

5.4. Kitaev chain with long-range interactions

In the numerical part of this chapter we consider a generalization of the fermionic Kitaev chain [Kit01] with long-range p-wave pairing of size L, whose Hamiltonian $H := H_{\mathrm{FR}} + H_{\mathrm{LR}}$ consists of a finite-range (nearest neighbor) part

$$H_{\mathrm{FR}} := -t \sum_{i=1}^{L} \left(a_i^\dagger \, a_{i+1} + \text{h.c} \right) - \mu \sum_{i=1}^{L} \left(n_i - 1/2 \right) \tag{5.16}$$

with tunneling rate t and chemical potential μ, and a power-law decaying long-range pair-creation/pair-annihilation term

$$H_{\mathrm{LR}} := \frac{\Delta}{2} \sum_{i=1}^{L} \sum_{j=1}^{L-1} d_j^{-\alpha} \left(a_i \, a_{i+j} + a_{i+j}^\dagger \, a_i^\dagger \right), \tag{5.17}$$

where $d_j := \min(j, L - j)$, Δ is the coupling strength, and α the coupling exponent [VLE$^+$14]. Whenever L is finite, we consider a closed chain with anti-periodic boundary conditions, i.e., for $i > L$ we set $a_i := -a_{i \bmod L}$ as otherwise the long-range term vanishes due to the fermionic commutation relations (see Appendix C.3). As in [VLE$^+$14], in the remainder of this work, we consider the case $\Delta = 2\,t = 1$. This model has a rich ground state phase diagram with two critical points at $\mu = \pm 1$ [VLEP16, VLE$^+$14].

The model described above falls into the class of so-called, quadratic, free, or non-interacting models. Their Hamiltonians can be written as $H = \sum_{i,j} c_i^\dagger \, h_{ij} \, c_j$ where $\vec{c} := (a_1, a_1^\dagger, \ldots, a_m, a_m^\dagger)$ and the Hamiltonian matrix h is hermitian. By diagonalizing $h = U^\dagger \, D \, U$ it can then be brought into the form $H = \sum_i b_i^\dagger \, D_{ii} \, b_i$, with $\vec{b} := U \, \vec{c}$. From this normal-mode decomposition one can compute the elements $\text{corr}(b_j, b_k^\dagger)_\beta$ of the covariance matrix of the thermal state and, finally, expectation values of the form $\text{corr}(a_j, a_k^\dagger)_\beta$, which are just complex linear combinations of the $\text{corr}(b_j, b_k^\dagger)_\beta$.

This allows one to calculate higher moments, including the experimentally directly accessible density-density correlations $\text{corr}(n_j, n_k)$, in terms of the second moments of the thermal states of quadratic Hamiltonians, which are Gaussian states, via Wick's theorem. Concretely, for fermionic systems we have (Lemma 6 in [GKF$^+$16])

$$\langle \prod_{k=1}^{m} c_{i_k} \rangle_\beta = \text{Pf}(\Gamma[i_1, \ldots, i_m]), \tag{5.18}$$

where Pf is the Pfaffian and Γ has matrix elements

$$\left(\Gamma[i_1,\ldots,i_m]\right)_{a,b} := \begin{cases} \langle c_{i_a} c_{i_b} \rangle_\beta & \text{if } a < b, \\ -\langle c_{i_b} c_{i_a} \rangle_\beta & \text{if } a > b, \\ 0 & \text{otherwise} \end{cases} \tag{5.19}$$

In particular, for the density-density correlations we find

$$\mathrm{corr}_\beta(n_i, n_j) = \langle a_i^\dagger a_i a_j^\dagger a_j \rangle_\beta - \langle a_i^\dagger a_i \rangle_\beta \langle a_j^\dagger a_j \rangle_\beta \tag{5.20}$$

$$= \langle a_i^\dagger a_j \rangle_\beta \langle a_i a_j^\dagger \rangle_\beta - \langle a_i^\dagger a_j^\dagger \rangle_\beta \langle a_i a_j \rangle_\beta. \tag{5.21}$$

Thus with Theorem 3 we can bound density-density correlations, as well as higher order correlation functions between even and odd operators in quadratic models.

5.4.1. Numerical analysis

We now present the numerical results on the decay of density-density correlations between two sites separated by a distance l for different values of the chemical potentials μ, inverse temperatures β and interaction decay exponents α. We consider different chain lengths ($L \in \{500, 1000, 2000\}$) in order to identify the influence of finite size effects. We observe that asymptotically correlations decay power-law like for any temperature and interaction strength (see Appendix C.4), that is for all i and large l

$$\mathrm{corr}_\beta(n_i, n_{i+l}) \propto l^{-\nu}, \tag{5.22}$$

where ν characterizes the decay of the correlations. Away from the critical point, we observe that ν depends on α. At the quantum critical point ($T = 0$, $\mu = 1$) we observe universal behaviour with ν being independent of α, namely $\nu \approx 2$. Everywhere else we find $\nu \approx 2$ when $\alpha \leq 1$ and $\nu \approx 2\alpha$ when $\alpha > 1$ (see Figure 5.1). These results are in agreement with the results for the ground state in [VLE+14].
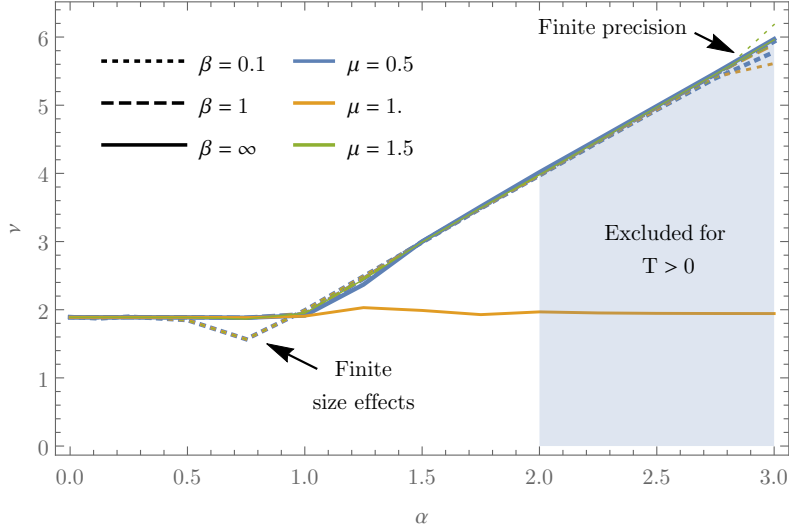
Figure 5.1.: Exponent ν as a function of the exponent of the interactions decay α extracted from the data for $L = 2000$. The blue, orange, and green lines correspond to $\mu = 0.5, 1.0, 1.5$. The line styles correspond to the inverse temperatures $\beta = 0.1, 1.0, \infty$. Exponents inside the shaded region are excluded by Theorem 3 whenever $T > 0$. For high temperatures and $\alpha < 1$ finite size effects slightly distort the results, for large α the finite precision is the limiting factor.

5.4.2. Application of the analytical bound

In this section we apply the Theorem 3 to the Kitaev chain. As the model is quadratic, we can use Eq. (5.20) to express the density-density correlations in terms of expectation values of odd operators and apply Theorem 3. This yields for any $0 < \delta < 1$

$$\mathrm{corr}_\beta(n_i, n_j) \in \mathcal{O}(l^{-2(1-\delta)\alpha}) \tag{5.23}$$

for any finite temperature $T > 0$ and for any $\alpha > 2\,D$.

A comparison with the numerics shows that Theorem 3 is asymptotically tight. The shaded region in Fig. 5.1 is the range of decay exponents excluded by Theorem 3. Despite the simplicity of the Kitaev chain, it shows correlations that are asymptotically as strong as possible for any fermionic system with power-law decaying two site interactions. Further, the restriction to $T > 0$ of Theorem 3 is not an artefact of our proof strategy but correlations actually do decay slower at the quantum critical point at $T = 0$ and $\mu = 1$.

5.5. High-temperature expansion

We perform a first-order high temperature expansion and see that the Kitaev model can be expected to essentially asymptotically saturate the bound from Theorem 3 for $T \to \infty$. For simplicity, consider only the long-range part of the Hamiltonian (5.17), then whenever correlations are analytic around $\beta = 0$ (not the case for $\alpha < 1$) one has in the limit $\beta \to 0$

$$| \operatorname{corr}_\beta(a_1, a_j)| = |\operatorname{tr}(a_1 \, a_j \, \mathrm{e}^{-\beta \, H_{\mathrm{LR}}})/\operatorname{tr}(\mathrm{e}^{-\beta \, H_{\mathrm{LR}}})| \qquad (5.24)$$

$$\geq |\operatorname{tr}(a_1 \, a_j \, \beta \, H_{\mathrm{LR}})/2^L - \mathcal{O}(\beta^2)| \qquad (5.25)$$

$$= |\beta \, \Delta \, d_{j-1}^{-\alpha}/4 - \mathcal{O}(\beta^2)|. \qquad (5.26)$$

More generally, for an arbitrary system with local dimension D and two-site interacting Hamiltonian $H := \sum_{i,j} H_{i,j}$ with $i, j \in [1, L]$ and any two traceless on-site operators O_i, O'_j one finds that if there is an interval $[0, \beta_0]$ in which $\operatorname{corr}_\beta(O_i, O'_j)$ is analytic, then for all $\beta \in [0, \beta_0]$

$$| \operatorname{corr}_\beta(O_i, O'_j)| \geq |\beta \, D^{-L}\operatorname{tr}(O_i \, O'_j \, H_{i,j}) - \mathcal{O}(\beta^2)|. \qquad (5.27)$$

Thus, two-site correlations are also lower-bounded for high temperature, with a lower bound that is proportional to the interactions between the two considered sites.

5.6. Conclusions

We have studied the correlation decay in fermionic systems with long-range interactions from analytical and numerical perspectives. More concretely, we consider systems described by two-site interacting Hamiltonians with power-law decaying interactions at thermal equilibrium at non-zero temperature $T > 0$. We then study the correlations between non-overlapping anti-commuting operators as a function of the distance between the operators and prove analytically an upper bound for the asymptotics of these correlations for an interaction exponent $\alpha > 2\,D$. The upper bound predicts that the correlations decay at least as a power-law with essentially the same exponent that characterizes the interactions of the system. Numerically, we study the density-density correlations for the Kitaev chain with long-range interactions at thermal equilibrium, which has a quantum phase transition. At the criticality, we obtain that correlations asymptotically decay with an universal exponent which is independent of the interactions. Away from the criticality, we obtain that correlations decay as a power-law with the smallest exponent allowed by the theoretical upper bound

for $\alpha > D$. Therefore, we are able to saturate the upper bound and we verify that our bound is asymptotically tight. We are also able to verify this by considering a high-temperature ($\beta \to 0$) expansion of the correlations.

5. Correlations in long-range interacting systems

6. Low-temperature thermometry enhanced by strong coupling

We consider the problem of estimating the temperature T of a very cold equilibrium sample. The temperature estimates are obtained from measurements performed on a quantum probe strongly coupled to it. We model this scenario by resorting to the canonical Caldeira-Leggett Hamiltonian and find analytically the exact stationary state of the probe for arbitrary coupling strength. In general, the probe does not reach thermal equilibrium with the sample, due to their non-perturbative interaction. We argue that this is advantageous for low-temperature thermometry, as we show in our model that (i) the thermometric precision at low T can be significantly enhanced by strengthening the probe-sampling coupling, (ii) the variance of a suitable quadrature of our thermometer can yield temperature estimates with nearly minimal statistical uncertainty, and (iii) the spectral density of the probe-sample coupling may be engineered to further improve thermometric performance. These observations may find applications in practical nanoscale thermometry at low temperatures, a regime which is particularly relevant to quantum technologies.

6.1. Introduction

The development of nanoscale temperature sensing techniques [CP15] has attracted an increasing interest over the last few years due to their potential applications to micro-electronics [WW86, ATMC05, LV05], biochemistry, or even to disease diagnosis [KN09, KMY+13, SCLD14, SG14]. In particular, thermometer miniaturization may be taken to the extreme of devising individual quantum thermometers [FVV+11, MB13, SHS+14, HIK14, NJD+13, KMY+13, JCM+16, HBPLB17]. The problem of measuring the temperature T of an equilibrium sample is most often tackled by thermally coupling it to a probe. After equilibration, one can estimate T by monitoring some temperature-dependent feature of the probe via a suitable measurement and data analysis scheme. Provided that the heat capacity of the probe is low, one usually assumes that the back-action on the sample can be neglected, and that the probe ends up in a Gibbs state at the sample temperature.

6. Low-temperature thermometry enhanced by strong coupling

Besides the nanometric spatial resolution of the ensuing temperature readings, using an individual quantum probe has the advantage of leaving the sample mostly unperturbed. In contrast, the direct manipulation of the sample, such as time-of-flight measurements of ultra-cold trapped atoms, is generally destructive and, thus, potentially problematic.

Such a simple picture runs into trouble if the sample is too cold, especially when using an individual quantum thermometer: The seemingly natural assumption of the probe reaching equilibrium at the sample temperature might break down at low T [NA02]. Furthermore, if the probe is too small, boundary effects become relevant and need to be taken into account to properly describe equilibration and thermalisation [GE16, FGSA12, KGK$^+$14, HSRH$^+$15]. As a result, thermometry with non-equilibrium quantum probes demands some knowledge about the internal structure of the sample, and the probe-sample coupling scheme.

One could still assume thermalisation at very low temperature if the probe-sample coupling is very weak. However, in this limit, the thermal sensitivity of the probe, which is proportional to its heat capacity [LL58, Man56, Man89, UvL99], drops quickly as the temperature decreases [Deb12]. This is an inherent problem of low-temperature thermometry [DRFG16].

In the following, we illustrate the difficulty of measuring low temperatures in the simplest case. We consider a quantum probe weakly coupled to a thermal sample, so that its steady state is thermal, i.e, $\Omega_T = e^{-\beta H_{\mathrm{p}}}/\mathrm{tr}(e^{-\beta H_{\mathrm{p}}})$ where H_{p} is the Hamiltonian of the probe, the inverse temperature $\beta = 1/T$ and T is the temperature of the sample. In order to quantify the maximum sensitivity attainable by the quantum probe, we make use of the quantum Fisher information (QFI) $\mathcal{F}_T$ (2.28), which sets a lower-bound on the estimation of the temperature via the quantum Cramér–Rao bound (2.27)

$$\delta T \geq 1/\sqrt{M\mathcal{F}_T}, \tag{6.1}$$

with M the number of measurements. If we consider a single-mode probe at equilibrium, we have its QFI $\mathcal{F}_T$ is such that

$$\mathcal{F}_T^{(\mathrm{eq})}(\omega) = \tfrac{\omega^2}{4T^4}\, \mathrm{csch}^2\left(\tfrac{\omega}{2T}\right), \tag{6.2}$$

which decays exponentially at low T, as can be inferred by expanding it as

$$\mathcal{F}_T^{(\mathrm{eq})}(\omega) = \tfrac{\omega^2}{2T^4} e^{-\omega/T} + \mathcal{O}(e^{-2\omega/T}) \tag{6.3}$$

for $T/\omega \ll 1$. This applies to harmonic probes and optimized finite-dimensional equilibrium thermometers [CMAS15]. This decay implies that even an estimate based on

the most informative measurements on an optimized equilibrium probe has an exponentially vanishing precision as $T/\omega \to 0$. Due to this inherent limitation, devising practical strategies to enhance low-temperature sensitivity becomes relevant.

The aim of this chapter is to find a proposal to fight the fundamental limitation of thermometry at low-temperature. In particular, we extend quantum thermometry to the strong coupling regime, by adopting a fully rigorous description of the probe and its dynamics. To that end, we make use of the Caldeira-Leggett Hamiltonian, one of the most paradigmatic dissipation models [Wei08]. The equilibrium sample is thus represented by a bosonic reservoir [CL83, RHW85] which is dissipatively coupled to a single harmonic oscillator, playing the role of the thermometer. We calculate the exact steady state of the probe analytically and show that the low-temperature sensitivity is significantly enhanced by increasing the coupling strength. We also find that the optimal measurements for strong coupling are given by the square of the position quadrature of the probe, contrary to the typical case of energy measurements [CMAS15]. It is important to stress that we are not limited by any of the simplifying assumptions usually adopted when dealing with open quantum systems, such as the Born-Markov or secular approximations, nor rely on perturbative expansions in the dissipation strength [BKP01, BGM06]. In fact, our methods are totally general and, thus, not limited to a specific probe-sample coupling scheme.

6.2. The model and its exact solution

We now present the details of the considered scenario. The Hamiltonian of our probe is

$$H_{\mathrm{p}} = \frac{1}{2}\omega_0^2 x^2 + \frac{1}{2}p^2 \tag{6.4}$$

(where the mass of the probe is $m = 1$), whereas the sample is described as an infinite collection of non-interacting harmonic oscillators

$$H_{\mathrm{s}} = \sum_i \frac{1}{2}\omega_i^2 m_i x_i^2 + \frac{1}{2m_i}p_i^2. \tag{6.5}$$

The probe-sample coupling is realized by a linear term of the form

$$H_{\mathrm{p-s}} = x \sum_i g_i x_i. \tag{6.6}$$

6. Low-temperature thermometry enhanced by strong coupling

In order to compensate exactly for the "distortion" caused on the probe by the coupling to the sample, one should replace ω_0^2 with $\omega_0^2 + \omega_R^2$ in H_p [CL83, Wei08], where

$$\omega_R^2 := \sum_i \frac{g_i^2}{m_i \omega_i^2} \tag{6.7}$$

This can be explained by splitting the Hamiltonian into a potential and a kinetic term: $H = U(x, x_i) + K(p, p_i)$. One can see that the effective potential "felt" by the probe is given by $U(x, x_i^\star)$, where

$$x_i^\star = -\frac{g_i x}{m_i \omega_i^2} \tag{6.8}$$

such that $\partial_{x_i} U = 0$ at $x_i^\star$ and, thus, $U(x, x_i^\star) = \frac{1}{2}(\omega_0^2 - \omega_R^2)x^2$. As a result, the high temperature limit of the reduced steady state of the probe obtained from the bare model $H = H_p + H_s + H_{p-s}$ is

$$\mathrm{tr}_s \rho \propto \exp\left(-\frac{1}{2T}(\omega^2 - \omega_R^2)x^2 - \frac{1}{2T}p^2\right), \tag{6.9}$$

which may differ significantly from the corresponding thermal state of the probe $\Omega_T = Z^{-1} \exp(-H_p/T)$ if the couplings g_i are strong. Therefore, it is necessary to introduce the frequency shift ω_R^2 in H_p ad hoc to correct this effect.

The coupling strengths between the probe and each of the sample modes are determined by the spectral density

$$J(\omega) := \pi \sum_i \frac{g_i^2}{2m_i \omega_i} \delta(\omega - \omega_i), \tag{6.10}$$

which is given a phenomenological analytical form. In the first part of this chapter, we shall work with an Ohmic spectral density with Lorentz-Drude cutoff [BP02], given by

$$J(\omega) = 2\gamma\omega\,\omega_c^2/(\omega^2 + \omega_c^2). \tag{6.11}$$

The dissipation strength γ carries the order of magnitude of the couplings g_i, and ω_c denotes the cutoff frequency, required to ensure convergence. Notice that it is possible to introduce a cutoff frequency ω_c due to the fact that even if the sample is very large (as compared to the probe), it is finite and, thus, it has a maximum energy. Besides, the non-equilibrium steady state of the central oscillator will unavoidably depend on the choice of ω_c but as long as $\omega_c \gg \omega_0$, this dependence should be weak and not change its qualitative features [CVA12].

The following quantum Langevin equation [GWT84, Wei08] can be obtained from the Heisenberg equations for x, p, x_i and p_i:

$$\ddot{x}(t) + (\omega_0^2 + \omega_R^2)x(t) - x(t)\,\chi(t) = f(t). \tag{6.12}$$

The first two terms in the left-hand side of Eq. (6.12) correspond to the coherent dynamics of a free harmonic oscillator of squared frequency $\omega_0^2 + \omega_R^2$ (the dots denote time derivative), while the incoherent superposition of all environmental modes, encompassed in $f(t)$, plays the role of a driving force with $\langle f(t) \rangle = 0$ (see Appendix D.1). The convolution

$$x(t)\,\chi(t) := \int_{-\infty}^{\infty} \mathrm{d}s\,\chi(t-s)\,x(s) \tag{6.13}$$

brings memory effects into the dissipative dynamics. Here,

$$\chi(t) := \frac{2}{\pi}\Theta(t)\int_0^{\infty} \mathrm{d}\omega\, J(\omega)\sin\omega t, \tag{6.14}$$

where $\Theta(t)$ stands for the step function.

It is important to remark that Eq. (6.12) is exact. The only assumption that we make when solving it is that probe and sample start uncorrelated at $t_0 \to -\infty$, i.e. in $\rho\otimes\Omega_T$, where Ω_T is the Gibbs state of the sample at temperature T. The initial state of the probe ρ is arbitrary. However, since the Hamiltonian H is overall quadratic in positions and momenta, its stationary state is Gaussian, and, thus, completely determined by its first and second-order moments: $\langle R_i(t) \rangle$ and

$$\Gamma_{ij}(t',t'') := \frac{1}{2}\langle\{R_i(t'), R_j(t'')\}\rangle, \tag{6.15}$$

where $R = (x,p)$ [GWT84]. The notation $\langle\cdots\rangle$ stands here for average on the initial state and $\{\cdot,\cdot\}$ denotes anti-commutator.

One may now take the Fourier transform ($\tilde{f}(\omega) := \int_{-\infty}^{\infty}\mathrm{d}t\,f(t)e^{i\omega t}$) in Eq. (6.12), such that

$$-\omega^2\tilde{x} + (\omega_0^2 + \omega_R^2)\tilde{x} + \tilde{x}\,\tilde{\chi} = \tilde{f}$$
$$\Rightarrow \tilde{x}(\omega) = \alpha(\omega)^{-1}\tilde{f}(\omega) \tag{6.16}$$

where $\alpha(\omega) := \omega_0^2 + \omega_R^2 - \omega^2 - \tilde{\chi}(\omega)$. The position correlator $\Gamma_{11}(t',t'')$ can be thus cast as

$$\Gamma_{11} = \frac{1}{2}\langle\{x(t'), x(t'')\}\rangle = \iint_{-\infty}^{\infty}\frac{\mathrm{d}\omega'\,\mathrm{d}\omega''}{8\pi^2}\,e^{-i(\omega't'+\omega''t'')}\,\langle\{\tilde{x}(\omega'), \tilde{x}(\omega'')\}\rangle. \tag{6.17}$$

Substituting equation (6.16) into the expression (6.17), we obtain that

$$\Gamma_{11} = \iint_{-\infty}^{\infty}\frac{\mathrm{d}\omega'\,\mathrm{d}\omega''}{8\pi^2}\,e^{-i(\omega't'+\omega''t'')}\,\alpha(\omega')^{-1}\,\alpha(\omega'')^{-1}\,\langle\{\tilde{f}(\omega'), \tilde{f}(\omega'')\}\rangle. \tag{6.18}$$

Similarly, Γ_{22} may be calculated by noticing that

$$\langle\{\tilde{p}(\omega')\tilde{p}(\omega'')\}\rangle = -\omega'\omega''\langle\{\tilde{x}(\omega')\tilde{x}(\omega'')\}\rangle. \tag{6.19}$$

The remaining covariances are $\Gamma_{12} = \Gamma_{21} = 0$. Note that since $\langle f(t) \rangle = 0$, its Fourier transform $\langle \tilde{f}(\omega) \rangle = 0$ and, thus, all the stationary first-order moments vanish as their Fourier transforms are proportional to $\langle \tilde{f}(\omega) \rangle$. Hence, all we need to know is the power spectrum of the noise $\langle\{\tilde{f}(\omega')\tilde{f}(\omega'')\}\rangle$ and the Fourier transform of the dissipation kernel $\tilde{\chi}(\omega)$, which appears in $\alpha(\omega)$. Since the sample was prepared in a Gibbs state, one can show that the noise is connected to the dissipation kernel through the following fluctuation-dissipation relation (see Appendix D.2)

$$\langle\{\tilde{f}(\omega'), \tilde{f}(\omega'')\}\rangle = 4\pi\,\delta(\omega' + \omega'')\coth\left(\tfrac{\omega'}{2T}\right)\mathrm{Im}\,\tilde{\chi}(\omega') \tag{6.20}$$

with $\tilde{\chi}(\omega) = 2\gamma\omega_c^2/(\omega_c - i\omega)$ for our spectral density.

Putting together the pieces from the above paragraphs, we can compute the steady-state covariances $\Gamma_{ij}(t, t)$ [CVA12, VCA13, VAK13, VRA15] (recall that $t_0 \to -\infty$). Importantly, our choice of $J(\omega)$ makes it possible to evaluate the covariances analytically (see Appendix D.4.1). These may be collected into the 2×2 matrix $\boldsymbol{\sigma}$, which provides a full description of the (Gaussian) non-equilibrium asymptotic state [FOP05].

6.3. Enhanced thermometry at low T

We show here how strong dissipation improves the achievable precision for thermometry at low T and how the estimation bound can be saturated by selecting suitable measurements.

6.3.1. Dissipation-driven thermometric enhancement

We can now calculate $\mathcal{F}_T$ from Eq. (2.28), using the fact that the Uhlmann fidelity between two single-mode Gaussian states with covariance matrices $\boldsymbol{\Gamma}_1$ and $\boldsymbol{\Gamma}_2$ is given by

$$\mathrm{F}\,(\boldsymbol{\Gamma}_1, \boldsymbol{\Gamma}_2) = 2\,(\sqrt{\Delta + \Lambda} - \sqrt{\Lambda})^{-1}, \tag{6.21}$$

where $\Delta := 4\det(\boldsymbol{\Gamma}_1 + \boldsymbol{\Gamma}_2)$ and $\Lambda := (4\det\boldsymbol{\sigma}_1 - 1)(4\det\boldsymbol{\sigma}_2 - 1)$ [Scu98]. In Figure 6.1.a we plot the best-case relative error $\delta T/T = 1/(T\sqrt{\mathcal{F}_T})$ (disregarding the factor $1/\sqrt{M}$) versus the temperature of the sample, for different dissipation strengths γ.
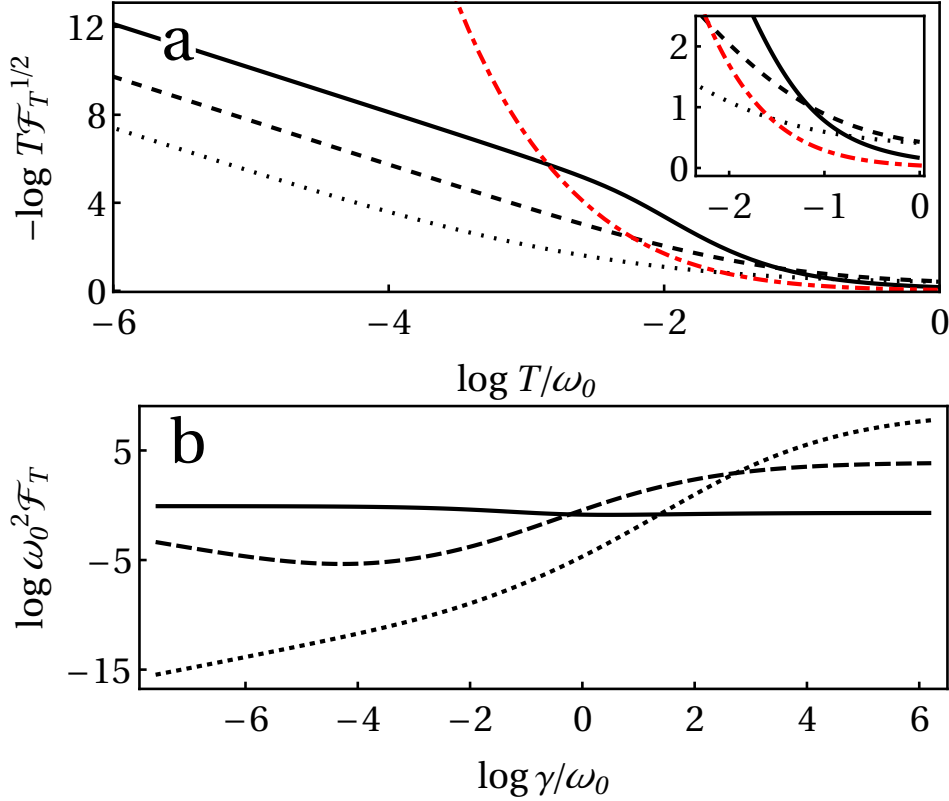
Figure 6.1.: a. Log-log plot of the best-case relative error $\delta T/T = 1/(T\sqrt{\mathcal{F}_T})$ vs. the sample temperature T for different dissipation strengths γ; namely, $\gamma/\omega_0 = 0.1$ (solid), $\gamma/\omega_0 = 1$ (dashed line), and $\gamma/\omega_0 = 5$ (dotted line). The relative error of a single-mode probe at thermal equilibrium (dot-dashed red) has been super-imposed for comparison. $\delta T/T$ diverges as $T \to 0$; while for the thermal mode it would diverge exponentially, our exact solution yields $\delta T/T \sim T^{-2}$ at low T. Whenever $T/\omega_0 \ll 1$, increasing the dissipation strength results in a significant reduction of the minimum $\delta T/T$. On the contrary, at larger temperatures, the best-case relative error need not be monotonically decreasing with γ. This is shown in the inset, which zooms into the bottom-right corner of the plot. Log-log plot of $\mathcal{F}_T$ as a function of γ for $T = 1$ (solid), $T = 0.1$ (dashed), and $T = 0.01$ (dotted). It becomes again clear that, while not strictly monotonic in γ, the QFI always grows with the dissipation strength for $\gamma/\omega_0 \gtrsim 1$ at $T/\omega_0 \ll 1$. Furthermore, as $T/\omega_0 \to 0$, we observe such a sensitivity enhancement at arbitrarily weak probe-sample coupling. In both cases $\omega_c = 100\,\omega_0$ and $\hbar = k_B = \omega_0 = 1$

We see how, at low T, the performance of our thermometer is significantly improved by strengthening its coupling to the sample. However, the QFI does not increase monotonically with γ, as illustrated in Figure 6.1.b . Instead, only at cold enough T is the performance of the probe monotonically enhanced by sufficiently strengthening the probe-sample interaction. In the limiting case of approaching zero temperature, such dissipation-assisted enhancement can be attained at arbitrarily low probe-sample coupling.

It is necessary to specify what we mean by cold enough and sufficiently strong in this context. The central energy scale of our problem is set by the frequency of the probe ω_0. We say that the sample is cold whenever $T/\omega_0 \ll 1$ so that the probe has a very low thermal population. On the other hand, we say that the coupling is strong whenever it is non-perturbative; that is, when $\gamma/\omega_0 \gtrsim 1$. In this situation, the probe will certainly end up in a non-equilibrium steady state [GWT84]. Thus going back to Figure 6.1.b , we see that, provided that $T/\omega_0 \ll 1$ and $\gamma/\omega_0 \gtrsim 1$, $\mathcal{F}_T$ increases monotonically with the dissipation strength. Hence, the probe-sample coupling can be thought of as a relevant control parameter in practical low-temperature quantum thermometry. This is our main result.

It is worth stressing that even though, in the above, we have resorted to an Ohmic spectral density with algebraic high-frequency cutoff, the exact same qualitative behaviour follows from a spectral density with exponential cutoff $J_s(\omega) := \frac{\pi}{2}\gamma\omega^s\omega_c^{1-s}e^{-\omega/\omega_c}$ and a tunable Ohmicity parameter s. In particular, we give full details on how to solve the ubiquitous super-Ohmic case $s > 1$ in Appendix D.3.

We shall now give an intuition about the origin of the observed dissipation-driven enhancement. To that end, let us consider not just the marginal of the probe but the global state of probe and sample. For simplicity we can model them as a finite N-mode star system, comprised of a central harmonic oscillator (playing the role of the probe), linearly coupled to $N-1$ independent peripheral oscillators with arbitrary frequencies (representing the sample). Let us further prepare the N-mode composite in a Gibbs state at the sample temperature T. Indeed, when such system is at thermal equilibrium, and provided that the number of modes N is large enough, the marginal of the central oscillator approximates well the actual steady state of the probe [SFTH12] (see Appendix D.5).

6.3.2. How to exploit strong dissipation in practice

Thus far, we have shown how strong coupling may improve the ultimate bounds on thermometric precision at low temperatures. However, we have not yet discussed how

to saturate those bounds in practice. We therefore need to find observables capable of producing temperature estimates that approach closely the precision bound set by the QFI.

In general, a temperature estimate based on M independent measurements of some
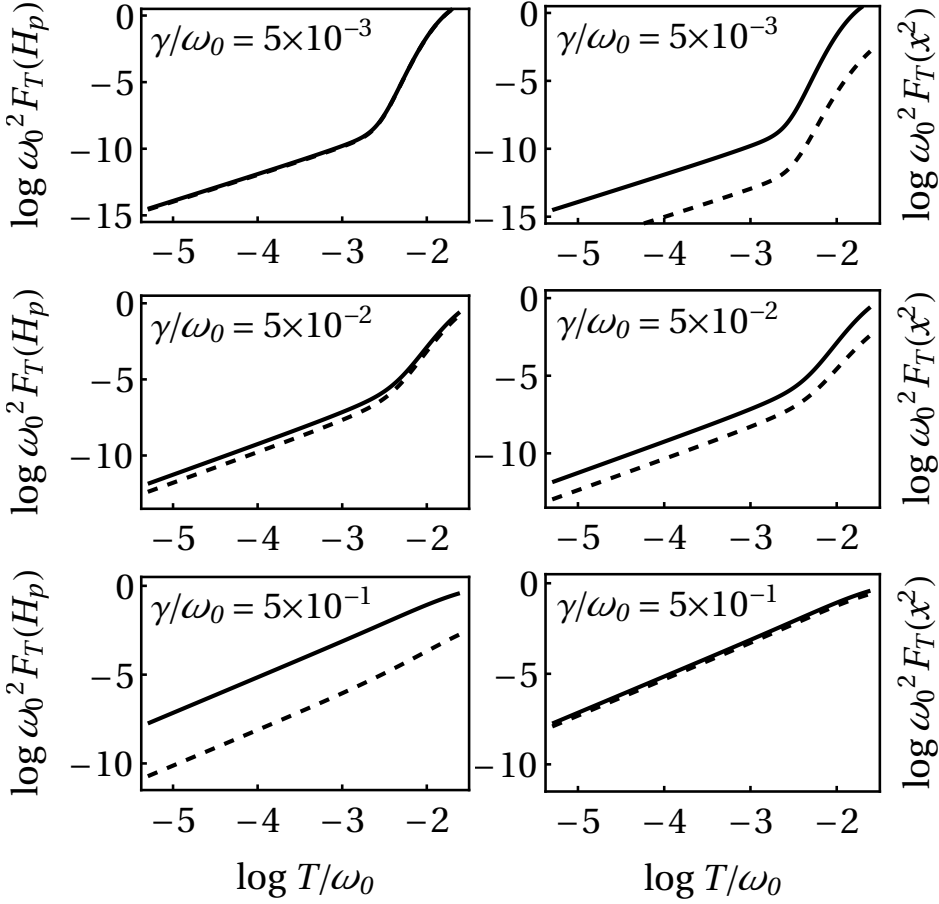
Figure 6.2.: Log-log plot of the QFI $\mathcal{F}_T$ (solid line on all panels), thermal sensitivity of the energy of the probe $F_T(H_\mathrm{p})$ (dashed line on the left-hand panels), and $F_T(x^2)$ (dashed line on the right-hand panels), for different values of the dissipation strength: $\gamma/\omega_0 = 5 \times 10^{-3}$ (top), $\gamma/\omega_0 = 5 \times 10^{-2}$ (middle), and $\gamma/\omega_0 = 0.5$ (bottom). Note that the thermal sensitivity H_p is deterred as the dissipation strength grows, whilst x^2 becomes a quasi-optimal temperature estimator. As in Figure 6.1, $\omega_c = 100$ and $\hbar = k_B = \omega_0 = 1$.

observable O on the steady state of the probe has uncertainty $\delta T \geq 1/\sqrt{M \, \mathscr{F}_T(O)}$, where $\mathscr{F}_T(O)$ stands for the classical Fisher information of O [BNG00]. This may be lower-bounded by the thermal sensitivity

$$F_T(O) := \frac{|\partial_T \langle O \rangle|^2}{(\Delta O)^2} \leq \mathscr{F}_T(O) \leq \mathcal{F}_T \equiv \sup_O f_T(O) \qquad (6.22)$$

[BC94, TA14]. Here, $\Delta O := \sqrt{\langle O^2 \rangle - \langle O \rangle^2}$ denotes standard deviation on the stationary state of the probe. The observable for which $F_T(O)$ is maximized (i.e. $F_T(O) = \mathscr{F}_T(O) = \mathcal{F}_T$) commutes with the so-called symmetric logarithmic derivative (SLD) L, which satisfies $\partial_T \rho = \frac{1}{2}(L\rho + \rho L)$. For instance, in the case of an equilibrium probe, i.e. $\Omega_T \propto \exp{(-H_{\mathrm{p}}/T)}$, one has $[L, H_{\mathrm{p}}] = 0$. Consequently, a complete projective measurement on the energy basis renders the best temperature estimate. However, as shown in Figure 6.2, when the strength of the interaction with the sample increases, energy measurements become less and less informative about the temperature of the sample—the larger the dissipation strength γ, the smaller $F_T(H_{\mathrm{p}})/\mathcal{F}_T$. Estimates based on energy measurements seem thus incapable of exploiting the extra low-temperature sensitivity enabled by the strong dissipation.

In searching for a more suitable measurement scheme, one can look at the SLD: Since Ω_T is an undisplaced Gaussian, L will be a quadratic form of x^2 and p^2 [Mon13]. Due to our choice for the probe-sample coupling ($x \sum_i g_i x_i$), the steady state Ω_T becomes squeezed in the position quadrature at $T/\omega_0 \ll 1$ and $\gamma/\omega_0 \gtrsim 1$ [GWT84, LLGML17]. Interestingly, we observe that $\langle x^2 \rangle$ is much more sensitive to temperature changes in this regime than $\langle p^2 \rangle$. We thus take $O = x^2$ as an ansatz for a quasi-optimal temperature estimator. $F_T(x^2)$ is also plotted in Figure 6.2, where we can see how it does approach closely the ultimate bound $\mathcal{F}_T$ as γ grows (at $T/\omega_0 \ll 1$). This numerical observation can be confirmed by taking the low-temperature limit on the analytic stationary covariances (see Appendix D.4.2).

Measuring the variance of the most relevant quadrature of a thermometer is therefore a practical means to exploit the thermometric advantage provided by strong dissipation at low temperatures. It is worth mentioning that quadratures of trapped particles are either directly measurable [BvZS06] or accessible via state tomography [DM96, PWC$^+$96], and that systems such as an impurity in a BEC may admit a Caldeira-Leggett description [LLGML17].
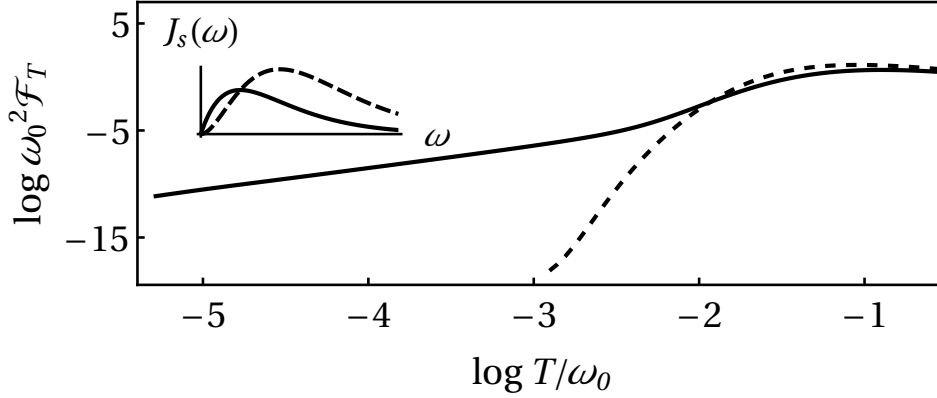
Figure 6.3.: Log-log plot of the QFI $\mathcal{F}_T$ as a function of temperature for Ohmic (solid) and super-Ohmic (dashed) spectral density $J_s(\omega)$ with exponential high-frequency cutoff ($s = 1$ and $s = 2$, respectively). In the inset, both spectral densities are compared. Note that the Ohmic form largely outperforms the super-Ohmic one at low temperatures ($\gamma/\omega_0 = 0.1$, $\omega_c = 100\omega_0$, and $\hbar = k_B = \omega_0 = 1$).

6.4. Further enhancement

The frequencies of the lowest normal modes of the global star system always decrease monotonically as the overall magnitude of the coupling strengths increases (see Appendix D.5). If the temperature T was so low that not even the first harmonic could get thermally populated, the sensitivity of the entire system and, by extension, also that of the central probe, would vanish. However, one could populate the first few normal modes by strengthening the couplings, as their frequencies would then decrease (see Figure 6.1.b). It is this effect which ultimately enables temperature sensing at low T. The magnitude of the enhancement is dictated by the specific frequency distribution of the probe-sample couplings which, in turn, determines the spectrum of the normal modes of the global system.

From the above reasoning it follows that the shape of the spectral density $J(\omega)$ could, in principle, be tailored to render more precise low-temperature probes. To see that this is indeed the case, we shall adopt a generic spectral density of the form $J_s(\omega) := \frac{\pi}{2}\gamma\omega^s\omega_c^{1-s}e^{-\omega/\omega_c}$. We can thus compare the performance of a single-mode thermometer coupled to the sample through an Ohmic ($s = 1$) and a super-Ohmic ($s > 1$) spectral density. Importantly, the dissipation kernel $\tilde{\chi}(\omega)$ needs to be re-calculated due to the change in spectral density [VRA15] (see Appendix D.3). Note as well that now $\omega_R^2 = \gamma\omega_c\Gamma_0(s)$, where $\Gamma(z)_0 := \int_0^\infty dt\, t^{z-1}e^{-t}$ is Euler's Gamma function.

In Figure 6.3 we can see how the Ohmic spectral density offers a clear advantage over the super-Ohmic one at low temperatures. This is in line with our qualitative argument explaining the dissipation-driven enhancement in precision: A thermometer coupled more strongly to the lower frequency modes of the sample (i.e. the only ones substantially populated at low T) should perform better.

6.5. Conclusions

We study how thermometry can be enhanced via strong coupling between the probe and the system for low temperatures. In particular, we consider a bosonic system described by the Caldeira-Leggett Hamiltonian [Wei08] and at thermal equilibrium, where the system is a bosonic reservoir and the probe is represented by a single-mode harmonic oscillator. We then show that the thermal sensitivity of the single-mode probe can be boosted by increasing the strength of its dissipative coupling to the sample under study. We also provide a concrete and feasible measurement scheme capable of producing nearly optimal temperature estimates in the relevant regime. Moreover, we suggest that the spectral density of the probe-sample coupling can be set to play an active role in enhanced low-temperature quantum thermometry.

7. Conclusions and outlook

In this chapter, we review the main conclusions of each work and discuss open questions.

7.1. Locality of temperature for one-dimensional spin systems

In Chapter 3, we study the problem of locality of temperature for quantum spin chains with strong but finite-range interactions. Upon noting that in the presence of strong interactions the marginal states of a global thermal state do not take the canonical form, we go on defining an effective thermal state for a subsystem. The effective thermal state refers to the reduced density matrix of the subsystem considered as a part of a slightly bigger, enveloping thermal system. Borrowing concepts from quantum information theory and employing methods from quantum statistical mechanics, we show that temperature is local for any quantum spin chain. In order to prove this, we have related the accuracy with which the effective thermal state describes the actual state of the subsystem to the correlations present in the whole system. Away from the critical point, we build a tensor network representation of the corresponding states of the subsystem to provide upper bounds on the aforementioned accuracy, depending on the size of the enveloping thermal system, the spectral gap of the global Hamiltonian and the global temperature. At the quantum critical point, we use already existing asymptotic formulas from conformal field theory to bound the accuracy.

Finally, we exemplify our analytical findings by analysing a model of a quantum Ising chain. The latter is complex enough to have a quantum phase transition point, but simple enough to allow for an exact diagonalization by standard tools of statistical mechanics, thereby serving as a perfect test-bed for our analytical upper bounds. In particular, we find that, e.g., away from criticality, the envelope which is bigger than the system only by one layer of spins, is enough to approximate the actual state with good precision. Investigating the properties of effective thermal states in higher dimensions is an interesting direction for further research. For instance, it would be interesting to study the problem of locality for generic quadratic Hamiltonians for

high dimensional systems. Another intriguing question is whether the locality of temperature is also satisfied by long-range interacting systems. Given its relation with correlations [KGK$^+$14], the different phenomenology of long-range interactions will affect the locality in a non-trivial manner. Other questions of interest are whether the locality of temperature is valid in 1D bosonic systems in a similar way to fermions or in a system with a non-zero-temperature phase transitions. In a more practical vein, another field where our findings may have implications is quantum thermometry [DRFG16], where our results may allow for new measurement schemes.

7.2. Locality of temperature and correlations in the presence of non-zero-temperature phase transitions

In Chapter 4, we analyse the problem of locality of temperature for a bosonic model with a phase transition at non-zero temperature. In particular, we consider a 3D bosonic model at the grand canonical state (4.2) with particle density n. This model represents a discrete version of the Bose-Einstein model as: (i) it reproduces its eigenvalues at the continuous limit; (ii) it undergoes a phase transition at temperature $T_c > 0$ when the particle density is fixed, below which all the particles have zero-momentum; and (iii) the chemical potential μ is negligible at temperature $T < T_c$ for a fixed density.

Following a similar scheme to Chapter 3, we study the distinguishability between the partial state of a subsystem embedded in a global system at thermal equilibrium and an effective thermal state. We obtain that the temperature is locally well-defined regardless of the phase transition at non-zero temperature. We also observe that the aforementioned distinguishability behaves qualitatively different above and below the critical temperature, depending on the temperature, the particle density and the size of the enveloping thermal system. Specifically, it behaves as a power-law decaying function with the boundary size for $T \leq T_c$ and exponentially for $T > T_c$. Additionally, we find that the partial state of the subsystem is highly mixed for any size of the global system. This implies that the partial state is highly independent of the system size L and it explains the high values of the fidelity, as $F > 0.98$ for any case. Finally, we study density-density correlations as a function of the distance for a large system size. We observe that the correlations decay in different ways below and above the critical temperature T_c, decaying up to a constant value as a power-law function for $T \leq T_c$ and decaying to zero as an exponential function for $T > T_c$. These results are qualitatively equivalent to the behaviours observed for the distinguishabil-

ity between the subsystem state and the effective thermal state for each temperature regime, showing a relation between locality and correlations. We remark that there are long-range correlations below the critical temperature, $T \leq T_c$, that do not affect the locality of temperature. Thus, we can only assure a non-trivial qualitative relation between correlations and locality, in opposition to the direct relation observed in previous works [HSRH$^+$15]. This raises an open problem about the role of correlations for non-zero-temperature phase transitions. In particular, it would be interesting to understand how the different quantum and classical contributions of the correlations affect the locality of temperature and whether the boundary conditions play a role on this problem. Another intriguing question is based on the numerical results about the highly mixed partial states of the considered system, where we wonder whether this is in general true for highly dimensional systems and whether this depends on the choice of periodic boundary conditions.

7.3. Correlations in long-range interacting systems

In Chapter 5, we study the correlation decay in fermionic systems with long-range interactions. More concretely, we consider systems described by two-site long-range interacting Hamiltonians with power-law decaying interactions at thermal equilibrium at non-zero temperature $T > 0$. We then study the correlations between non-overlapping anti-commuting operators as a function of the distance between the operators and prove analytically an upper bound for the asymptotics of these correlations for an interaction exponent $\alpha > 2D$. The upper bound predicts that the correlations decay at least as a power-law with the same exponent that characterizes the interactions of the system, α. Numerically, we study the density-density correlations for the Kitaev chain with long-range interactions at thermal equilibrium, model which has a quantum phase transition at $T = 0$. At criticality, we obtain that correlations asymptotically decay with a universal exponent which is independent of the interactions. Away from the criticality, we obtain that correlations decay as a power-law with the smallest exponent allowed by the theoretical upper bound for $\alpha > D$, with $D = 1$ for the chain. Therefore, we are able to saturate the upper bound and, thus, we verify that our bound is asymptotically tight. We are also able to verify this by considering a high-temperature ($\beta \to 0$) expansion of the correlations, regime where the correlations are lower bounded by a power law with exponent α. These results suggest an absence of non-zero-temperature phase transitions observed in the asymptotic decay of correlations for the models where the bound applies, as the decay of correlations for high temperature is typically the strongest decay. Notice here that these phase transitions do not exist for one-dimensional systems with short-range interactions. Therefore, it

might be possible that the absence of phase transition at non-zero temperature for one-dimensional systems can be extended to long-range interacting systems. Nonetheless, we do not actually prove the absence of phase transitions in the considered models. This constitutes a fundamental question in long-range systems and an interesting problem for future research.

7.4. Low-temperature thermometry enhanced by strong coupling

In Chapter 6, we study how thermometry can be enhanced via strong coupling between the probe and the system for low temperatures. In particular, we consider a bosonic system described by the Caldeira-Leggett Hamiltonian and at thermal equilibrium, where the system is a bosonic reservoir and the probe is represented by a single-mode harmonic oscillator. We then show that the thermal sensitivity of the single-mode probe can be boosted by increasing the strength of its dissipative coupling to the sample under study. We also provide a concrete and feasible measurement scheme capable of producing nearly optimal temperature estimates in the relevant regime. Moreover, we suggest that the spectral density of the probe-sample coupling can be set to play an active role in enhanced low-temperature quantum thermometry. This calls for a more in-depth analysis of the potential role of reservoir engineering techniques [KKS94] or even dynamical control [ZÁK16] in enhanced low-T quantum thermometry. As a final remark, we note that, since the equilibrium state of the probe corresponds to the marginal of a global thermal state [SFTH12], we can think of our results as an instance of thermometry on a macroscopic sample through local measurements, as studied in [DRFG16]. While local thermometry in translationally-invariant gapped systems is exponentially inefficient at low temperatures, our exact results display a polynomial decay $\mathcal{F}_T \sim T^{-2}$ as $T \to 0$. Such an advantage can be related to the fact that the Caldeira-Leggett model maps into a gapless harmonic chain [HC18].

APPENDICES

A. Appendix of Chapter 3: *Locality of temperature for one-dimensional spin systems*

A.1. Proofs of the Lemmas

In this section, we present the proofs of the lemma's used in Secs. 3.3 and 3.4. to get statements on the locality of temperature for gapped systems. They consist of how different covariances decay for one dimensional systems with a gapped transfer matrix T.

Lemma 4. *[Infinite chain] Given a gapped transfer matrix T with eigenvalues λ_k labelled in decreasing order, i. e. $|\lambda_k| \geq |\lambda_{k'}|$ for all $k < k'$, and right (left) dominant eigenvector $|1_R\rangle$ ($\langle 1_L|$), and a covariance between any two operators O and O' separated by a distance ℓ defined as*

$$\operatorname{cov}(\ell; O, O', T) := \frac{\langle 1_L|O^\dagger T^\ell O'|1_R\rangle}{\langle 1_L|T^\ell|1_R\rangle} - \frac{\langle 1_L|O^\dagger T^\ell|1_R\rangle}{\langle 1_L|T^\ell|1_R\rangle}\frac{\langle 1_L|T^\ell O'|1_R\rangle}{\langle 1_L|T^\ell|1_R\rangle}. \quad \text{(A.1)}$$

Then, the covariance can be proven to decay exponentially in ℓ

$$|\operatorname{cov}(\ell; O, O', T)| \leq \sigma_L(O)\sigma_R(O')e^{-\ell/\xi} \quad \text{(A.2)}$$

where $\xi = \left(\ln(\lambda_1/\lambda_2)\right)^{-1}$ is the correlation length and

$$\sigma_{L/R}(O) = \left\|(O - \langle 1_L|O|1_R\rangle)\,|1_{L/R}\rangle\right\|. \quad \text{(A.3)}$$

Proof of Lemma 4. Let us first introduce the operator $\tilde{O}^\dagger = O^\dagger - \langle 1_L|O^\dagger|1_R\rangle$ (and analogously for $\tilde{O}'$) to rewrite the covariance as

$$\operatorname{cov}(\ell; O, O', T) = \frac{1}{\lambda_1^\ell}\langle 1_L|\tilde{O}^\dagger T^\ell \tilde{O}'|1_R\rangle. \quad \text{(A.4)}$$

By using the Cauchy-Schwarz inequality one gets

$$\left|\lambda_1^{-\ell}\langle 1_L|\tilde{O}^\dagger T^\ell \tilde{O}'|1_R\rangle\right| \leq \left\|\tilde{O}'|1_R\rangle\right|\left(|\lambda_1|^{-2\ell}\langle 1_L|\tilde{O}^\dagger T^\ell (T^\dagger)^\ell \tilde{O}|1_L\rangle\right)^{1/2}. \quad \text{(A.5)}$$

Let us now consider second factor separately. By inserting a resolution of the identity, a straight forward calculation leads to

$$\begin{aligned}
|\lambda_1|^{-2\ell}\langle 1_L|\tilde{O}^\dagger T^\ell (T^\dagger)^\ell \tilde{O}|1_L\rangle &= \sum_{k\geq 2}\left(\frac{|\lambda_k|}{|\lambda_1|}\right)^{2\ell}\langle 1_L|\tilde{O}^\dagger|k_R\rangle\langle k_R|\tilde{O}|1_L\rangle \\
&\leq \left(\frac{|\lambda_2|}{|\lambda_1|}\right)^{2\ell}\sum_{k\geq 2}\langle 1_L|\tilde{O}^\dagger|k_R\rangle\langle k_R|\tilde{O}|1_L\rangle \\
&\leq \left(\frac{|\lambda_2|}{|\lambda_1|}\right)^{2\ell}\left\|\tilde{O}|1_L\rangle\right\|^2 \quad \text{(A.6)}
\end{aligned}$$

where we have used that $|\lambda_2|$ is an upper-bound for all the $|\lambda_k|$ with $k \geq 2$ and the Parseval inequality.

Finally, we put everything together and get

$$|\text{cov}(\ell; O, O', T)| \leq \left(\frac{\lambda_2}{\lambda_1}\right)^\ell \left\||\tilde{O}|1_L\rangle\right\| \left\||\tilde{O}'|1_R\rangle\right\| = \sigma_L(O)\sigma_R(O')\text{e}^{-\ell/\xi}, \quad \text{(A.7)}$$

where we have introduced the correlation length ξ and identified $\sigma_{L/R}$. Note that in the case that the transfer matrix T is Hermitian, $\sigma_L(O)$ and $\sigma_R(O)$ coincide and correspond to the fluctuations of the operator O on the dominant eigenvector of T. $\quad \square$

Lemma 5. *[3-point correlation function for an infinite chain] Given a gapped transfer matrix T with eigenvalues λ_k labelled in decreasing order, i. e. $|\lambda_k| \geq |\lambda_{k'}|$ for all $k < k'$, and right (left) dominant eigenvector $|1_R\rangle$ ($\langle 1_L|$), and a 3-point correlation function defined for any operators Y and X separated by a distance ℓ as*

$$\text{cov}_3(\ell; X, Y, T) = \frac{\langle 1_L|XT^\ell YT^\ell X|1_R\rangle}{\langle 1_L|T^{2\ell}|1_R\rangle} - \frac{\langle 1_L|T^\ell YT^\ell|1_R\rangle}{\langle 1_L|T^{2\ell}|1_R\rangle} \frac{\langle 1_L|XT^{2\ell}X|1_R\rangle}{\langle 1_L|T^{2\ell}|1_R\rangle}.$$
$$\text{(A.8)}$$

Then, the covariance can be proven to decay exponentially in ℓ

$$|\text{cov}_3(\ell; X, Y, T)| \leq 2 \|Y\|_\infty \sigma_L(X^\dagger)\sigma_R(X)\text{e}^{-2\ell/\xi}$$
$$+ \left(\sigma_L(X^\dagger)\sigma_R(Y) + \sigma_L(Y^\dagger)\sigma_R(X)\right) \langle 1_L|X|1_R\rangle\text{e}^{-\ell/\xi} \quad \text{(A.9)}$$

where $\xi = \left(\ln(\lambda_1/\lambda_2)\right)^{-1}$ is the correlation length, and

$$\sigma_{L/R}(O) = \left\|(O - \langle 1_L|O|1_R\rangle)\,|1_{L/R}\rangle\right\|. \quad \text{(A.10)}$$

Proof of Lemma 5. Let us first introduce the operator $\tilde{X} = X - \langle 1_L|X|1_R\rangle$ (and analogously for Y) to rewrite the 3-point function as

$$\text{cov}_3(\ell; X, Y, T) = \frac{1}{\lambda_1^{2\ell}}\langle 1_L|\tilde{X}T^\ell\tilde{Y}T^\ell\tilde{X}|1_R\rangle$$
$$+ \langle 1_L|X|1_R\rangle \left(\langle 1_L|\tilde{Y}T^\ell\tilde{X}|1_R\rangle + \langle 1_L|\tilde{X}T^\ell\tilde{Y}|1_R\rangle\right) \text{(A.11)}$$

The second term can be bounded by means of Lemma 4. Concerning the first term, let us rewrite it by introducing new operator $O := \tilde{Y}T^\ell\tilde{X}$ and use Lemma 4 again to obtain

$$|\lambda_1^{-2\ell}\langle 1_R|\tilde{X}T^\ell\tilde{Y}T^\ell\tilde{X}|1_L\rangle| = |\lambda_1^{-2\ell}\langle 1_L|\tilde{X}T^\ell O|1_R\rangle|$$
$$\leq \left\|\tilde{X}^\dagger|1_L\rangle\right\| \left(|\lambda_1|^{-\ell} \left\|O|1_R\rangle\right\|\right) \text{e}^{-\ell/\xi}. \quad \text{(A.12)}$$

The norm of the vector $O|1_R\rangle$ is given by

$$\|O|1_R\rangle\| = \left(\langle 1_R|\tilde{X}^\dagger(T^\dagger)^\ell \tilde{Y}^\dagger \tilde{Y}T^\ell \tilde{X}|1_R\rangle\right)^{1/2} \tag{A.13}$$

$$= \left(\sum_y |\mu_y|^2 \langle 1_R|\tilde{X}^\dagger(T^\dagger)^\ell|y_L\rangle\langle y_L|T^\ell \tilde{X}|1_R\rangle\right)^{1/2} \tag{A.14}$$

where we have introduced a resolution of the identity in the left eigenbasis of Y, $|y_L\rangle$, with associated eigenvalues μ_y. Notice that $\langle 1_R|\tilde{X}^\dagger(T^\dagger)^\ell|y_L\rangle\langle y_L|T^\ell \tilde{X}|1_R\rangle$ are positive. Thus,

$$\|O|1_R\rangle\| \leq \left(\|Y\|_\infty^2 \sum_y \langle 1_R|\tilde{X}^\dagger(T^\dagger)^\ell|y_L\rangle\langle y_L|T^\ell \tilde{X}|1_R\rangle\right)^{1/2}$$

$$= \|Y\|_\infty \left(\langle 1_R|\tilde{X}^\dagger(T^\dagger)^\ell T^\ell \tilde{X}|1_R\rangle\right)^{1/2} . \tag{A.15}$$

where $\langle 1_R|\tilde{X}^\dagger(T^\dagger)^\ell T^\ell \tilde{X}|1_R\rangle$ can be bounded analogously to Eq. (A.6). The three point correlation function is then bounded by

$$|\lambda_1^{-2\ell}\langle 1_R|\tilde{X}T^\ell \tilde{Y}T^\ell \tilde{X}|1_L\rangle| \leq \|Y\|_\infty \left\|\tilde{X}^\dagger|1_L\rangle\right\| \left\|\tilde{X}|1_R\rangle\right\| e^{-2\ell/\xi} \tag{A.16}$$

Finally, by putting everything together and using that $\left\|\tilde{Y}\right\|_\infty \leq 2\|Y\|_\infty$, Eq. (A.9) is obtained. $\qquad\square$

Lemma 6. *[Periodic boundary conditions] Given a system with periodic boundary conditions, an Hermitian transfer matrix T with a gap Δ and a covariance between any two operators O and O' separated by a distance ℓ defined as*

$$\mathrm{cov}(\ell; n, O, O', T) = \frac{\mathrm{tr}(OT^\ell O'T^{n-\ell})}{\mathrm{tr}(T^n)} - \frac{\mathrm{tr}(OT^n)}{\mathrm{tr}(T^n)}\frac{\mathrm{tr}(O'T^n)}{\mathrm{tr}(T^n)} . \tag{A.17}$$

where $0 \leq \ell \leq n$ and n is the system size. Therefore, the covariance $\mathrm{cov}(\ell) = \mathrm{cov}(\ell; n, O, O', T)$ as a function of ℓ fulfills following properties:

(i) Its real part is symmetric respect to the $n/2$ and the interchange of A and B, i. e.

$$\mathrm{cov}(n - \ell; n, O, O', T) = \mathrm{cov}(\ell; n, O, O', T)^* = \mathrm{cov}(\ell; n, O, O', T) . \tag{A.18}$$

(ii) Given two operators O and O', there always exist two other operators O_M and O'_M such that

$$|\mathrm{cov}(\ell; n, O, O', T)| \leq \mathrm{cov}(\ell; n, O_M, O'_M, T) \tag{A.19}$$

and where $\mathrm{cov}(\ell; n, O_M, O'_M, T)$ is a convex function in ℓ that is maximum at $\ell = 0$ and 1, and reaches its minimum at $\ell = n/2$.

Proof of Lemma 6. Statement (*i*) is a simple consequence of the following elementary equalities

$$
\begin{aligned}
\left(\operatorname{tr}(OT^\ell O'T^{n-\ell})\right)^* &= \operatorname{tr}\left((OT^\ell O'T^{n-\ell})^\dagger\right) \\
&= \operatorname{tr}(T^{n-\ell}O'T^\ell O) = \operatorname{tr}(O'T^\ell OT^{n-\ell}) \,. \quad \text{(A.20)}
\end{aligned}
$$

In order to prove (*ii*), let us focus on the first term in Eq. (A.17), since note that the second one does not depend on ℓ. With this aim, we define

$$
f(\ell; O, O') = \mathbb{R}\left[\frac{\operatorname{tr}(OT^\ell O'T^{n-\ell})}{\operatorname{tr}(T^n)}\right] \,. \quad \text{(A.21)}
$$

By introducing the transfer matrix in its spectral representation, $f(\ell)$ can be written as

$$
\begin{aligned}
f(\ell; O, O') &= \frac{s_1^n}{\operatorname{tr}(T^n)}\left[\langle 1|O|1\rangle\langle 1|O'|1\rangle + \sum_{k\geq 2} c_k \left(\left(\frac{\lambda_k}{\lambda_1}\right)^\ell + \left(\frac{\lambda_k}{\lambda_1}\right)^{n-\ell}\right)\right. \\
&\quad \left. + \sum_{k,k'\geq 2} d_{kk'}\left(\frac{\lambda_k}{\lambda_1}\right)^\ell \left(\frac{\lambda_{k'}}{\lambda_1}\right)^{n-\ell}\right] \,, \quad \text{(A.22)}
\end{aligned}
$$

where $c_k = \mathfrak{R}\left(\langle 1|O|k\rangle\langle k|O'|1\rangle\right)$ and $d_{kk'} = \mathfrak{R}\left(\langle k|O|k'\rangle\langle k'|O'|k\rangle\right)$. Note now that

$$
\left(\frac{\lambda_k}{\lambda_1}\right)^\ell + \left(\frac{\lambda_k}{\lambda_1}\right)^{n-\ell} = 2e^{-\frac{n}{2\xi_k}}\cosh\left(\frac{\ell - n/2}{\xi_k}\right) \,, \quad \text{(A.23)}
$$

where the correlation length ξ_k is defined as

$$
\xi_k^{-1} := \ln\left(\frac{\lambda_1}{\lambda_k}\right) \,. \quad \text{(A.24)}
$$

Note that as the eigenvalues of the transfer matrix are ordered, a larger k implies a shorter correlation length ξ_k.

In a similar way, we can also simplify the terms in the last sum in Eq. (A.22). Note that

$$
\begin{aligned}
\left(\frac{\lambda_k}{\lambda_1}\right)^\ell\left(\frac{\lambda_{k'}}{\lambda_1}\right)^{n-\ell} + \left(\frac{\lambda_{k'}}{\lambda_1}\right)^\ell\left(\frac{\lambda_k}{\lambda_1}\right)^{n-\ell} &= e^{-\frac{n}{\xi_{k'}} - \frac{\ell}{\xi_{kk'}}} + e^{-\frac{n}{\xi_k} + \frac{\ell}{\xi_{kk'}}} \\
&= 2e^{-\frac{n}{2\xi_{kk'}}}\cosh\left(\frac{\ell - n/2}{\xi_{kk'}}\right) \,. \quad \text{(A.25)}
\end{aligned}
$$

where the length $\xi_{kk'}$ has been defined as $\xi_{kk'}^{-1} = \xi_k^{-1} - \xi_{k'}^{-1}$. Puting the previous steps together, we get

$$f(\ell; A, B) = \frac{\lambda_1^n}{\mathrm{tr}(T^n)} \left[\langle 1|A|1\rangle\langle 1|B|1\rangle + 2\sum_{k\geq 2} e^{-\frac{n}{2\xi_k}} c_k \cosh\left(\frac{\ell - n/2}{\xi_k}\right) \right.$$
$$\left. + 2\sum_{k\geq 2} d_{kk} e^{-\frac{n}{\xi_k}} + 2\sum_{2\leq k<k'} d_{kk'} e^{-\frac{n}{2\xi_{kk'}}} \cosh\left(\frac{\ell - n/2}{\xi_{kk'}}\right) \right]. \quad \text{(A.26)}$$

Note that in general the covariance could oscilate in ℓ, since c_k and $d_{kk'}$ could take negative values for some k and k'. Nevertheless, given two operators A and B for which some c_k and $d_{kk'}$ are negative, there always exist two operators O_M and O'_M such that their respective $\tilde{c}_k = |c_k|$ and $\tilde{d}_{kk'} = |d_{kk'}|$. For instance, $\langle k|O_M|k'\rangle = -\langle k|O|k'\rangle$ for the k' and k-s with negative coefficients and $\langle k|O_M|k'\rangle = \langle k|O_M|k'\rangle$ otherwise, and $O'_M = O'$. This covariance $f(\ell; O_M, O'_M)$ is an upper bound to the absolute value of the previous one covariance $f(\ell; O, O')$,

$$f(\ell; O_M, O'_M) = \frac{\lambda_1^n}{\mathrm{tr}(T^n)} \left[|\langle 1|O|1\rangle\langle 1|O'|1\rangle| + 2\sum_{k\geq 2} e^{-\frac{n}{2\xi_k}} |c_k| \cosh\left(\frac{\ell - n/2}{\xi_k}\right) \right.$$
$$\left. + 2\sum_{k\geq 2} |d_{kk}| e^{-\frac{n}{\xi_k}} + 2\sum_{2\leq k<k'} |d_{kk'}| e^{-\frac{n}{2\xi_{kk'}}} \cosh\left(\frac{\ell - n/2}{\xi_{kk'}}\right) \right]$$
$$\text{(A.27)}$$
$$\geq f(\ell; O, O'). \quad \text{(A.28)}$$

As the sum in Eq. (A.27) is a linear combination of convex functions with positive coefficents, $f(\ell; O_M, O'_M)$ is also convex. It is also obvious from the properties of the $\cosh()$ function, that $f(\ell; O_M, O'_M)$ reaches its maximum at $\ell = 0$ and n, and its minimum at $\ell = n/2$. $\qquad\square$

A.2. Solving the quantum Ising model

In this appendix we find the states (3.38) and (3.39) using formalism of covariance matrices.

Jordan-Wigner transformation

Let us first apply the *Jordan-Wigner transformation*, $\sigma_i^x \otimes \sigma_{i+1}^x = (a_i^\dagger - a_i)(a_{i+1} + a_{i+1}^\dagger)$ and $\sigma_i^z = a_i a_i^\dagger - a_i^\dagger a_i$, to the Hamiltonian (3.36). We obtain,

$$H_n = \sum_{i,j=1}^{N} A_{ij} a_i a_j^\dagger + \frac{1}{2} \sum_{i,j=1}^{N} B_{ij} (a_i^\dagger a_j^\dagger - a_i a_j), \tag{A.29}$$

with $A_{ij} = h\delta_{i,j} + \frac{1}{2}(\delta_{i+1,j} + \delta_{i,j+1})$ and $B_{ij} = \frac{1}{2}(\delta_{i+1,j} - \delta_{i,j+1})$ and where a_i and $a_i^\dagger$ denote annihilation and creation operators, respectively. From this form of the Hamiltonian, we notice it is quadratic, and thus the thermal state (an their partial states) are gaussian states. Therefore we can deal with them using the covariance matrix formalism.

The correlation matrix

In this formalism, we define the global correlation matrix, Γ, as

$$\Gamma(X) := \langle XX^\dagger \rangle$$

$$= \begin{bmatrix} \| \langle a_i a_j^\dagger \rangle \|_{N \times N} & \| \langle a_i a_j \rangle \|_{N \times N} \\ \| \langle a_i^\dagger a_j^\dagger \rangle \|_{N \times N} & \| \langle a_i^\dagger a_j \rangle \|_{N \times N} \end{bmatrix} \quad \text{with} \quad X := \begin{bmatrix} a_1 \\ \vdots \\ a_N \\ a_1^\dagger \\ \vdots \\ a_N^\dagger \end{bmatrix}, \tag{A.30}$$

where $\| \dots \|_{N \times N}$ refers to a $N \times N$ matrix. Given Γ, we can obtain the correlation matrix corresponding to a reduced state by just selecting the corresponding matrix elements of Γ. For example, the correlation matrix of the fermions $k, k+1$ is given by,

$$\Gamma_{k,k+1} = \begin{pmatrix} \langle a_k a_k^\dagger \rangle & \langle a_k a_{k+1}^\dagger \rangle & \langle a_k a_k \rangle & \langle a_k a_{k+1} \rangle \\ \langle a_{k+1} a_k^\dagger \rangle & \langle a_{k+1} a_{k+1}^\dagger \rangle & \langle a_{k+1} a_k \rangle & \langle a_{k+1} a_{k+1} \rangle \\ \langle a_k^\dagger a_k^\dagger \rangle & \langle a_k^\dagger a_{k+1}^\dagger \rangle & \langle a_k^\dagger a_k \rangle & \langle a_k^\dagger a_{k+1} \rangle \\ \langle a_{k+1}^\dagger a_k^\dagger \rangle & \langle a_{k+1}^\dagger a_{k+1}^\dagger \rangle & \langle a_{k+1}^\dagger a_k \rangle & \langle a_{k+1}^\dagger a_{k+1} \rangle \end{pmatrix}. \tag{A.31}$$

Since the Jordan Wigner transformation is local, in the sense that it maps the kth fermion to the kth spin in the chain, this correlation matrix also corresponds to the two-spin subsystem at sites k and $k + 1$. This subsystem is precisely the region of interest A in section 3.5.2, and thus (A.31) corresponds to the correlation matrix of ρ_A in (3.38).

Given the reduced correlation matrix, the explicit form of ρ_A can be easily obtained. As the reduced state of a thermal state is gaussian, there is a one-to-one connection between (A.31) and ρ_A. Indeed, for any gaussian state, with

$$\rho = \frac{e^{-X^\dagger M X}}{Tr[e^{-X^\dagger M X}]} \text{ with } M \text{ a coefficient matrix,} \tag{A.32}$$

it is straightforward to prove that, provided that M is diagonalizable,

$$\Gamma(X) = \frac{1}{(\mathbb{1} + e^{-2M})} \tag{A.33}$$

or, equivalently, that

$$M = -\frac{1}{2} \log(\Gamma(X)^{-1} - \mathbb{1}). \tag{A.34}$$

Explicit computation

Now we explicitly compute (A.31) for a finite and an infinite chain, in order to obtain ρ'_A and ρ_A, respectively, using relation (A.34).

- Finite chain

  For the case of a finite chain, we need to obtain the correlation matrix (A.38) corresponding to the global state. It is then useful to first diagonalize the Hamiltonian (A.29) by applying the Bogoliubov transformation

  $$\tilde{a}_j := \sum_{k=1}^{N} \frac{1}{2}(\phi_0 + \psi_0)_{jk} \, a_k - \frac{1}{2}(\phi_0 - \psi_0)_{jk} \, a_k^\dagger, \tag{A.35}$$

  where ϕ_0 and ψ_0 are real matrices and verify $\sum_{k=1}^{N} \phi_{0,jk}^2 = \sum_{k=1}^{N} \psi_{0,jk}^2 = 1$. The Hamiltonian can then take the form,

  $$H = \sum_{k=1}^{N} \varepsilon_k (\tilde{a}_k^\dagger \tilde{a}_k - 1/2), \tag{A.36}$$

where ε_k are the fermionic excitation energies and $\tilde{a}_k$ and $\tilde{a}_k^\dagger$ denote annihilation and creation operators, respectively. The excitation energies, ε_k, and the matrices ϕ_0 and ψ_0 are obtained by solving the equation

$$(A - B)\phi_0 = \psi_0 D_\varepsilon, \tag{A.37}$$

where D_ε is a diagonal matrix whose entries correspond to the excitation energies, ε_k.

Once the Hamiltonian is diagonalized, it is easy to compute the correlation matrix of a thermal state at inverse temperature β in the diagonalized basis, obtaining

$$\Gamma(Y) = \begin{bmatrix} \frac{1}{1+e^{-\beta D_\varepsilon}} & 0_{N \times N} \\ 0_{N \times N} & \frac{1}{1+e^{\beta D_\varepsilon}} \end{bmatrix} \quad \text{with} \quad Y := \begin{bmatrix} \tilde{a}_1 \\ \vdots \\ \tilde{a}_N \\ \tilde{a}_1^\dagger \\ \vdots \\ \tilde{a}_N^\dagger \end{bmatrix}, \tag{A.38}$$

where the non-zero matrices are diagonal.

From that expression we can obtain the correlation matrix in the original basis, $\Gamma(X)$, via

$$\Gamma(X) = T^\dagger \Gamma(Y) T, \tag{A.39}$$

where T is the transformation matrix defined by the Bogoliubov transformation (A.35). That is, $Y = TX$, with

$$T = \begin{bmatrix} \gamma_0 & \mu_0 \\ \mu_0^* & \gamma_0^* \end{bmatrix}. \tag{A.40}$$

and

$$\gamma_0 = \frac{1}{2}(\phi_0 + \psi_0) \text{ and } \mu_0 = -\frac{1}{2}(\phi_0 - \psi_0). \tag{A.41}$$

- Infinite chain ($N \to \infty$)

A. Appendix of Chapter 3: Locality of temperature for one-dimensional spin systems

In the case of an infinite chain, (A.31) can be obtained relying on the analytical results from [BM71]. The partial state of a two-spin subsystem is

$$\rho_2^{n\to\infty} = \frac{1}{4}\left[1 + \langle\sigma_k^z\rangle(\sigma_k^z + \sigma_{k+1}^z) + \sum_{l=x,y,z}^{3}\langle\sigma_k^l\sigma_{k+1}^l\rangle\sigma_k^l\otimes\sigma_{k+1}^l\right], \quad \text{(A.42)}$$

where the average $\langle\sigma_k^z\rangle$ and the two-spin correlation functions $\{\langle\sigma_k^l\sigma_{k+1}^l\rangle\}_{l=\{x,y,z\}}$ are given by [BM71]. In order to express the state in the fermionic basis, we can compute the reduced correlation matrix (A.31) from this state,

$$\Gamma_{k,k+1} = \begin{pmatrix} 2(1+\alpha_0) & -(\beta_0+\gamma_0) & 0 & -(\beta_0-\gamma_0) \\ -(\beta_0+\gamma_0) & 2(1+\alpha_0) & \beta_0-\gamma_0 & 0 \\ 0 & \beta_0-\gamma_0 & 2(1-\alpha_0) & \beta_0+\gamma_0 \\ -(\beta_0-\gamma_0) & 0 & \beta_0+\gamma_0 & 2(1-\alpha_0) \end{pmatrix},$$

(A.43)

with $\alpha_0 = \langle\sigma_k^z\rangle$, $\beta_0 = \langle\sigma_k^x\sigma_{k+1}^x\rangle$ and $\gamma_0 = \langle\sigma_k^y\sigma_{k+1}^y\rangle$.

B. Appendix of Chapter 4: *Locality of temperature and correlations for non-zero temperature PT*

B.1. Equivalence to the Bose-Einsten model at continuous limit

We consider the Hamiltonian (4.1) with periodic boundary conditions (PBC). Then, we diagonalize the Hamiltonian by applying the Fourier transform $b_{\mathbf{n}} = \frac{1}{L^{3/2}} \sum_{\mathbf{k}} b_{\mathbf{k}} e^{i\mathbf{k}\mathbf{n}}$ and the orthogonal relation $\sum_{\mathbf{k}} e^{i(\mathbf{k}-\mathbf{k}')\mathbf{n}} = L^3 \delta(\mathbf{k} - \mathbf{k}')$, such that

$$H = \sum_{\mathbf{k}} \varepsilon(\mathbf{k}) b_{\mathbf{k}}^{\dagger} b_{\mathbf{k}} \tag{B.1}$$

where the momentum $\mathbf{k} := 2\pi\mathbf{n}/L$ and the eigenvalues $\varepsilon(\mathbf{k})$ are defined as

$$\varepsilon(\mathbf{k}) := 2t(3 - cos(k_x) - cos(k_y) - cos(k_z)). \tag{B.2}$$

When one applies the continuous limit, $L \to \infty$ and $|\mathbf{k}| \to 0$, which gives that $cos(k_x) \approx (1 - k_x^2/2)$. Substituting this equation into (B.19), we obtain that

$$H \approx t \sum_{\mathbf{k}} \mathbf{k}^2 b_{\mathbf{k}}^{\dagger} b_{\mathbf{k}}, \tag{B.3}$$

an equivalent expression to the well-known Bose-Einstein model that reproduces the same type of dispersion relation.

Notice that this result is also valid for open boundary conditions, since the results are independent on the boundary conditions at the continuous limit.

B.2. Condensation is not possible for dimension $D \leq 2$

For a system with Hamiltonian (B.19) at the grand canonical state (4.2), the total number of particles, N, and the number of particles with 0-momentum ($\mathbf{k} = \mathbf{0}$), N_0, are given by

$$N = \sum_{\mathbf{k}} \frac{1}{e^{\beta \, \varepsilon(\mathbf{k}) - \mu} - 1} \quad \text{and} \tag{B.4}$$

$$N_0 = \frac{1}{e^{-\mu} - 1} \quad \text{with } \mu \leq 0. \tag{B.5}$$

Given this, we can formally express the presence of a condensate as the saturation of the number of particles at excited states $N' = N - N_0$, that is,

$$N' \leq N'_{max} = \sum_{\mathbf{k} \neq \mathbf{0}} \frac{1}{e^{\beta \varepsilon(\mathbf{k})} - 1} \tag{B.6}$$

where N'_{max} must be a finite number. In order to verify this, we analyse N'_{max} for the 3D Hamiltonian (4.1) and its 1D and 2D versions at the thermodynamic limit ($L \rightarrow \infty$), that is,

$$N'_{max} = \int \frac{\mathrm{d}^D \mathbf{k}}{e^{\beta \varepsilon(\mathbf{k})} - 1}. \qquad (B.7)$$

where D is the physical dimension of the system and the eigenvalues $\varepsilon(\mathbf{k})$ are given by the expressions

$$\varepsilon(\mathbf{k}) = 2t(1 - cos(k_x)) \qquad \qquad \text{for the 1D case,} \qquad (B.8)$$
$$\varepsilon(\mathbf{k}) = 2t(2 - cos(k_x) - cos(k_y)) \qquad \qquad \text{for the 2D case,} \qquad (B.9)$$
$$\varepsilon(\mathbf{k}) = 2t(3 - cos(k_x) - cos(k_y) - cos(k_z)) \qquad \text{and for the 3D case.} \qquad (B.10)$$

In particular, we are able to compute a lower-bound for N'_{max} by choosing $k := |\mathbf{k}| < \delta$ and applying the Tailor approximation $cos(k_x) \approx 1 - k_x^2/2$, such that $\varepsilon(\mathbf{k}) \approx t k^2$ and

$$N'_{max} > \int_\delta \frac{\mathrm{d}^D \mathbf{k}}{\beta t k^2}. \qquad (B.11)$$

We are able to solve this integral analytically for $D = 1, 2, 3$ and obtain that

$$\int_\delta \frac{\mathrm{d}\mathbf{k}}{\beta t k^2} \propto \int_0^\delta \frac{\mathrm{d}\mathbf{k}}{k^2} \sim \infty \qquad \qquad \text{for the 1D case,} \qquad (B.12)$$

$$\int_\delta \frac{\mathrm{d}^2\mathbf{k}}{\beta t k^2} \propto \int_0^\delta \frac{\mathrm{d}\mathbf{k}}{k} \sim \infty \qquad \qquad \text{for the 2D case,} \qquad (B.13)$$

$$\int_\delta \frac{\mathrm{d}^3\mathbf{k}}{\beta t k^2} \propto \int_0^\delta \mathrm{d}\mathbf{k} = \delta \qquad \qquad \text{and for the 3D case.} \qquad (B.14)$$

Therefore, we are able to prove that N'_{max} diverges for $D \leq 2$ and, thus, condensation is only possible for $D = 3$.

B.3. Correlations decay to n_0^2 at low temperature

In this section, we show that at low temperature and large distances, the density-density correlations decay with the inverse of the distance to n_0:

$$\langle a_n^\dagger a_n a_m^\dagger a_m \rangle - \langle a_n^\dagger a_n \rangle \langle a_m^\dagger a_m \rangle \approx n_0^2 + \frac{n_0}{2\pi\beta} \frac{1}{|n - m|} \qquad (B.15)$$

We prove first that

$$\langle a_n^\dagger a_n a_m^\dagger a_m \rangle - \langle a_n^\dagger a_n \rangle \langle a_m^\dagger a_m \rangle = \langle a_n^\dagger a_m \rangle \langle a_m^\dagger a_n \rangle. \qquad (B.16)$$

Let us rewrite the above expression. Notice that

$$\langle a_n^\dagger a_n \rangle \cdot \langle a_m^\dagger a_m \rangle = n_0^2 = \frac{1}{L^6} \sum_{k,l} \langle n_k \rangle \langle n_l \rangle. \tag{B.17}$$

The first term also can be expanded with help of the Fourier transforms:

$$\langle a_n^\dagger a_n a_m^\dagger a_m \rangle = \frac{1}{L^6} \sum_{klrs} \exp\left\{ \frac{2\pi i}{L} \left(n(k-l) + m(r-s) \right) \right\} \langle a_k^\dagger a_l a_r^\dagger a_s \rangle. \tag{B.18}$$

Notice that as the state has the form

$$\prod_k \exp\{(-\beta \varepsilon_k + \mu) a_k^\dagger a_k\}, \tag{B.19}$$

it commutes with n_k, and thus the expectation value is 0 unless the indices k, l, r, s pairwise coincide. Let us therefore divide the non-zero elements of the sum over k, l, r, s to three distinct sums:

- For $k = l = r = s$,

- for $k = l, r = s, k \neq s$, and

- for $k = s, l = r, k \neq l$.

The sum in the first case is

$$\frac{1}{L^6} \sum_k \langle a_k^\dagger a_k a_k^\dagger a_k \rangle = \frac{1}{L^6} \sum_k \langle n_k^2 \rangle. \tag{B.20}$$

Note that

$$\sum_n x^n = \frac{1}{1-x} \tag{B.21}$$

$$\sum_n n x^n = \frac{x}{(1-x)^2} \tag{B.22}$$

$$\sum_n n^2 x^n = \frac{x}{(1-x)^2} + \frac{2x^2}{(1-x)^3} \tag{B.23}$$

Thus

$$\langle n_k^2 \rangle = 2\langle n_k \rangle^2 + \langle n_k \rangle, \tag{B.24}$$

Meaning that

$$\frac{1}{L^6} \sum_k \langle a_k^\dagger a_k a_k^\dagger a_k \rangle = \frac{2}{L^6} \sum_k \langle n_k \rangle^2 + \frac{1}{L^6} \sum_k \langle n_k \rangle. \tag{B.25}$$

In the case of $k = l, r = s, k \neq s$, after renaming the running indices the sum can be written as

$$\frac{1}{L^6} \sum_{k \neq l} \langle a_k^\dagger a_k a_l^\dagger a_l \rangle = \frac{1}{L^6} \sum_{k \neq l} \langle n_k \rangle \cdot \langle n_l \rangle. \tag{B.26}$$

Finally, in the case $k = s, l = r, k \neq l$, the sum reads as

$$\frac{1}{L^6} \sum_{k \neq l} \exp \left\{ \frac{2\pi i}{L} (n - m)(k - l) \right\} \langle a_k^\dagger a_l a_l^\dagger a_k \rangle \tag{B.27}$$

$$= \frac{1}{L^6} \sum_{k \neq l} \exp \left\{ \frac{2\pi i}{L} (n - m)(k - l) \right\} \langle a_k^\dagger a_k a_l a_l^\dagger \rangle \tag{B.28}$$

$$= \frac{1}{L^6} \sum_{k \neq l} \exp \left\{ \frac{2\pi i}{L} (n - m)(k - l) \right\} \langle n_k n_l \rangle + \frac{1}{L^6} \sum_{k \neq l} \exp \left\{ \frac{2\pi i}{L} (n - m)(k - l) \right\} \langle n_k \rangle \tag{B.29}$$

$$= \frac{1}{L^6} \sum_{k \neq l} \exp \left\{ \frac{2\pi i}{L} (n - m)(k - l) \right\} \langle n_k \rangle \langle n_l \rangle + \delta_{nm} \frac{1}{L^3} \sum_k \langle n_k \rangle - \frac{1}{L^6} \sum_k \langle n_k \rangle \tag{B.30}$$

Therefore

$$\langle a_n^\dagger a_n a_m^\dagger a_m \rangle - \langle a_n^\dagger a_n \rangle \langle a_m^\dagger a_m \rangle = \delta_{nm} \frac{N}{L^3} + \frac{1}{L^6} \sum_{k,l} \exp \left\{ \frac{2\pi i}{L} (n - m)(k - l) \right\} \langle n_k \rangle \langle n_l \rangle \tag{B.31}$$

Or

$$\langle a_n^\dagger a_n a_m^\dagger a_m \rangle - \langle a_n^\dagger a_n \rangle \langle a_m^\dagger a_m \rangle = \delta_{nm} \frac{N}{L^3} + \left| \frac{1}{L^3} \sum_k \exp \left\{ \frac{2\pi i}{L} (n - m)k \right\} \langle n_k \rangle \right|^2 \tag{B.32}$$

Thus

$$\langle n_n n_m \rangle - \langle n_n \rangle \langle n_m \rangle = \delta_{nm} \frac{N}{L^3} + \left| \frac{1}{L^3} \sum_k \exp \left\{ \frac{2\pi i}{L} (n - m)k \right\} \langle n_k \rangle \right|^2 \tag{B.33}$$

Consequently, if $n \neq m$,

$$\langle n_n n_m \rangle - \langle n_n \rangle \langle n_m \rangle = \left| \frac{1}{L^3} \sum_k \exp \left\{ \frac{2\pi i}{L} (n - m)k \right\} \frac{1}{e^{\beta \varepsilon_k - \mu} - 1} \right|^2 \tag{B.34}$$

Note that below (and at) phase transition $\mu = 0$ and n_0 is macroscopic, above $\mu < 0$. The latter expression is exactly $\langle a_n^\dagger a_m \rangle$.

Long-range order?

In the continuous limit,

$$\langle a_n^\dagger a_m \rangle - n_0 = \frac{1}{8\pi^3} \int_{-\pi}^{\pi} d^3k \exp\left\{i(n-m)k\right\} \frac{1}{e^{\beta\varepsilon_k - \mu} - 1}. \tag{B.35}$$

Substituting $\varepsilon_k \approx k^2$ and $\mu = 0$, the dispersion has spherical symmetry, and thus

$$\langle a_n^\dagger a_m \rangle - n_0 \approx \frac{1}{4\pi^2} \int_0^\infty dk \int_0^\pi d\Theta \exp\left\{i|n-m|k\cos\Theta\right\} \frac{k^2 \sin\Theta}{e^{\beta k^2} - 1}. \tag{B.36}$$

Substituting $y = -\cos\Theta$, we get

$$\langle a_n^\dagger a_m \rangle - n_0 \approx \frac{1}{4\pi^2} \int_0^\infty dk \int_{-1}^1 dy \exp\left\{-i|n-m|ky\right\} \frac{k^2}{e^{\beta k^2} - 1}. \tag{B.37}$$

Evaluating the integral over y, the integral takes the form

$$\langle a_n^\dagger a_m \rangle - n_0 \approx \frac{1}{2\pi^2} \int_0^\infty dk \frac{k}{|n-m|} \frac{\sin\left\{|n-m|k\right\}}{e^{\beta k^2} - 1}. \tag{B.38}$$

When cutting the integral at some finite value, the integral in the upper half is a constant times $1/|n-m|$ and at the lower half sin is upper bounded with linear. Then the integral there is constant. This works for every cut. Thus the value goes to zero as $|n-m|$ goes to infinity.

At low temperature only small values of k contribute to the integral, thus

$$e^{\beta k^2} - 1 \approx \beta k^2. \tag{B.39}$$

By substituting, we obtain that

$$\int_0^\infty \frac{k\sin(|n-m|k)}{e^{\beta k^2} - 1} dk \approx \frac{1}{\beta} \int_0^\infty \frac{\sin(|n-m|k)}{k} dk = \frac{1}{\beta} \int_0^\infty \frac{\sin(k')}{k'} dk' = \frac{\pi}{2\beta}. \tag{B.40}$$

In conclusion,

$$\langle a_n^\dagger a_m \rangle - n_0 \approx \frac{1}{4\pi\beta} \frac{1}{|n-m|} \quad \text{for } \beta \gg 1 \tag{B.41}$$

and thus the density-density correlation also decays with the inverse of the distance:

$$\langle a_n^\dagger a_n a_m^\dagger a_m \rangle - \langle a_n^\dagger a_n \rangle \langle a_m^\dagger a_m \rangle \approx n_0^2 + \frac{n_0}{2\pi\beta} \frac{1}{|n-m|}. \tag{B.42}$$

C. Appendix of Chapter 5: *Correlations in long-range interacting systems*

C.1. Proof of Lemma 1

For the readers convenience we include a proof of our Lemma 1, which is a result from [Has04b] of the main text.

Proof of Lemma 1. Let us consider the operator O with matrix elements O_{ij} in some basis of eigenvectors of the Hamiltonian H. Let E_i, be the energy of the i-th eigenvector. Define O_ω element wise via $(O_\omega)_{ij} := O_{ij}\,\delta(E_i - E_j - \omega)$, then $O = \int O_\omega\,\mathrm{d}\omega$ and we can write $\langle O_\omega B\rangle_\beta = Z^{-1}\sum_{i,j}\delta(E_i - E_j - \omega)\,O_{ij}\,O'_{ji}\,\mathrm{e}^{-\beta E_i}$ and similarly $\langle O' O_\omega\rangle_\beta = Z^{-1}\sum_{i,j}\delta(E_i - E_j - \omega)\,O'_{ji}\,O_{ij}\,\mathrm{e}^{-\beta E_j}$. However, $\delta(E_i - E_j - \omega)\,\mathrm{e}^{-\beta E_j} = \delta(E_i - E_j - \omega)\,\mathrm{e}^{-\beta E_i}\,\mathrm{e}^{\beta\omega}$, and thus, $\langle O' O_\omega\rangle_\beta = \langle O_\omega O'\rangle_\beta\,\mathrm{e}^{\beta\omega}$. Hence,

$$\langle O_\omega O'\rangle_\beta = \frac{1}{1 + \mathrm{e}^{\beta\omega}}\langle\{O_\omega, O'\}\rangle_\beta. \tag{C.1}$$

Next, we use that $(1 + \mathrm{e}^{\beta\omega})^{-1} = 1/2 - \beta^{-1}\sum_{n\,\mathrm{odd}}(\omega - \mathrm{i}\,n\,\pi/\beta)^{-1}$, where the sum ranges over all positive and negative odd n. For $n > 0$, we have $(\omega - \mathrm{i}\,n\,\pi/\beta)^{-1} = \mathrm{i}\int_0^\infty \mathrm{e}^{-(\mathrm{i}\omega + n\,\pi/\beta)\,t}\,\mathrm{d}t$. Similarly, for $n < 0$, we have $(\omega - \mathrm{i}\,n\,\pi/\beta)^{-1} = -\mathrm{i}\int_0^\infty \mathrm{e}^{(\mathrm{i}\omega + n\,\pi/\beta)\,t}\,\mathrm{d}t$. Thus,

$$\frac{1}{1 + \mathrm{e}^{\beta\omega}} = \frac{1}{2} + \frac{\mathrm{i}}{\beta}\int_0^\infty \frac{\mathrm{e}^{\mathrm{i}\omega t} - \mathrm{e}^{-\mathrm{i}\omega t}}{\mathrm{e}^{\pi t/\beta} - \mathrm{e}^{-\pi t/\beta}}\,\mathrm{d}t. \tag{C.2}$$

Due to the linearity of time evolution $O(t) := \mathrm{e}^{\mathrm{i}Ht}O\,\mathrm{e}^{-\mathrm{i}Ht}$ we have $O_\omega(t) = \mathrm{e}^{\mathrm{i}\omega t}O_\omega$. Therefore, substituting Eq. (C.2) into Eq. (C.1), we get

$$\begin{aligned}\langle O_\omega O'\rangle_\beta &= \frac{1}{2}\langle\{O_\omega, O'\}\rangle_\beta \\ &+ \frac{\mathrm{i}}{\beta}\int_0^\infty \frac{\langle\{O_\omega(t) - O_\omega(-t), O'\}\rangle_\beta}{\mathrm{e}^{\pi t/\beta} - \mathrm{e}^{-\pi t/\beta}}\,\mathrm{d}t.\end{aligned} \tag{C.3}$$

Finally, by integrating Eq. (C.3) over ω we get Eq. (5.4). $\qquad\square$

C.2. Proof of Lemma 2

Here we discuss how to prove Lemma 2 following the strategy outlined in [FFGCG15] of the main text.

Proof of Lemma 2. As in [FFGCG15] of the main text the Hamiltonian is separated into a finite-range and a long-range part. All interactions over distances up to some length ϑ go into the finite-range part of the Hamiltonian

$$H_{\mathrm{FR}} := \sum_{\kappa,i,j:\, d_{i,j}\leq\vartheta} J_{i,j}^{(\kappa)} V_i^{(\kappa)} V_j^{(\kappa)} \qquad (C.4)$$

and all others into the long-range part. As ϑ is later chosen to grow with time, one should think of both parts of the Hamiltonian as piece wise constant in time. For any operator O let $\mathcal{O}(t)$ be the time evolution of O under H_{FR} only. Due to standard Lieb-Robinson bounds [Has04a, NVZ11, KGE14] the time evolution under the finite-range part is quasi-local, i.e., $\mathcal{O}(t)$ can be decomposed into a sum of operators $\sum_l^\infty \mathcal{O}^l(t)$, each supported only on the support of O and a border of width $\vartheta\, l$ around it. The norm of these operators can be bounded proportional to $\exp(v(\vartheta)\, t - l)$ with the speed

$$v(\vartheta) := 4\,\exp(1)\,\sup_i \sum_{\kappa,j:\, d_{i,j}\leq\vartheta} J_{i,j}^{(\kappa)} \qquad (C.5)$$

$$\leq 4\,\exp(1)\, J\, 2^D \sum_{d=1}^{\vartheta} d^{D-1-\alpha}. \qquad (C.6)$$

It is crucial that the speed $v(\vartheta)$ of the finite-range Hamiltonian H_{FR} can be bounded independently of ϑ by $v(\vartheta) \leq v := 4\, J\, \exp(1)\, 2^D\, \zeta(1+\alpha-D) \leq 8\, J\, \exp(1)\, 2^D$, where ζ is the Riemann zeta function and we have used that $\alpha > 2\, D$. In particular Eqs. (S3) and (S8) from the Supplemental Information of [FFGCG15] from the main text also hold in our setting with an anti-commutator instead of a commutator.

As a side remark, as was already noted in the main text, one can use the same approach to derive a Lieb-Robinson type bound very similar to Lemma 2 also for Hamiltonians with long-range interactions between patches of particles whose diameter is bounded by a constant. The finite range part H_{FR} is then to be constructed such that it contains all the terms in which the maximum distance between any two sites in the coupled patches is smaller than or equal to ϑ and only those. The value of v changes with the size of the patches, but it remains independent of ϑ. In the rest of the proof, all one has to do is to replace balls with radius r around sites with such that contain the respective patch and separated it from the boundary of the ball with a distance r. For finite t and l this leads to corrections in the right-hand side of Eq. (5.5), but these become negligible in the limit of large l. Apart from this, only the numerical values of the constants v, c_0 and c_1 change.

Returning to the proof for the case considered here, one then makes use of the interaction picture to bound the additional growth of the support due to the long-range part.

C. Appendix of Chapter 5: Correlations in long-range interacting systems

We define $C_r(t) := \|\{O(t), O'\}\|$ in analogy to the quantity introduced in Eq. (S9) of the Supplementary Information of [FFGCG15] from the main text and proceed as in Section S2. Let $\mathcal{U}(t)$ be the interaction picture unitary, i.e., the unitary for which for any operator O it holds that $O(t) = \mathcal{U}^\dagger(t)\, \mathcal{O}(t)\, \mathcal{U}(t)$. The idea is now to introduce the generalized (two-time) anti-commutator

$$C_r^l(t, \tau) := \{\mathcal{O}^l(t), \mathcal{U}(t)\, O'\, \mathcal{U}^\dagger(t)\} \tag{C.7}$$

(instead of the commutator) with the property that $\|\sum_l C_r^l(t, t)\| = C_r(t)$. By using the von Neumann equation and the equality

$$\{A, [B, C]\} = \{C, [A, B]\} + [B, \{C, A\}], \tag{C.8}$$

(instead of the Jacobi identity) one obtains a differential equation for $C_r^l(t, \tau)$ equivalent to Eqs. (S11) and (S16) from [FFGCG15] of the main text with the outer commutator in the second term replaced by an anti-commutator. After employing the bound (S17), also in the fermionic case, a part of the right-hand side can be identified to be $C_r^l(t)$ allowing for the same type of recursive bound on $\|C_r^l(t, t)\|$. As everything is now reduced to scalars, one can proceed completely analogous to the proof in [FFGCG15] of the main text to obtain, with c_0, c_1, and ϑ constants,

$$C_r(t) \leq c_0 e^{v\,t - r/\vartheta} + c_1 e^{v_\vartheta\, t}(\vartheta\, v\, t/r)^\alpha \tag{C.9}$$

where

$$v_\vartheta \leq \vartheta\, t^D\, \vartheta^{2\,D - \alpha}, \tag{C.10}$$

which is the analogue to Eq. (18) in [FFGCG15] of the main text.

That Lemma 2 is restricted to $\alpha > 2\,D$ is a consequence of the above bound on v_ϑ, which becomes small for large ϑ only if $\alpha > 2\,D$. It can be shown to hold as follows.

The quantity v_ϑ is defined as $v_\vartheta := \vartheta'\,(\vartheta\, v\, t)^D\, \lambda_\vartheta$ with

$$\lambda_\vartheta \leq \sum_{d = \vartheta + 1}^{\infty} J\, d^{-\alpha}\, 2\,(2\, d)^{D-1} \tag{C.11}$$

$$= 2^D\, J \sum_{d = \vartheta + 1}^{\infty} d^{D - \alpha - 1} \tag{C.12}$$

$$= 2^D\, J\, \zeta(\alpha - D + 1, \vartheta + 1) \tag{C.13}$$

where ζ is the Hurwitz zeta function (a generalization of the Riemann zeta function). In total this gives

$$v_\vartheta \leq \vartheta'\,(2\, \vartheta\, v\, t)^D\, J\, \zeta(\alpha - D + 1, \vartheta + 1), \tag{C.14}$$

and it remains to show a bound on ζ for large ϑ. We make use of the following integral representation of ζ, valid for all $\alpha - D + 1 > 0$ and $\vartheta > 0$:

$$\zeta(\alpha - D + 1, \vartheta) = \Gamma(\alpha - D + 1)^{-1} \int_0^\infty \frac{x^{\alpha - D} \, \mathrm{e}^{-\vartheta x}}{1 - \mathrm{e}^{-x}} \, \mathrm{d}x \qquad (C.15)$$

The integrand can be bounded using

$$\frac{1}{\mathrm{e}^{x/2} - \mathrm{e}^{-x/2}} \le \frac{1}{x} \implies \frac{1}{1 - \mathrm{e}^{-x}} \le \frac{\mathrm{e}^{x/2}}{x}, \qquad (C.16)$$

which, as long as $\alpha > D$, allows to compute the resulting integral explicitly

$$\int_0^\infty x^{\alpha - D - 1} \, \mathrm{e}^{-(\vartheta - 1/2)\, x} \, \mathrm{d}x \qquad (C.17)$$

$$= \Gamma(\alpha - D)\,(\vartheta - 1/2)^{D - \alpha}, \qquad (C.18)$$

which yields the following bound on v_ϑ

$$v_\vartheta \le \vartheta'\,(2\,v)^D\,J\,\frac{\Gamma(\alpha - D)}{\Gamma(\alpha - D + 1)}\,t^D\,\vartheta^D(\vartheta - 1/2)^{D - \alpha}. \qquad (C.19)$$

Proceeding as in [FFGCG15] of the main text one obtains Lemma 2 as stated in the main text. □

C.3. PBC implies short-range interactions

Here we show that the long-range contribution of the Hamiltonian (5.17),

$$H_{\mathrm{LR}} := \frac{\Delta}{2} \sum_{i=1}^{L} \sum_{j=1}^{L-1} d_j^{-\alpha} \left(a_i\, a_{i+j} + a_{i+j}^\dagger\, a_i^\dagger \right), \qquad (C.20)$$

is only non-negligible when antiperiodic boundary conditions are considered, that is, for $i > L$ we set $a_i := -a_{i \mod L}$. For simplicity, we study the problem for both periodic and antiperiodic boundary conditions and make use of a parameter p_{BC} which characterizes the boundary conditions, such that $p_{BC} = +1$ corresponds to periodic boundary conditions (PBC) and $p_{BC} = -1$ corresponds to antiperiodic (ABC).

C. Appendix of Chapter 5: Correlations in long-range interacting systems

First, we analyse the first term of the long-range term (5.17) (the annihilation-annihilation term) and divide the sum in j into two contributions, such as

$$H_{\text{LR}}^{\text{a}-\text{a}} = \sum_{i=1}^{L} \sum_{j=1}^{L-1} d_j^{-\alpha} \, a_i \, a_{i+j} \qquad (\text{C}.21)$$

$$= \sum_{i=1}^{L} \left(\sum_{j=1}^{L-i} d_j^{-\alpha} \, a_i \, a_{i+j} + \sum_{j=L-i+1}^{L-1} d_j^{-\alpha} a_i \, a_{i+j} \right). \qquad (\text{C}.22)$$

Given this, we apply the boundary conditions and introduce a change of indexes $j' = i + j - L$ for the second term, such that

$$\sum_{i=1}^{L} \sum_{j'=1}^{i-1} d_{j'+L-i}^{-\alpha} \, a_i \, a_{j'+L} = p_{BC} \sum_{i=1}^{L} \sum_{j'=1}^{i-1} d_{j'+L-i}^{-\alpha} \, a_i \, a_{j'}. \qquad (\text{C}.23)$$

Then we reorder the sums as follows,

$$p_{BC} \sum_{i=1}^{L} \sum_{j'=1}^{i-1} d_{j'+L-i}^{-\alpha} \, a_i \, a_{j'} = p_{BC} \sum_{j'=1}^{L} \sum_{i=j'+1}^{L} d_{j'+L-i}^{-\alpha} \, a_i \, a_{j'}. \qquad (\text{C}.24)$$

We apply the canonical commutation relation $\{a_i, a_k\} = 0$, make two changes of indexes: first, $j'' \to i - j'$ and, second, $i \to j'$ and $j \to j''$; and apply $d_{L-j} = d_j$. Finally, we get

$$p_{BC} \sum_{j'=1}^{L} \sum_{i=j'+1}^{L} d_{j'+L-i}^{-\alpha} \, a_i \, a_{j'} = -p_{BC} \sum_{j'=1}^{L} \sum_{j''=1}^{L-j'} d_{L-j''}^{-\alpha} \, a_{j'} \, a_{j'+j''} \qquad (\text{C}.25)$$

$$= -p_{BC} \sum_{i=1}^{L} \sum_{j=1}^{L-i} d_j^{-\alpha} \, a_i \, a_{i+j}. \qquad (\text{C}.26)$$

We substitute the equation (C.26) into the term (C.22), such that

$$H_{\text{LR}}^{\text{a}-\text{a}} = \sum_{i=1}^{L} \left(\sum_{j=1}^{L-i} d_j^{-\alpha} \, a_i \, a_{i+j} - p_{BC} \sum_{j=1}^{L-i} d_j^{-\alpha} \, a_i \, a_{i+j} \right). \qquad (\text{C}.27)$$

Given this expression, it is clear that this term and its conjugate cancel for periodic boundary conditions. We can conclude then that the long-range term does not contribute for PBC and for any interaction exponent α. On the other hand, the long-range term (5.17) for antiperiodic boundary conditions is not null and can be reexpressed as

$$H_{\text{LR}} = \Delta \sum_{i=1}^{L} \sum_{j=1}^{L-i} d_j^{-\alpha} \left(a_i \, a_{i+j} + a_{i+j}^\dagger \, a_i^\dagger \right). \qquad (\text{C}.28)$$

C.4. Power-law decay of correlations in the Kitaev chain
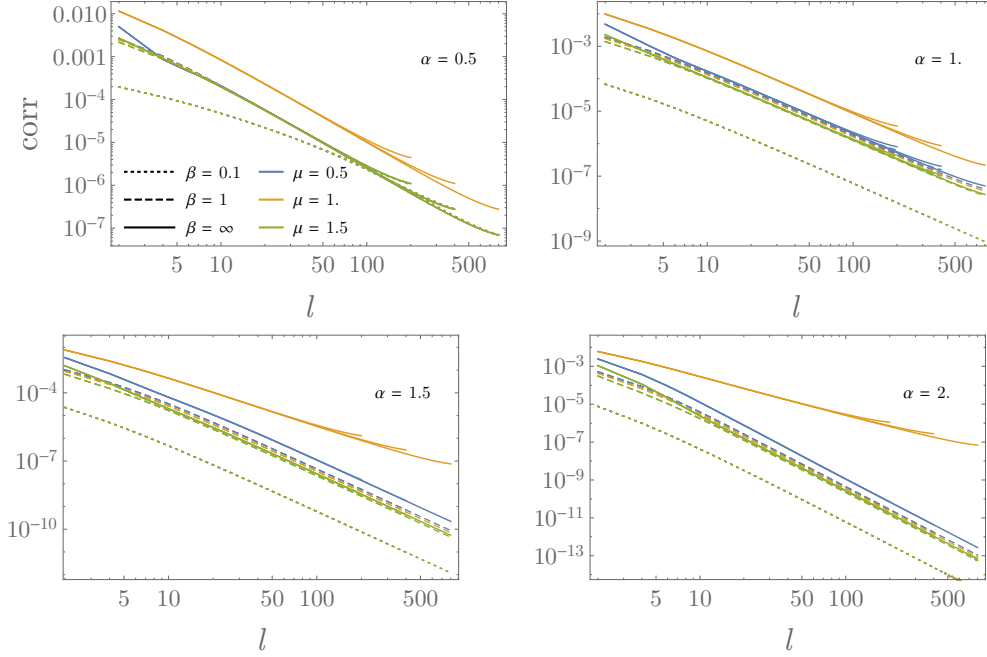
Figure C.1.: Double logarithmic plots of the correlations corr as a function of the distance l for $\alpha = 0.5, 1, 1.5, 2$ from left to right. The blue, orange and green lines correspond to $\mu = 0.5, 1.0, 1.5$. The different line styles indicate different inverse temperatures, namely $\beta = 0.1, 1.0, \infty$ respectively. For each combination we overlay curves for chain lengths $L = 500, 1000, 2000$ to visualize the influence of finite size effects. For large α and high temperatures a bending of the curves at short distances is visible, reminiscent of the transient behavior observed for $\alpha > 1$ at $T = 0$ in [VLE$^+$14] of the main text. The exponents shown in Figure 5.1 in the main text were determined by linear fits to the logarithmized data in the range $l \in [l_{\min}, 300]$ with $l_{\min} = 200$ except for $\alpha \geq 2$, where $l_{\min} = 50$ for $\beta = 1, \infty$ and $l_{\min} = 20$ for $\beta = 0.1$. Data with corr $< \mathrm{e}^{-32}$ were discarded. The remaining data is almost perfectly linear in the double logarithmic plot.

## C.5. Correlations for different values of Δ
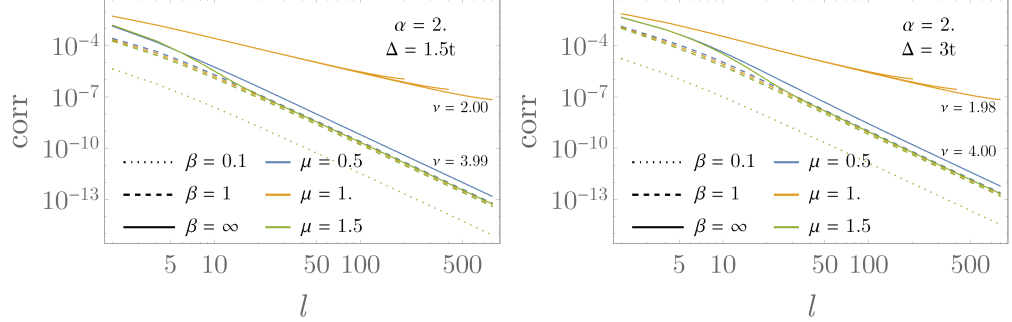
Figure C.2.: Double logarithmic plots of the correlations corr as a function of the distance l for $\Delta/t = 1.5, 3$ from left to right. The blue, orange and green lines correspond to $\mu = 0.5, 1.0, 1.5$. The different line styles indicate different inverse temperatures, namely $\beta = 0.1, 1.0, \infty$ respectively. For each combination we overlay curves for chain lengths $L = 500, 1000, 2000$ to visualize the influence of finite size effects. The exponents have been extracted in the same way than described in Figure C.1. Notice that the plots are equivalent in the asymptotics with the only exception of the quantitative value of the correlations, which are greater when Δ increases.

C.6. Fourier analysis

Here we compare our result with what can be obtained using tools from Fourier analysis. It is known that one can essentially show the following (some additional conditions omitted for the sake of brevity, see [Kat04, Section I.4] of the main text for more details):

i. If the absolute values $|f_k|$ of the Fourier coefficients of a function f decay slightly faster than $|k|^{-\alpha}$, then f is almost $(\alpha - 1)$-times continuously differentiable.

ii. If a function f is α'-times continuously differentiable, then the absolute values $|f_k|$ of its Fourier coefficients decay like $|k|^{-\alpha'}$.

If the Hamiltonian H of a 1D long range system is quadratic and translation invariant, then the Hamiltonian matrix $h_{ij} \in \mathcal{O}(|i - j|^{-\alpha})$ is circulant and its first row can be thought of as the Fourier coefficients of a function $f(x)$ that is almost $(\alpha - 1)$-times

continuously differentiable. In turn, $\mathrm{corr}(a_i, a_{i+l})_\beta$ can be thought of as the Fourier coefficients of the function $g(x) := 1/(1+\mathrm{e}^{\beta\, f(x)})$, which is also almost $(\alpha-1)$-times continuously differentiable, and thus $\mathrm{corr}(a_i, a_{i+l}) \in \mathcal{O}(|l|^{-\alpha+1})$.

C. Appendix of Chapter 5: Correlations in long-range interacting systems

D. Appendix of Chapter 6: *Low-temperature thermometry enhanced by strong coupling*

D.1. From the Heisenberg equations to the QLE

We can write down the Heisenberg equations of motion $\left(\frac{d}{dt}A(t) = i[H, A(t)] + \partial_t A(t)\right)$ for all degrees of freedom $\{x, p, x_i, p_i\}$ of the total system $H = H_p + H_s + H_{p-s}$. These read

$$\dot{x} = p \tag{D.1a}$$

$$\dot{p} = -\left(\omega_0^2 + \omega_R^2\right)x - \sum_i g_i x_i \tag{D.1b}$$

$$\dot{x}_i = \frac{p_i}{m_i} \tag{D.1c}$$

$$\dot{p}_i = -m_i \omega_i^2 x_i - g_i x. \tag{D.1d}$$

Differentiating Eq. (D.1c) and inserting in it Eq. (D.1d) yields $\ddot{x}_i + \omega_i^2 x_i = -\frac{g_i}{m_i}x$, which results in

$$x_i(t) = x_i(t_0) \cos \omega_i(t - t_0) + \frac{p_i(t_0)}{m_i \omega_i} \sin \omega_i(t - t_0)$$
$$- \frac{g_i}{m_i \omega_i} \int_{t_0}^t ds \sin \omega_i(t - s)\, x(s). \tag{D.2}$$

Similarly, one can differentiate Eq. (D.1a) and use Eqs. (D.1b) and (D.2) to eliminate $\dot{p}$ and x_i. This results in the following integro-differential equation

$$\ddot{x} + \left(\omega_0^2 + \omega_R^2\right)x - \int_{t_0}^t ds \sum_i \frac{g_i^2}{m_i \omega_i} \sin \omega_i(t - s)\, x(s)$$
$$= -\sum_i g_i \left(x_i(t_0) \cos \omega_i(t - t_0)\right.$$
$$\left. + \frac{p_i(t_0)}{m_i \omega_i} \sin \omega_i(t - t_0)\right). \tag{D.3}$$

This is the quantum Langevin equation (QLE) for our probe. Since we are interested in the steady state of the central oscillator, we may let $t_0 \to -\infty$ without loss of generality. Defining the stochastic quantum force

$$f(t) := -\sum_i g_i \left(x_i(t_0) \cos \omega_i(t - t_0)\right.$$
$$\left. + \frac{p_i(t_0)}{m_i \omega_i} \sin \omega_i(t - t_0)\right), \tag{D.4}$$

and the dissipation kernel

$$
\begin{aligned}
\chi(t) &:= \sum_i \frac{g_i^2}{m_i \omega_i} \sin \omega_i t \, \Theta(t) \\
&= \frac{2}{\pi} \int_0^\infty \mathrm{d}\omega \, J(\omega) \sin \omega t \, \Theta(t),
\end{aligned}
\tag{D.5}
$$

one may rewrite the QLE as

$$
\ddot{x}(t) + \left(\omega_0^2 + \omega_R^2 \right) x(t) - x(t) \, \chi(t) = f(t),
\tag{D.6}
$$

where $*$ denotes convolution. Note that, so far, the initial state of the sample has not been specified and is thus completely general. In Sec. D.2 below we shall adopt a thermal equilibrium preparation.

D.2. Steady-state solution of the QLE: The fluctuation-dissipation relation

Let us start by computing $\frac{1}{2}\langle\{\tilde{f}(\omega'), \tilde{f}(\omega'')\}\rangle_T = \mathrm{Re}\,\langle \tilde{f}(\omega')\tilde{f}(\omega'')\rangle_T$ from Eq. (D.4), where the subscript in $\langle \cdots \rangle_T$ emphasizes that the average is taken over the initial Gibbs state of the sample. Taking into account that $\langle x_i(t_0)x_i'(t_0)\rangle_T = \delta_{ii'}(2m_i\omega_i)^{-1}[1+ 2n_i(T)]$, $\langle p_i(t_0)p_i'(t_0)\rangle_T = \delta_{ii'}\frac{1}{2}m_i\omega_i[1+2n_i(T)]$ and $\langle x_i(t_0)p_i(t_0)\rangle_T = \langle p_i(t_0)x_i(t_0)\rangle_T^* = i/2$, one has

$$
\begin{aligned}
\frac{1}{2}\langle\{\tilde{f}(t'), \tilde{f}(t'')\}\rangle_T &= \frac{1}{\pi}\sum_i \frac{\pi g_i^2}{2m_i\omega_i}[1 + 2n_i(T)] \\
&\quad \times \Bigg[\cos\omega_i(t' - t_0)\cos\omega_i(t'' - t_0) \\
&\qquad\qquad + \sin\omega_i(t' - t_0)\sin\omega_i(t'' - t_0)\Bigg] \\
&= \frac{1}{\pi}\int_0^\infty \mathrm{d}\omega \, J(\omega)\coth\frac{\omega}{2T}\cos\omega(t' - t''),
\end{aligned}
\tag{D.7}
$$

where we have used $2n_i(T)+1 = \coth\left(\omega_i/2T\right)$, which follows from the definition of the bosonic thermal occupation number $n_i(T) := [\exp\left(\omega/2T\right) - 1]^{-1}$. Now, taking

the Fourier transform of Eq. (D.7) yields

$$\frac{1}{2}\langle\{\tilde{f}(\omega'), \tilde{f}(\omega'')\}\rangle_T$$

$$= 2\pi \int\limits_{-\infty}^{\infty} \frac{\mathrm{d}t'}{2\pi} e^{i\omega't'} \int\limits_{-\infty}^{\infty} \frac{\mathrm{d}t''}{2\pi} e^{i\omega''t''} \int\limits_{0}^{\infty} \mathrm{d}\omega\, J(\omega) \coth\frac{\omega}{2T} \left(e^{i\omega(t'-t'')} + e^{-i\omega(t'-t'')}\right)$$

$$= 2\pi \int\limits_{-\infty}^{\infty} \frac{\mathrm{d}t'}{2\pi} \int\limits_{-\infty}^{\infty} \frac{\mathrm{d}t''}{2\pi} \int\limits_{0}^{\infty} \mathrm{d}\omega\, J(\omega) \coth\frac{\omega}{2\pi} \left(e^{it'(\omega+\omega')}e^{it''(\omega''-\omega)} + e^{it'(\omega'-\omega)}e^{it''(\omega''+\omega)}\right)$$

$$= 2\pi \int\limits_{0}^{\infty} \mathrm{d}\omega\, J(\omega) \coth\frac{\omega}{2T} \left[\delta(\omega+\omega')\delta(\omega''-\omega) + \delta(\omega'-\omega)\delta(\omega''+\omega)\right]$$

$$= 2\pi\, \delta(\omega'+\omega'') \coth\frac{\omega'}{2T} \left[J(\omega')\,\Theta(\omega') - J(-\omega')\,\Theta(-\omega')\right], \tag{D.8}$$

where we have used the identity $\int_{-\infty}^{\infty} \mathrm{d}t\, e^{i\omega t} = 2\pi\, \delta(\omega)$. On the other hand, we may find $\operatorname{Im}\tilde{\chi}(\omega)$ from Eq. (D.5). Note that

$$\operatorname{Im}\tilde{\chi}(\omega) = \operatorname{Im}\sum_i \frac{g_i^2}{m_i\omega_i} \int\limits_{-\infty}^{\infty} \mathrm{d}t\, e^{i\omega t}\, \Theta(t)\, \sin\omega_i t = \sum_i \frac{g_i^2}{m_i\omega_i} \int\limits_{0}^{\infty} \mathrm{d}t\, \sin\omega t \sin\omega_i t$$

$$= -\frac{1}{4}\sum_i \frac{g_i^2}{m_i\omega_i} \int\limits_{0}^{\infty} \mathrm{d}t\, [e^{i(\omega+\omega_i)t} - e^{i(\omega-\omega_i)t} - e^{i(-\omega+\omega_i)t} + e^{-i(\omega+\omega_i)t}]$$

$$= -\frac{1}{4}\sum_i \frac{g_i^2}{m_i\omega_i} \left(\int\limits_{-\infty}^{\infty} \mathrm{d}t\, e^{i(\omega+\omega_i)t} - \int\limits_{-\infty}^{\infty} \mathrm{d}t\, e^{i(\omega-\omega_i)t}\right)$$

$$= \frac{\pi}{2}\sum_i \frac{g_i^2}{m_i\omega_i}[\delta(\omega-\omega_i) - \delta(\omega+\omega_i)] = \int\limits_{0}^{\infty} \mathrm{d}\omega'\, J(\omega')[\delta(\omega-\omega') - \delta(\omega+\omega')]$$

$$= J(\omega)\,\Theta(\omega) - J(-\omega)\,\Theta(-\omega). \tag{D.9}$$

Hence the fluctuation-dissipation relation $\langle\{\tilde{f}(\omega'), \tilde{f}(\omega'')\}\rangle$
$= 4\pi\, \delta(\omega'+\omega'') \coth(\omega'/2T) \operatorname{Im}\tilde{\chi}(\omega')$. When it comes to its real part, the calculation is not so straightforward. Recall from Eq. (D.5) that the response function $\chi(t)$ is *causal* due to the accompanying Heaviside step function. Causal response functions have analytic Fourier transform in the upper-half of the complex plane and therefore, the Kramers-Kronig relations hold [Wei08]. In particular

$$\operatorname{Re}\tilde{\chi}(\omega) = \frac{1}{\pi}\,\mathrm{P}\int\limits_{-\infty}^{\infty} \mathrm{d}\omega' \frac{\operatorname{Im}\tilde{\chi}(\omega')}{\omega'-\omega} := \mathcal{H}\operatorname{Im}\tilde{\chi}(\omega), \tag{D.10}$$

where we have introduced the Hilbert transform $g(y) = \mathcal{H} f(x) := \pi^{-1} \mathrm{P} \int_{-\infty}^{\infty} dx\, f(x)/(x-y)$ [Bat54], and P denotes Cauchy principal value.

D.3. Dissipation kernel for Ohmic and super-Ohmic spectral densities with exponential cutoff

We will now obtain $\mathbb{R}\,\tilde{\chi}(\omega)$ for two instances of the family of spectral densities $J_s(\omega) := \frac{\pi}{2}\gamma\omega^s\omega_c^{1-s}e^{-\omega/\omega_c}$, namely $s = 1$ (Ohmic case) and $s = 2$ (super-Ohmic case) [VRA15]. To begin with, let us list four useful properties of the Hilbert transform that we shall use in what follows

$$f(-ax) \stackrel{\mathcal{H}}{\longmapsto} -g(-ay)a > 0 \tag{D.11a}$$

$$x f(x) \stackrel{\mathcal{H}}{\longmapsto} y\, g(y) + \frac{1}{\pi} \int\limits_{-\infty}^{\infty} dx\, f(x) \tag{D.11b}$$

$$\exp(-a|x|) \stackrel{\mathcal{H}}{\longmapsto} \frac{1}{\pi}\mathrm{sign}\, y \left[e^{a|y|}\,\mathrm{Ei}(-a|y|) - e^{-a|y|}\,\overline{\mathrm{Ei}}(a|y|) \right], \quad a > 0 \tag{D.11c}$$

$$\mathrm{sign}\, x \exp(-a|x|) \stackrel{\mathcal{H}}{\longmapsto} -\frac{1}{\pi}\left[\exp(a|y|)\,\mathrm{Ei}(-a|y|) + \exp(-a|y|)\,\overline{\mathrm{Ei}}(a|y|) \right], \quad a > 0, \tag{D.11d}$$

where $\mathrm{Ei}(x) := -\int_{-x}^{\infty} dt\, t^{-1}e^{-t}$ is the exponential integral, and $\overline{\mathrm{Ei}}(x)$ denotes its principal value.

D.3.1. Ohmic case ($s = 1$)

According to Eqs. (D.10) and (D.9), one has

$$\mathbb{R}\,\tilde{\chi}(\omega) = \frac{\pi\gamma}{2}\left\{ \mathcal{H}[\Theta(\omega')\,\omega' \exp(-\omega'/\omega_c)](\omega) - \mathcal{H}[-\Theta(-\omega')\,\omega' \exp(\omega'/\omega_c)](\omega) \right\}. \tag{D.12}$$

Using Eqs. (D.11a) and (D.11b), this rewrites as

$$\mathbb{R}\,\tilde{\chi}(\omega) = \frac{\pi\gamma}{2}\left\{ \mathcal{H}[\Theta(\omega')\,\omega' \exp(-\omega'/\omega_c)](\omega) + \mathcal{H}[\Theta(\omega')\,\omega' \exp(-\omega'/\omega_c)](-\omega) \right\}$$
$$= \frac{\pi\gamma}{2}\left\{ \omega\,\mathcal{H}[\Theta(\omega')\,\exp(-\omega'/\omega_c)](\omega) - \omega\,\mathcal{H}[\Theta(\omega')\,\exp(-\omega'/\omega_c)](-\omega) + \frac{2\omega_c}{\pi} \right\}. \tag{D.13}$$

Now, using first Eq. (D.11a) again, and then Eq. (D.11c), one finds

$$
\begin{aligned}
\mathbb{R}\,\tilde{\chi}(\omega) &= \gamma\omega_c + \frac{\pi\gamma}{2}\omega\,\mathcal{H}[\exp\left(-|\omega'|/\omega_c\right)](\omega) \\
&= \gamma\omega_c - \frac{\gamma}{2}\omega\left[\exp\left(-\omega/\omega_c\right)\overline{\mathrm{Ei}}(\omega/\omega_c) - \exp\left(\omega/\omega_c\right)\mathrm{Ei}(-\omega/\omega_c)\right],\quad \text{(D.14)}
\end{aligned}
$$

which can also be expressed in terms of the incomplete Euler's Gamma function $\Gamma(0,x) = -\mathrm{Ei}(-x)$.

D.3.2. Super-Ohmic case ($s = 2$)

Using the properties of Eq. (D.11) it is also straightforward to obtain $\mathbb{R}\,\tilde{\chi}(\omega)$ in the case of $s = 2$:

$$
\begin{aligned}
\mathbb{R}\,\tilde{\chi}(\omega) &= \frac{\pi\gamma}{2\omega_c}\left\{\mathcal{H}[\Theta(\omega')\,\omega'^2\exp\left(-\omega'/\omega_c\right)](\omega) - \mathcal{H}[\Theta(-\omega')\,\omega'^2\exp\left(\omega'/\omega_c\right)](\omega)\right\} \\
&= \frac{\pi\gamma}{2\omega_c}\left\{\mathcal{H}[\Theta(\omega')\,\omega'^2\exp\left(-\omega'/\omega_c\right)](\omega) + \mathcal{H}[\Theta(\omega')\,\omega'^2\exp\left(-\omega'/\omega_c\right)](-\omega)\right\} \\
&= \frac{\pi\gamma}{2\omega_c}\left\{\omega\,\mathcal{H}[\Theta(\omega')\,\omega'\exp\left(-\omega'/\omega_c\right)](\omega) - \omega\,\mathcal{H}[\Theta(\omega')\,\omega'\exp\left(-\omega'/\omega_c\right)](-\omega) + \frac{2\omega_c^2}{\pi}\right\} \\
&= \gamma\omega_c + \frac{\pi\gamma}{2\omega_c}\left\{\omega^2\,\mathcal{H}[\Theta(\omega')\exp\left(-\omega'/\omega_c\right)](\omega) + \omega^2\,\mathcal{H}[\Theta(\omega')\exp\left(-\omega'/\omega_c\right)](-\omega)\right\} \\
&= \gamma\omega_c + \frac{\pi\gamma}{2\omega_c}\omega^2\,\mathcal{H}[\mathrm{sign}\,\omega\,\exp\left(-|\omega'|/\omega_c\right)](\omega) \\
&= \gamma\omega_c - \frac{\gamma}{2\omega_c}\omega^2\left[\exp\left(-\omega/\omega_c\right)\overline{\mathrm{Ei}}(\omega/\omega_c) + \exp\left(\omega/\omega_c\right)\mathrm{Ei}(-\omega/\omega_c)\right].
\end{aligned}
$$

$$\text{(D.15)}$$

D.4. Calculation of the steady-state covariances

Now we have all the ingredients to compute the steady-state covariances of the central oscillator. Note that

$$\frac{1}{2}\langle\{x(t'), x(t'')\}\rangle = \frac{1}{2}\int\limits_{-\infty}^{\infty}\frac{d\omega'}{2\pi}\,e^{-i\omega't'}\int\limits_{-\infty}^{\infty}\frac{d\omega''}{2\pi}\,e^{-i\omega''t''}\alpha(\omega')^{-1}\alpha(\omega'')^{-1}\langle\{\tilde{f}(\omega'),\tilde{f}(\omega'')\}\rangle_T$$

(D.16)

$$= \int\limits_{-\infty}^{\infty}\frac{d\omega'}{2\pi}\,e^{-i\omega't'}\int\limits_{-\infty}^{\infty}d\omega''\,e^{-i\omega''t''}\alpha(\omega')^{-1}\alpha(\omega'')^{-1}\times$$

$$\times\,[J(\omega')\Theta(\omega') - J(-\omega')\Theta(-\omega')]\coth\frac{\omega'}{2T}\,\delta(\omega'+\omega'')$$

(D.17)

$$= \int\limits_{-\infty}^{\infty}\frac{d\omega'}{2\pi}\,e^{-i\omega'(t'-t'')}\alpha(\omega')^{-1}\alpha(-\omega')^{-1}[J(\omega')\Theta(\omega') - J(-\omega')\Theta(-\omega')]\coth\frac{\omega'}{2T}.$$

(D.18)

This gives a closed expression for the position-position covariance. Note that, since $\tilde{p}(\omega) = -i\omega\,\tilde{x}(\omega)$, one has $2^{-1}\langle\{\tilde{p}(\omega'), \tilde{x}(\omega'')\}\rangle = 0$ and

$$\frac{1}{2}\langle\{p(t'), p(t'')\}\rangle$$

$$= \int\limits_{-\infty}^{\infty}\frac{d\omega'}{2\pi}\,e^{-i\omega'(t'-t'')}\,\omega'^2\,\alpha(\omega')^{-1}\alpha(-\omega')^{-1}[J(\omega')\Theta(\omega') - J(-\omega')\Theta(-\omega')]\coth\frac{\omega'}{2T}.$$

(D.19)

Therefore, we have fully characterized the steady state of a single harmonic oscillator in a bosonic bath. Note that the *only* underlying assumption is that the sample was prepared in an equilibrium state at temperature T. Specifically, this was required when evaluating the correlators $\langle\{x_i(t_0), x_i(t_0)\}\rangle_T$ and $\langle\{p_i(t_0), p_i(t_0)\}\rangle_T$ in Eq. (D.7). Otherwise, our calculation is *completely general*. For a non-equilibrium sample, one would only need to recalculate Eqs. (D.7) and (D.8).

D.4.1. Explicit calculation for Ohmic spectral density with Lorentz-Drude cutoff

The integrals in Eqs. (D.18) and (D.19) are easy to evaluate numerically. However, when dealing with the simple Ohmic spectral density with Lorentz-Drude cutoff introduced in the main text as $J(\omega) = 2\gamma\omega_c^2\omega/(\omega^2 + \omega_c^2)$, it is possible to calculate the

covariances analytically. This will allow us to get some insight into the temperature-dependence of the covariances at very low T and about the squeezing in the position quadrature described in the main text.

Let us start calculating $\langle x^2 \rangle$. For our choice of spectral density Eq. (D.18) reads

$$\langle x^2 \rangle = \frac{\gamma \omega_c^2}{\pi} \int_{\infty}^{\infty} d\omega \, \frac{\frac{\omega}{\omega^2 + \omega_c^2} \coth \frac{\omega}{2T}}{(\omega_0^2 - \omega^2 + 2\gamma\omega_c - \frac{2\gamma\omega_c^2}{\omega_c - i\omega})(\omega_0^2 - \omega^2 + 2\gamma\omega_c - \frac{2\gamma\omega_c^2}{\omega_c + i\omega})},$$
(D.20)

which can be re-written as

$$\langle x^2 \rangle = \frac{2T\gamma\omega_c^2}{\pi} \left(\sum_{n=1}^{\infty} \int_{-\infty}^{\infty} d\omega \, \frac{\omega^2}{h_4(\omega) h_4(-\omega)} + \int_{-\infty}^{\infty} \frac{d\omega}{h_3(\omega) h_3(-\omega)} \right), \quad \text{(D.21)}$$

where $h_4(\omega) := (\omega - i\nu_n)[(\omega_0^2 - \omega^2 + 2\gamma\omega_c)(\omega_c + i\omega) - 2\gamma\omega_c^2]$, $h_3(\omega) = (\omega_0^2 - \omega^2 + 2\gamma\omega_c)(\omega_c + i\omega) - 2\gamma\omega_c^2$, and owing to the identity $\coth \frac{\omega}{2T} = 2\sum_{n=1}^{\infty} \frac{2T\omega}{\nu_n^2 + \omega^2} + \frac{2T}{\omega}$, where $\nu_n := 2\pi T n$ are the Matsubara frequencies.

Integrals such as those in Eq. (D.21) can be evaluated using the following formula [GR07]

$$\int_{-\infty}^{\infty} dx \, \frac{g_n(x)}{h_n(x) h_n(-x)} = \frac{i\pi}{a_0} \frac{\det \mathsf{M}_n}{\det \Delta_n}, \quad \text{(D.22)}$$

where $g_n(x) := b_0 x^{2n-2} + b_1 x^{2n-4} + \cdots + b_{n-1}$ and $h_n(x) := a_0 x^n + a_1 x^{n-1} + \cdots + a_n$ and the matrices Δ_n and M_n are defined as

$$\Delta_n := \begin{pmatrix} a_1 & a_3 & \cdots & 0 \\ a_0 & a_2 & \cdots & 0 \\ 0 & a_1 & \cdots & 0 \\ \vdots & \vdots & \ddots & \vdots \\ 0 & 0 & \cdots & a_n \end{pmatrix}, \qquad \mathsf{M}_n := \begin{pmatrix} b_0 & b_1 & \cdots & b_{n-1} \\ a_0 & a_2 & \cdots & 0 \\ 0 & a_1 & \cdots & 0 \\ \vdots & \vdots & \ddots & \vdots \\ 0 & 0 & \cdots & a_n \end{pmatrix}. \quad \text{(D.23)}$$

For (D.22) to be valid, $h_n(x)$ must have all its roots in the upper half of the complex plane, which is the case for us. The covariance $\langle x^2 \rangle$ thus rewrites as

$$\langle x^2 \rangle = 2 \sum_{n=1}^{\infty} \frac{T(\nu_n + \omega_c)}{\nu_n(\nu_n^2 + \omega_0^2) + (\nu_n^2 + 2\gamma\nu_n + \omega_0^2)\omega_c} + \frac{1}{2\omega_0^2}. \quad \text{(D.24)}$$

To proceed further, we shall resort to the *digamma* function $\psi(z)$, defined as the logarithmic derivate of Euler's gamma function [AS65]; that is $\psi(z) := \frac{d}{dz} \ln \Gamma_0(z)$, where $\Gamma(z)_0 := \int_0^{\infty} dt \, t^{z-1} e^{-t}$. The digamma function satisfies the following identity [AS65]

$$\sum_{n=1}^{\infty} \frac{G(n)}{H(n)} = \sum_{n=0}^{\infty} \frac{G(n+1)}{H(n+1)} = \sum_{n=0}^{\infty} \sum_{m=1}^{N} \frac{c_m}{n - d_m}$$

$$= -\sum_{m=1}^{N} c_m \psi(-d_m), \qquad (D.25)$$

where $G(n)$ and $H(n)$ are polynomials in n, d_m are the N roots (assumed to be simple) of $H(n+1)$, and c_m are the coefficients of the simple-fraction decomposition of $G(n+1)/H(n+1)$ ($\sum_{m=1}^{N} c_m = 0$). In our specific case, the c_m evaluate to

$$c_m =$$
$$\frac{1}{2\pi} \frac{\nu_1(d_m + 1) + \omega_c}{\omega_0^2 + 2\gamma\omega_c + \nu_1(d_m + 1) + \nu_1(d_m + 1)[3\nu_1(d_m + 1) + 2\omega_c]}, \qquad (D.26)$$

and the d_m are the three solutions to

$$\nu_1^3(d + 1)^3 + \nu_1^2(d + 1)^2 \omega_c + \nu_1(d + 1)(\omega_0^2 + 2\gamma\omega_c)$$
$$+ \omega_0^2 \omega_c = 0. \qquad (D.27)$$

Therefore, the covariance $\langle x^2 \rangle$ is

$$\langle x^2 \rangle = \frac{1}{2\omega_0^2} - 2 \sum_{m=1}^{3} c_m \psi_m(-d_m). \qquad (D.28)$$

Similarly, the momentum covariance can be found to be

$$\langle p^2 \rangle = \frac{1}{2} - 2 \sum_{m=1}^{3} c_m' \psi_m(-d_m), \qquad (D.29)$$

where the coefficients c_m' are now given by

$$c_m' = \frac{\nu_1}{\pi} \frac{\omega_0^2 \omega_c + \nu_1(d_m + 1)(\omega_0^2 + 2\gamma\omega_c)}{\omega_0^2 + 2\gamma\omega_c + \nu_1(d_m + 1)[3\nu_1(d_m + 1) + 2\omega_c]}. \qquad (D.30)$$

It must be noted that Eqs. (D.28) and (D.29) are *exact*, though not very informative. In the next section we will try to simplify their expressions by taking the low temperature limit.

D.4.2. Low T and large ω_c limit

Let us consider again Eq. (D.27). To begin with, let us assume that $\gamma/\omega_c \lll 1$ so that $d_m \simeq d_m^{(0)} + \frac{\gamma}{\omega_c} d_m^{(1)}$. One thus has

$$
\begin{aligned}
d_{1,2} = &- \left(1 + \frac{\gamma\omega_c^2}{\nu_1(\omega_0^2 + \omega_c^2)} \right) \\
&\pm i \frac{\omega_0}{\nu_1} \frac{\omega_0^2 + \omega_c(\gamma + \omega_c)}{\omega_0^2 + \omega_c^2} + \mathcal{O}\left(\frac{\gamma}{\omega_c} \right)^2 \\
d_3 = &- \left(1 + \frac{\omega_c}{\nu_1} \right) + \frac{2\gamma\omega_c^2}{\nu_1(\omega_0^2 + \omega_c^2)} + \mathcal{O}\left(\frac{\gamma}{\omega_c} \right)^2 .
\end{aligned} \tag{D.31}
$$

Notice that the roots diverge as $T \to 0$ due to the ν_1 appearing in the denominators. It is thus possible to replace the digamma by the first term in its asymptotic expansion $\psi(z) \sim \ln z$.

Eqs. (D.28) and (D.29) can be further simplified by retaining terms only up to first order in ω_0/ω_c and T/ω_0. When expanding the expressions above, care must be taken with the divergence of terms proportional to $\ln \frac{\omega_c}{\omega_0}$. One eventually arrives to the following approximate covariances

$$
\langle x^2 \rangle \simeq \frac{1}{2\omega_0} - \frac{1}{2\omega_0} \left(\frac{2\gamma}{\pi\omega_0} + \frac{2T}{\omega_0} + \frac{4\gamma\omega_0}{\pi\omega_c^2} \ln \frac{\omega_c}{\omega_0} \right) \tag{D.32a}
$$

$$
\langle p^2 \rangle \simeq \frac{\omega_0}{2} + \frac{\omega_0}{2} \left[\frac{4\gamma}{\pi\omega_0} \ln \frac{\omega_c}{\omega_0} + \frac{3\gamma}{\omega_c} - \left(\frac{2T}{\omega_0} + \frac{2\gamma}{\pi\omega_0} \right) \right] . \tag{D.32b}
$$

From Eq. (D.32a) we can see how the variance in the position quadrature is reduced below its thermal equilibrium value of $\langle x^2 \rangle_T = (2\omega_0)^{-1} \coth \frac{\omega_0}{2T} \sim (2\omega_0)^{-1}$, as noted in the main text. On the other hand, the 'quantum correction' over $\langle p^2 \rangle_T$ [i.e., the bracketed term in Eq. (D.32b)] is dominated by the non-perturbative logarithmic divergence, and will therefore be positive. In particular, for strong dissipation, i.e. $\gamma/\omega_0 \gtrsim 1$, $\langle p^2 \rangle \simeq \langle p^2 \rangle_T + \frac{2\gamma}{\pi} \ln \frac{\omega_c}{\omega_0}$ and hence $\partial_T \langle p^2 \rangle \simeq 0$. On the contrary, there is no reason to drop the temperature dependence of $\langle x^2 \rangle$ in the strong dissipation regime. This intuitively justifies our observation that the dispersion in the position quadrature exhibits a quasi-optimal thermal sensitivity in the ultra-cold strongly-coupled regime, whilst the dispersion in momentum performs very poorly as a temperature estimator.

Unfortunately, Eqs. (D.32) are unsuitable to derive a qualitatively accurate and equally simple analytical expression for the low-temperature QFI. One should proceed instead

directly from Eqs. (D.28) and (D.29) and expand the resulting expression again to first order in the small parameters γ/ω_c, ω_0/ω_c, and T/ω_0. Although this is in principle straightforward, the algebra quickly becomes unmanageable.

D.5. Dependence of the normal-mode frequencies on the coupling strength in a 'star system'

Let us consider a finite *star system* with N modes. As already explained in the main text, this will be comprised of a central harmonic oscillator of bare frequency ω_0 (playing the role of the probe), dissipatively coupled to $N-1$ independent peripheral oscillators with arbitrary frequencies $\omega_{i\in\{1,\cdots,N-1\}}$ (representing the sample). We will choose linear probe-sample couplings of the form $x\,G\sum_{i=1}^{N-1}g_i x_i$. Therefore, adjusting G simply amounts to rescaling the probe-sample interaction without changing the overall frequency distribution of the couplings. This is exactly what happens when the dissipation strength γ is tuned in the spectral density $J(\omega)$ of the continuous Caldeira-Leggett model from the main text. Note that we also allow for an *arbitrary* frequency-distribution of the coupling constants g_i.

Hence, the total N-particle Hamiltonian may be written as $\hat{H} = \frac{1}{2}\bar{x}^{\mathsf{t}}\mathsf{V}\bar{x} + \frac{1}{2}|\bar{p}|^2$. Here, the N-dimensional vectors $\bar{x}$ and $\bar{p}$ are $\bar{x} = (x, x_1, \cdots, x_{N-1})$ and $\bar{p} = (p, p_1, \cdots, p_{N-1})$. For simplicity, we will take unit mass for all particles. The $N \times N$ interaction matrix V may thus be written as

$$\mathsf{V} = G\begin{pmatrix} G^{-1}\Upsilon_0^2 & g_1 & g_2 & \cdots & g_{N-2} & g_{N-1} \\ g_1 & G^{-1}\omega_1^2 & 0 & \cdots & 0 & 0 \\ g_2 & 0 & \omega_2^2 & \cdots & 0 & 0 \\ \vdots & \vdots & \vdots & \ddots & \vdots & \vdots \\ g_{N-2} & 0 & 0 & \cdots & G^{-1}\omega_{N-2}^2 & 0 \\ g_{N-1} & 0 & 0 & \cdots & 0 & G^{-1}\omega_{N-1}^2 \end{pmatrix}. \qquad \text{(D.33)}$$

The frequencies of the normal modes of the system are given by the square root of the N solutions v_i of $P_N(v_i) = |\mathsf{V} - v_i\mathbb{1}| = 0$. Note that we have shifted the frequency of the central oscillator $\omega_0^2 \rightarrow \Upsilon_0^2 := \omega_0^2 + \sum_i g_i^2/\omega_i^2$ to ensure that all $v_i > 0$.

While it is hard to obtain closed expressions for v_i, one may easily see the following: The frequencies of the modes above Υ_0 increase with the coupling strength, whereas those of the modes below Υ_0 decrease with G (i.e. $\partial_G v_i > 0$ for $v_i > \Upsilon_0^2$ and $\partial_G v_i < 0$ for $v_i < \Upsilon_0^2$). Indeed, expanding $P_N(v)$ by minors along the last row,

yields the recurrence relation

$$P_N(v) = (\omega_{N-1}^2 - v)P_{N-1}(v) - G^2 \, g_{N-1}^2 \Pi_{k=1}^{N-2}(\omega_k^2 - v), \qquad (D.34)$$

$$\Upsilon_0^2 - v_i = \frac{1}{\prod_{l=1}^{N-1} \omega_l^2 - v_i} \sum_{k=1}^{N-1} G^2 g_k^2 \prod_{l=1}^{N-1} \frac{\omega_l^2 - v_i}{\omega_k^2 - v_i} = \sum_{k=1}^{N-1} \frac{G^2 g_k^2}{\omega_k^2 - v_i}. \qquad (D.35)$$

Consequently, the derivative of any eigenvalue v_i with respect to the coupling strength G evaluates to

$$\partial_G v_i = -\frac{2G \sum_{k=1}^{N-1} g_k^2 (\omega_k^2 - v_i)^{-1}}{1 + \sum_{k=1}^{N-1} G^2 g_k^2 (\omega_k^2 - v_i)^{-2}}. \qquad (D.36)$$

Comparing Eqs. (D.35) and (D.36) we can see that $\partial_G v_i > 0$ for $v_i > \Upsilon_0^2$, and that, on the contrary, $\partial_G v_i < 0$ for $v_i < \Upsilon_0^2$.

Now consider the situation in which the star system is prepared in a Gibbs state at temperature T. Paraphrasing the line of reasoning of the main text, if T happens to be so low that not even the fundamental mode is significantly populated, the thermal sensitivity of the entire system, and also that of the central temperature probe, vanishes. However, if we were to increase the coupling strength G, the frequencies of the lowest normal modes would decrease monotonically. As a result, the first few modes could get thermally populated thus enabling temperature sensing.

This intuition can be made more precise by explicitly writing the total QFI of the star system $\mathcal{F}_T^{(\text{star})}$. Its global thermal state can be expressed as $\Omega_T \propto \exp(-H/T) = \bigotimes_{i=1}^N \Omega_T^{(i)}$, where $\Omega_T^{(i)}$ stands for the Gibbs state of the normal mode at frequency $\sqrt{v_i}$. Since the QFI is additive with respect to tensor products, one has $\mathcal{F}_T^{(\text{star})} = \sum_{i=1}^N \mathcal{F}_T^{(\text{eq})}(\sqrt{v_i})$, where the QFI for temperature estimation in a thermal mode $\mathcal{F}_T^{(\text{eq})}$ was defined in the main text.

If the temperature T is low enough, only the terms corresponding to the lowest-frequency normal modes will contribute significantly to the sum in $\mathcal{F}_T^{(\text{star})}$. Crucially, $\mathcal{F}_T^{(\text{eq})}(\omega)$ also increases monotonically as $\omega \to 0$ which, in turn, entails a *monotonic* increase of $\mathcal{F}_T^{(\text{star})}$ with G at low T. If, on the contrary, the temperature were large enough to thermally populate modes above Υ_0, the situation would become less clear: The global QFI could either increase or decrease with G. Due to its central position, the QFI of the reduced state of the probe qualitatively follows $\mathcal{F}_T^{(\text{star})}$ (although $\mathcal{F}_T \ll \mathcal{F}_T^{(\text{star})}$).

Bibliography

[AS65]   M. Abramowitz and I. A. Stegun (eds.). *Handbook of mathematical functions: with formulas, graphs, and mathematical tables*. Dover Publications (1965).

[ATMC05]   L. Aigouy, G. Tessier, M. Mortier and B. Charlot. Scanning thermal imaging of microelectronic circuits with a fluorescent nanoprobe. *Applied Physics Letters* **87**, 184105 (2005).

[Bal07]   R. Balian. *From Microphysics to Macrophysics*. Springer-Verlag Berlin Heidelberg (2007).

[Bat54]   H. Bateman. *Tables of integral transforms (vol. II)*. McGraw-Hill (1954).

[BC94]   S. L. Braunstein and C. M. Caves. Statistical distance and the geometry of quantum states. *Physical Review Letters* **72**, 3439 (1994).

[BC15]   F. G. S. L. Brandao and M. Cramer. Equivalence of statistical mechanical ensembles for non-critical quantum systems (2015). ArXiv:1502.03263 [quant-ph].

[BCW09]   M.-C. Bañuls, J. I. Cirac and M. M. Wolf. Entanglement in systems of indistinguishable fermions. *Journal of Physics: Conference Series* **171**, 012032 (2009).

[BDN12]   I. Bloch, J. Dalibard and S. Nascimbène. Quantum simulations with ultracold quantum gases. *Nature Physics* **8**, 267 (2012).

[BGM06]   H. P. Breuer, J. Gemmer and M. Michel. Non-Markovian quantum dynamics: Correlated projection superoperators and Hilbert space averaging. *Physical Review E* **73**, 016139 (2006).

[Bha97]   R. Bhatia. *Matrix analysis*. Springer-Verlag Berlin Heidelberg (1997).

[BK13]   R. Bachelard and M. Kastner. Universal threshold for the dynamical

behavior of lattice systems with long-range interactions. *Physical Review Letters* **110**, 170603 (2013).

[BKP01]   H.-P. Breuer, B. Kappler and F. Petruccione. The time-convolutionless projection operator technique in the quantum theory of dissipation and decoherence. *Annals of Physics* **291**, 36 (2001).

[BM71]   E. Barouch and B. M. McCoy. Statistical mechanics of the XY model. II. spin-correlation functions. *Physical Review A* **3**, 786 (1971).

[BNG00]   O. E. Barndorff-Nielsen and R. D. Gill. Fisher information in quantum statistics. *Journal of Physics A* **33**, 4481 (2000).

[Boh49]   N. Bohr. Discussion with einstein on epistemological problems in atomic physics. In: P. A. Schilpp (ed.), *Albert Einstein, Philosopher-Scientist: The Library of Living Philosophers Volume VII*. Open Court (1949).

[BP02]   H.-P. Breuer and F. Petruccione. *The Theory of Open Quantum Systems*. Oxford University Press (2002).

[BSK$^+$12]   J. W. Britton, B. C. Sawyer, A. C. Keith, C. C. J. Wang, J. K. Freericks, H. Uys, M. J. Biercuk and J. J. Bollinger. Engineered two-dimensional Ising interactions in a trapped-ion quantum simulator with hundreds of spins. *Nature* **484**, 489 (2012).

[BvZS06]   T. Bastin, J. von Zanthier and E. Solano. Measure of phonon-number moments and motional quadratures through infinitesimal-time probing of trapped ions. *Journal of Physics B: Atomic, Molecular and Optical Physics* **39**, 685 (2006).

[Car84]   J. L. Cardy. Conformal invariance and surface critical behavior. *Nuclear Physics B* **240**, 514 (1984).

[Car86]   J. L. Cardy. Effect of boundary conditions on the operator content of two-dimensional conformally invariant theories. *Nuclear Physics B* **275**, 200 (1986).

[Car06]   J. Cardy. Boundary conformal field theory. In: J.-P. Françoise, G. L. Naber and T. S. Tsun (eds.), *Encyclopedia of Mathematical Physics*. Academic Press (2006).

[CL83]   A. O. Caldeira and A. J. Leggett. Path integral approach to quantum Brownian motion. *Physica A* **121**, 587 (1983).

[CMAS15]   L. A. Correa, M. Mehboudi, G. Adesso and A. Sanpera. Individual Quantum Probes for Optimal Thermometry. *Physical Review Letters* **114**, 220405 (2015).

[CP15]   L. Carlos and F. Palacio (eds.). *Thermometry at the Nanoscale: Techniques and Selected Applications*. Royal Society of Chemistry (2015).

[CPLH$^+$17]   L. A. Correa, M. Perarnau-Llobet, K. V. Hovhannisyan, S. Hernández-Santana, M. Mehboudi and A. Sanpera. Enhancement of low-temperature thermometry by strong coupling. *Physical Review A* **96**, 062103 (2017).

[Cra99]   H. Cramér. *Mathematical methods of statistics*. Princeton University Press (1999).

[CT96]   S. A. Cannas and F. A. Tamarit. Long-range interactions and nonextensivity in ferromagnetic spin models. *Physical Review B* **54**, R12661 (1996).

[CVA12]   L. A. Correa, A. A. Valido and D. Alonso. Asymptotic discord and entanglement of nonresonant harmonic oscillators under weak and strong dissipation. *Physical Review A* **86**, 012110 (2012).

[DB01]   A. Dutta and J. Bhattacharjee. Phase transitions in the quantum Ising and rotor models with a long-range interaction. *Physical Review B* **64**, 184106 (2001).

[Deb12]   P. Debye. Zur theorie der spezifischen wärmen. *Annalen der Physik (Berlin)* **344**, 789 (1912).

[DFMS97]   P. Di Francesco, P. Mathieu and D. Senechal. *Conformal Field Theory*. Springer-Verlag New York (1997).

[DM96]   C. D'Helon and G. J. Milburn. Reconstructing the vibrational state of a trapped ion. *Physical Review A* **54**, R25 (1996).

[DPC05]   X. L. Deng, D. Porras and J. I. Cirac. Effective spin quantum phases in systems of trapped ions. *Physical Review A* **72**, 063407 (2005).

[DPZ10]   M. Dalmonte, G. Pupillo and P. Zoller. One-dimensional quantum liquids with power-law interactions: The luttinger staircase. *Physical Review Letters* **105**, 140401 (2010).

[DRFG16]   A. De Pasquale, D. Rossini, R. Fazio and V. Giovannetti. Local quantum thermal susceptibility. *Nature Communications* **7**, 12782 (2016).

Bibliography

[dRrR+11]   L. del Rio, J. Åberg, R. Renner, O. Dahlsten and V. Vedraland. The thermodynamic meaning of negative entropy. *Nature* **474**, 61 (2011).

[Dys69]   F. J. Dyson. Existence of a phase-transition in a one-dimensional Ising ferromagnet. *Communications in Mathematical Physics* **12**, 91 (1969).

[EGM+17]   Z. Eldredge, Z.-X. Gong, A. H. Moosavian, M. Foss-Feig and A. V. Gorshkov. Fast state transfer and entanglement renormalization using long-range interactions. *Physical Review Letters* **119**, 170503 (2017).

[EVDWMK13]   J. Eisert, M. Van Den Worm, S. R. Manmana and M. Kastner. Breakdown of quasilocality in long-range quantum lattice models. *Physical Review Letters* **111**, 260401 (2013).

[FFGCG15]   M. Foss-Feig, Z.-X. Gong, C. W. Clark and A. V. Gorshkov. Nearly linear light cones in long-range interacting quantum systems. *Physical Review Letters* **114**, 157201 (2015).

[FGSA12]   A. Ferraro, A. García-Saez and A. Acín. Intensive temperature and quantum correlations for refined quantum measurements. *Europhysics Letters* **98**, 10009 (2012).

[FMN72]   M. E. Fisher, S.-k. Ma and B. G. Nickel. Critical exponents for long-range interactions. *Physical Review Letters* **29**, 917 (1972).

[FOP05]   A. Ferraro, S. Olivares and M. G. A. Paris. *Gaussian states in quantum information*. Bibliopolis, Napoli (2005).

[FV99]   C. A. Fuchs and J. Van De Graaf. Cryptographic distinguishability measures for quantum-mechanical states. *IEEE Transactions on Information Theory* **45**, 1216 (1999).

[FVV+11]   M. Falcioni, D. Villamaina, A. Vulpiani, A. Puglisi and A. Sarracino. Estimate of temperature and its uncertainty in small systems. *American Journal of Physics* **79**, 777 (2011).

[GE16]   C. Gogolin and J. Eisert. Equilibration, thermalisation, and the emergence of statistical mechanics in closed quantum systems. *Reports on Progress in Physics* **79**, 56001 (2016).

[GFFMG14]   Z.-X. Gong, M. Foss-Feig, S. Michalakis and A. V. Gorshkov. Persistence of locality in systems with power-law interactions. *Physical Review Letters* **113**, 030602 (2014).

[GKF$^+$16]   M. Gluza, C. Krumnow, M. Friesdorf, C. Gogolin and J. Eisert. Equilibration via gaussification in fermionic lattice systems. *Physical Review Letters* **117**, 190602 (2016).

[GLTZ06]   S. Goldstein, J. L. Lebowitz, R. Tumulka and N. Zanghi. Canonical typicality. *Physical Review Letters* **96**, 050403 (2006).

[GMM04]   J. Gemmer, M. Michel and G. Mahler. *Quantum Thermodynamics*. Springer-Verlag Berlin Heidelberg (2004).

[GR07]   I. S. Gradshteyn and I. M. Ryzhik. *Table of Integrals, Series, and Products*. Academic Press (2007).

[GSFA09]   A. García-Saez, A. Ferraro and A. Acín. Local temperature in quantum thermal states. *Physical Review A* **79**, 052340 (2009).

[GTHC$^+$15]   A. González-Tudela, C. L. Hung, D. E. Chang, J. I. Cirac and H. J. Kimble. Subwavelength vacuum lattices and atom–atom interactions in two-dimensional photonic crystals. *Nature Photonics* **9**, 320 (2015).

[GWT84]   H. Grabert, U. Weiss and P. Talkner. Quantum theory of the damped harmonic oscillator. *Zeitschrift für Physik B* **55**, 87 (1984).

[Has04a]   M. Hastings. Lieb-Schultz-Mattis in higher dimensions. *Physical Review B* **69**, 104431 (2004).

[Has04b]   M. B. Hastings. Decay of correlations in Fermi systems at nonzero temperature. *Physical Review Letters* **93**, 126402 (2004).

[Has06]   M. B. Hastings. Solving gapped Hamiltonians locally. *Physical Review B* **73**, 085115 (2006).

[HBPLB17]   P. P. Hofer, J. B. Brask, M. Perarnau-Llobet and N. Brunner. Quantum thermal machine as a thermometer. *Physical Review Letters* **119**, 090603 (2017).

[HC18]   K. V. Hovhannisyan and L. A. Correa. Measuring the temperature of cold many-body quantum systems. *Physical Review B* **98**, 045101 (2018).

[HCMH$^+$10]   P. Hauke, F. M. Cucchietti, A. Müller-Hermes, M. C. Bañuls, J. I. Cirac and M. Lewenstein. Complete devil's staircase and crystal-superfluid transitions in a dipolar XXZ spin chain: A trapped ion quantum simulation. *New Journal of Physics* **12**, 113037 (2010).

Bibliography

[HIK14]   F. Haupt, A. Imamoglu and M. Kroner. Single quantum dot as an optical thermometer for millikelvin temperatures. *Physical Review Applied* **2**, 024001 (2014).

[HK06]   M. B. Hastings and T. Koma. Spectral gap and exponential decay of correlations. *Communications in Mathematical Physics* **265**, 781 (2006).

[HO13]   M. Horodecki and J. Oppenheim. Fundamental limitations for quantum and nanoscale thermodynamics. *Nature Communications* **4**, 2059 (2013).

[HSGCA17]   S. Hernández-Santana, C. Gogolin, J. I. Cirac and A. Acín. Correlation decay in fermionic lattice systems with power-law interactions at non-zero temperature. *Physical Review Letters* **119**, 110601 (2017).

[HSRH$^+$15]   S. Hernández-Santana, A. Riera, K. V. Hovhannisyan, M. Perarnau-Llobet, L. Tagliacozzo and A. Acín. Locality of temperature in spin chains. *New Journal of Physics* **17**, 085007 (2015).

[IEK$^+$11]   R. Islam, E. E. Edwards, K. Kim, S. Korenblit, C. Noh, H. Carmichael, G.-D. Lin, L.-M. Duan, C.-C. J. Wang, J. K. Freericks and C. Monroe. Onset of a quantum phase transition with a trapped ion quantum simulator. *Nature Communications* **2**, 377 (2011).

[JCM$^+$16]   T. H. Johnson, F. Cosco, M. T. Mitchison, D. Jaksch and S. R. Clark. Thermometry of ultracold atoms via nonequilibrium work distributions. *Physical Review A* **93**, 053619 (2016).

[JLH$^+$14]   P. Jurcevic, B. P. Lanyon, P. Hauke, C. Hempel, P. Zoller, R. Blatt and C. F. Roos. Quasiparticle engineering and entanglement propagation in a quantum many-body system. *Nature* **511**, 202 (2014).

[Kas11]   M. Kastner. Diverging equilibration times in long-range quantum spin models. *Physical Review Letters* **106**, 130601 (2011).

[Kas17]   M. Kastner. N-Scaling of timescales in long-range N-body quantum systems. *Journal of Statistical Mechanics* **2017**, 014003 (2017).

[Kat04]   Y. Katznelson. *An Introductrion to Harmonic Analysis*. Cambridge University Press (2004).

[KGE14]   M. Kliesch, C. Gogolin and J. Eisert. Lieb-Robinson bounds and the simulation of time evolution of local observables in lattice systems.

132

In: V. Bach and L. Delle Site (eds.), *Many-Electron Approaches in Physics, Chemistry and Mathematics*. Springer International Publishing (2014).

[KGK⁺14] M. Kliesch, C. Gogolin, M. J. Kastoryano, A. Riera and J. Eisert. Locality of Temperature. *Physical Review X* **4**, 31019 (2014).

[Kit01] A. Y. Kitaev. Unpaired Majorana fermions in quantum wires. *Physics-Uspekhi* **44**, 131 (2001).

[KKS94] A. G. Kofman, G. Kurizki and B. Sherman. Spontaneous and induced atomic decay in photonic band structures. *Journal of Modern Optics* **41**, 353 (1994).

[KLT12] T. Koffel, M. Lewenstein and L. Tagliacozzo. Entanglement entropy for the long-range Ising chain in a transverse field. *Physical Review Letters* **109**, 267203 (2012).

[KMY⁺13] G. Kucsko, P. C. Maurer, N. Y. Yao, M. Kubo, H. J. Noh, P. K. Lo, H. Park and M. D. Lukin. Nanometre-scale thermometry in a living cell. *Nature* **500**, 54 (2013).

[KN09] B. Klinkert and F. Narberhaus. Microbial thermosensors. *Cellular and Molecular Life Sciences* **66**, 2661 (2009).

[KRJP13] J. Kai, A. Retzker, F. Jelezko and M. B. Plenio. A large-scale quantum simulator on a diamond surface at room temperature. *Nature Physics* **9**, 168 (2013).

[LBR⁺16] H. Labuhn, D. Barredo, S. Ravets, S. de Léséleuc, T. Macrì, T. Lahaye and A. Browaeys. Tunable two-dimensional arrays of single Rydberg atoms for realizing quantum Ising models. *Nature* **534**, 667 (2016).

[LCB14] M. Lubasch, J. I. Cirac and M.-C. Bañuls. Algorithms for finite Projected Entangled Pair States. *Physical Review B* **90**, 064425 (2014).

[LG18] T.-C. Lu and T. Grover. Singularity in entanglement negativity across finite temperature phase transitions (2018). ArXiv:1808.04381 [cond-mat.stat-mech].

[LL58] L. D. Landau and E. M. Lifshitz. *Statistical Physics*. Pergamon Press (1958).

[LLGML17] A. Lampo, S. H. Lim, M. Á. García-March and M. Lewenstein. Bose

polaron as an instance of quantum Brownian motion. *Quantum* **1**, 30 (2017).

[LPS10]   N. Linden, S. Popescu and P. Skrzypczyk. How small can thermal machines be? The smallest possible refrigerator. *Physical Review Letters* **105**, 130401 (2010).

[LR72]   E. H. Lieb and D. W. Robinson. The finite group velocity of quantum spin systems. In: B. Nachtergaele, J. Solovej and J. Yngvason (eds.), *Statistical Mechanics*. Springer-Verlag Berlin Heidelberg (1972).

[LV05]   S. Lefèvre and S. Volz. 3ω-scanning thermal microscope. *Review of Scientific Instruments* **76**, 033701 (2005).

[MAMW15]   M. P. Müller, E. Adlam, L. Masanes and N. Wiebe. Thermalization and canonical typicality in translation-invariant quantum lattice systems. *Communications in Mathematical Physics* **340**, 499 (2015).

[Man56]   B. B. Mandelbrot. An outline of a purely phenomenological theory of statistical thermodynamics: I. Canonical ensembles. *IRE Transactions on Information Theory* **2**, 190 (1956).

[Man89]   B. B. Mandelbrot. Temperature fluctuation: a well-defined and unavoidable notion. *Physics Today* **42**, 71 (1989).

[MB13]   U. Marzolino and D. Braun. Precision measurements of temperature and chemical potential of quantum gases. *Physical Review A* **88**, 063609 (2013).

[MBZ06]   A. Micheli, G. K. Brennen and P. Zoller. A toolbox for lattice-spin models with polar molecules. *Nature Physics* **2**, 341 (2006).

[MGFFG16] M. F. Maghrebi, Z.-X. Gong, M. Foss-Feig and A. V. Gorshkov. Causality and quantum criticality in long-range lattice models. *Physical Review B* **93**, 125128 (2016).

[MKN17]   T. Matsuta, T. Koma and S. Nakamura. Improving the Lieb-Robinson bound for long-range interactions. *Annales Henri Poincaré* **18**, 519 (2017).

[MNV09]   K. Maruyama, F. Nori and V. Vedral. Colloquium: The physics of Maxwell's demon and information. *Reviews of Modern Physics* **81**, 1 (2009).

[Mon13]   A. Monras. Phase space formalism for quantum estimation of Gaussian states (2013). ArXiv:1303.3682 [quant-ph].

[MSC18]   M. Mehboudi, A. Sanpera and L. A. Correa. Thermome-
            try in the quantum regime: Recent theoretical progress (2018).
            ArXiv:1811.03988 [quant-ph].

[MSVC14]   A. Molnár, N. Schuch, F. Verstraete and J. I. Cirac. Approximating
            Gibbs states of local Hamiltonians efficiently with PEPS. *Physical
            Review B* **91**, 045138 (2014).

[NA02]   T. M. Nieuwenhuizen and A. E. Allahverdyan. Statistical thermo-
            dynamics of quantum Brownian motion: Construction of perpetuum
            mobile of the second kind. *Physical Review E* **66**, 036102 (2002).

[NC00]   M. A. Nielsen and I. L. Chuang. *Quantum Computation and Quan-
            tum Information*. Cambridge University Press (2000).

[NJD+13]   P. Neumann, I. Jakobi, F. Dolde, C. Burk, R. Reuter, G. Wald-
            herr, J. Honert, T. Wolf, A. Brunner, J. H. Shim et al. High-
            precision nanoscale temperature sensing using single defects in di-
            amond. *Nano Letters* **13**, 2738 (2013).

[NVZ11]   B. Nachtergaele, A. Vershynina and V. A. Zagrebnov. Lieb-Robinson
            bounds and existence of the thermodynamic limit for a class of irre-
            versible quantum dynamics. *AMS Contemporary Mathematics* **552**,
            161 (2011).

[PC04]   D. Porras and J. I. Cirac. Effective quantum spin systems with
            trapped ions. *Physical Review Letters* **92**, 207901 (2004).

[PGVWC07]   D. Perez-García, F. Verstraete, M. M. Wolf and J. I. Cirac. Matrix
            product state representations. *Quantum Information & Computation*
            7, 401 (2007).

[PMWB12]   D. Peter, S. Müller, S. Wessel and H. P. Büchler. Anomalous behavior
            of spin systems with dipolar interactions. *Physical Review Letters*
            109, 025303 (2012).

[PNP17]   K. Patrick, T. Neupert and J. K. Pachos. Topological quantum liq-
            uids with long-range couplings. *Physical Review Letters* **118**, 267002
            (2017).

[PS99]   G. S. Paraoanu and H. Scutaru. Fidelity for multimode thermal
            squeezed states. *Physical Review A* **61**, 5 (1999).

[PS16]   L. Pitaevskii and S. Stringari. *Bose-Einstein Condensation and Su-
            perfluidity*. Oxford University Press (2016).

Bibliography

[PSSV11]   A. Polkovnikov, K. Sengupta, A. Silva and M. Vengalattore. Colloquium: Nonequilibrium dynamics of closed interacting quantum systems. *Reviews of Modern Physics* **83**, 863 (2011).

[PSW06]   S. Popescu, A. J. Short and A. Winter. Entanglement and the foundations of statistical mechanics. *Nature Physics* **2**, 754 (2006).

[PTZB14]   L. A. Pachon, J. F. Triana, D. Zueco and P. Brumer. Influence of non-markovian dynamics in thermal-equilibrium uncertainty-relations (2014). ArXiv:1401.1418 [quant-ph].

[PVVT12]   B. Pirvu, G. Vidal, F. Verstraete and L. Tagliacozzo. Matrix product states for critical spin chains: Finite-size versus finite-entanglement scaling. *Physical Review B* **86**, 075117 (2012).

[PWC$^+$96]   J. F. Poyatos, R. Walser, J. I. Cirac, P. Zoller and R. Blatt. Motion tomography of a single trapped ion. *Physical Review A* **53**, R1966 (1996).

[Rei98]   L. E. Reichl. *A Modern Course in Statistical Physics*. Wiley-VCH (1998).

[RGL$^+$14]   P. Richerme, Z.-X. Gong, A. Lee, C. Senko, J. Smith, M. Foss-Feig, S. Michalakis, A. V. Gorshkov and C. Monroe. Non-local propagation of correlations in quantum systems with long-range interactions. *Nature* **511**, 198 (2014).

[RHW85]   P. S. Riseborough, P. Hänggi and U. Weiss. Exact results for a damped quantum-mechanical harmonic oscillator. *Physical Review A* **31**, 471 (1985).

[SBC16]   L. F. Santos, F. Borgonovi and G. L. Celardo. Cooperative shielding in many-body systems with long-range interaction. *Physical Review Letters* **116**, 250402 (2016).

[SBM$^+$11]   J. Simon, W. S. Bakr, R. Ma, M. E. Tai, P. M. Preiss and M. Greiner. Quantum simulation of antiferromagnetic spin chains in an optical lattice. *Nature* **472**, 307 (2011).

[SCLD14]   R. Schirhagl, K. Chang, M. Loretz and C. L. Degen. Nitrogen-vacancy centers in diamond: nanoscale sensors for physics and biology. *Annual Review of Physical Chemistry* **65**, 83 (2014).

[Scu98]   H. Scutaru. Fidelity for displaced squeezed thermal states and the os-

cillator semigroup. *Journal of Physics A: Mathematical and General* **31**, 3659 (1998).

[SF12]   A. J. Short and T. C. Farrelly. Quantum equilibration in finite time. *New Journal of Physics* **14**, 013063 (2012).

[SFTH12]   Y. Subaşı, C. H. Fleming, J. M. Taylor and B. L. Hu. Equilibrium states of open quantum systems in the strong coupling regime. *Physical Review E* **86**, 061132 (2012).

[SG14]   B. Somogyi and A. Gali. Computational design of in vivo biomarkers. *Journal of Physics: Condensed Matter* **26**, 143202 (2014).

[SHS$^+$14]   F. Seilmeier, M. Hauck, E. Schubert, G. J. Schinner, S. E. Beavan and A. Högele. Optical thermometry of an electron reservoir coupled to a single quantum dot in the millikelvin range. *Physical Review Applied* **2**, 024002 (2014).

[SPS12]   C. Schneider, D. Porras and T. Schaetz. Experimental quantum simulations of many-body physics with trapped ions. *Reports on Progress in Physics* **75**, 024401 (2012).

[SSD59]   H. E. D. Scovil and E. O. Schulz-DuBois. Three-level masers as heat engines. *Physical Review Letters* **2**, 262 (1959).

[SVK15]   D. M. Storch, M. Van Den Worm and M. Kastner. Interplay of sound-cone and supersonic propagation in lattice models with power law interactions. *New Journal of Physics* **17**, 063021 (2015).

[TA14]   G. Tóth and I. Apellaniz. Quantum metrology from a quantum information science perspective. *Journal of Physics A: Mathematical and Theoretical* **47**, 424006 (2014).

[Thi02]   W. Thirring. *Quantum mathematical physics*. Springer-Verlag Berlin Heidelberg (2002).

[UvL99]   J. Uffink and J. van Lith. Thermodynamic uncertainty relations. *Foundations of Physics* **29**, 655 (1999).

[VAK13]   A. A. Valido, D. Alonso and S. Kohler. Gaussian entanglement induced by an extended thermal environment. *Physical Review A* **88**, 042303 (2013).

[VC06]   F. Verstraete and J. I. Cirac. Matrix product states represent ground states faithfully. *Physical Review B* **73**, 094423 (2006).

Bibliography

[VCA13]   A. A. Valido, L. A. Correa and D. Alonso. Gaussian tripartite entanglement out of equilibrium. *Physical Review A* **88**, 012309 (2013).

[VLE⁺14]   D. Vodola, L. Lepori, E. Ercolessi, A. V. Gorshkov and G. Pupillo. Kitaev chains with long-range pairing. *Physical Review Letters* **113**, 156402 (2014).

[VLEP16]   D. Vodola, L. Lepori, E. Ercolessi and G. Pupillo. Long-range Ising and Kitaev models: Phases, correlations and edge modes. *New Journal of Physics* **18**, 015001 (2016).

[VN29]   J. Von Neumann. Beweis des Ergodensatzes und des H-Theorems in der neuen Mechanik. *Zeitschrift für Physik* **57**, 30 (1929).

[VRA15]   A. A. Valido, A. Ruiz and D. Alonso. Quantum correlations and energy currents across three dissipative oscillators. *Physical Review E* **91**, 062123 (2015).

[Wei08]   U. Weiss. *Quantum dissipative systems*. World Scientific Pub Co. (2008).

[WW86]   C. C. Williams and H. K. Wickramasinghe. Scanning thermal profiler. *Applied Physics Letters* **49**, 1587 (1986).

[ZÁK16]   A. Zwick, G. A. Álvarez and G. Kurizki. Maximizing information on the environment by dynamically controlled qubit probes. *Physical Review Applied* **5**, 014007 (2016).